**Effective Resource Allocation for Non-Cooperative Spectrum Sharing**

Dany Jacob-David

Thesis submitted to the
Faculty of Graduate and Postdoctoral Studies
in partial fulfillment of the requirements
for the Master's degree in Electrical and Computer Engineering

Department of Electrical and Computer Engineering
Faculty of Engineering
University of Ottawa

# Abstract

Spectrum access protocols have been proposed recently to provide flexible and efficient use of the available bandwidth. Game theory has been applied to the analysis of the problem to determine the most effective allocation of the users' power over the bandwidth. However, prior analysis has focussed on Shannon capacity as the utility function, even though it is known that real signals do not, in general, meet the Gaussian distribution assumptions of that metric. In a non-cooperative spectrum sharing environment, the Shannon capacity utility function results in a water-filling solution. In this thesis, the suitability of the water-filling solution is evaluated when using non-Gaussian signalling first in a frequency non-selective environment to focus on the resource allocation problem and its outcomes. It is then extended to a frequency selective environment to examine the proposed algorithm in a more realistic wireless environment. It is shown in both scenarios that more effective resource allocation can be achieved when the utility function takes into account the actual signal characteristics. Further, it is demonstrated that higher rates can be achieved with lower transmitted power, resulting in a smaller spectral footprint, which allows more efficient use of the spectrum overall. Finally, future spectrum management is discussed where the waveform adaptation is examined as an additional option to the well-known spectrum agility, rate and transmit power adaptation when performing spectrum sharing.

# Acknowledgements

First and foremost, I would like to thank Dr. Tricia Willink, my supervisor at Communications Research Centre (CRC). Her dedication, patience and advices have provided me with the determination to see this thesis through to completion. I particularly enjoyed the many discussions with her which have challenged me and strengthened my knowledge in spectrum management. I would surely not have reached this point without her encouragement and outstanding support.

Further, I owe special gratitude to the CRC for providing an excellent and supportive atmosphere throughout the work of my thesis. They were always opened for helpful discussions and accepted me as a full member of their group.

I would also like to thank Dr. Abbas Yongacoglu, my academic supervisor at University of Ottawa, for the support and guidance offered during my graduate studies program. My thanks and appreciation to my thesis committee members, Dr. I Marsland and Dr. C. D'Amours. I am greatly indebted to my degree sponsor, the Department of National Defence, for nominating me to pursue a master degree in electrical engineering.

Lastly, I am grateful to my family who has always support me through the thesis. I would like to thank my husband, Cédrick for the motivation he gave me during those tiring times when I had doubts about my studies. Finally, special thanks to my two daughters, Laurielle and Dorothée, to have dealt outstandingly well with having a mother not always present to share their important moments.

# Contents

# List of Figures

# List of Tables

# List of Abbreviations

| | |
|---|---|
| DSA: | dynamic spectrum access |
| REM: | radio environment map |
| SNR: | signal to noise ratio |
| QoS: | quality of service |
| TDMA: | time division multiple access |
| CDMA: | code division multiple access |
| FDM: | frequency division multiplexing |
| FDMA: | frequency division multiple access |
| SF: | spreading factor |
| OFDM: | orthogonal frequency division multiplexing |
| DSSS: | direct sequence spread spectrum |
| IFC: | interference frequency channel |
| CSI: | channel state information |
| SER: | symbol error rate |
| SIR: | signal to noise ratio |
| GR: | greedy algorithm |
| WF: | water-filling algorithm |
| MRC: | maximum ratio combining |
| AWGN: | additive white Gaussian noise |

# List of Symbols

| | |
|---|---|
| $N$ | Total number of available channels |
| $\mathcal{Q}_i$ | Desired signal at receiver $i$ |
| $\mathcal{I}_i$ | Interference signal from transmitter $j$ at receiver $i$ |
| $Q_i$ | Average power of desired signal at receiver $i$ |
| $I_i$ | Average power of interference signal at receiver $i$ |
| $k$ | index for the channel number |
| $x_i$ | Transmitted signal for user $i$ |
| $P_i(k)$ | Transmit power of user $i$ on channel $k$ |
| $h_ij(k)$ | Channel attenuations between receiver $i$ and transmitter $j$ |
| $N_o$ | Power spectral density |
| $B_c$ | Bandwidth for each channel |
| $\Upsilon_i(k)$ | Signal to noise ratio for user $i$ on channel $k$ |
| $P_{tot}$ | Total transmit power |
| $P_i^{WF}(k)$ | Water-filling transmit power allocation for user $i$ on channel $k$ |
| $P_i^{GR}(k)$ | Greedy transmit power allocation for user $i$ on channel $k$ |
| $P_{rem}$ | Unused power for the greedy algorithm |
| $R_{i,max}$ | Maximum sum rate for user $i$ |
| $\Delta Q$ | Differential received power |
| $\Delta P$ | Differential transmit power |
| $N_{it}$ | Number of iteration for the iterative game |
| $\beta$ | Cross-talk factor |
| $\kappa_{ii}(k)$ | Scaling factor to normalize the average received powers (multipath channel) |
| $M$ | Total number of delay lines |

| | |
|---|---|
| $T$ | Symbol duration |
| $U$ | Size of the Fast Fourier Transform |
| $\tau_m$ | Delay |
| $\alpha_{ij}(k, \tau_m)$ | Variance power for channel $k$ at delay $m$ |
| $w_i$ | Additive white Gaussian noise for user $i$ |
| $y_i$ | Received signal for user $i$ |
| $b_i(n)$ | $\mathrm{n}^{\mathrm{th}}$ transmit symbol for user $i$ |
| $T_s$ | Symbol duration for DSSS waveform |
| $T_c$ | Chip duration for DSSS waveform |
| $V$ | Spreading factor |
| $a(\frac{nT_s - v}{T_c})$ | pseudo-noise random sequence for DSSS waveform |
| $h^*$ | Complex conjugate for the channel attenuations |
| $a^*$ | Complex conjugate for the pseudo-noise random sequence |
| $P_{loss}$ | Path loss |
| $\lambda$ | Wavelength |
| $D$ | Maximal distance $D$ |
| $d$ | Distance between a receiver and a transmitter |
| $\alpha$ | Path loss exponent |

# Chapter 1

# Introduction

With the increasing demand for high data rates, unallocated spectrum has become scarce due to current spectrum management policies, which are designed to avoid mutual interference by limiting access to a spectrum band in the same geographical area. However, due to the unprecedent development and deployment of bandwidth-intense delay-sensitive multimedia devices (teleconferencing, distributed gaming, mobile video streaming), requirements for wireless spectrum access capacity are increasing more and more. To obtain a licence for unallocated spectrum, it has now become very expensive and can take years.

As a result, the discrepancy between the quasi-exponential growth of wireless bandwidth demands and the very limited wireless spectrum resource is a crucial issue that must be resolved in the near future to allow further development and deployment of new wireless services and technologies. Some steps have been taken to remedy this situation. For example the White House has established the Presidential Spectrum Policy Initiative and created a multi-agency Federal Government Spectrum Task Force to direct efforts on interagency initiatives to use spectrum more efficiently [1].

## 1.1 Literature Review

The present spectrum assignment policy leads itself to underutilization of the wireless spectrum resource. It has been shown through measurements that usage of licensed bands, especially in the cellular and TV broadcast bands, remains highly sporadic both geographically and temporally [2]. To remedy this situation, the cognitive radio paradigm has been

proposed in [3]. In [4], it is discussed how cognitive radios should be capable of sensing and learning from their environment to optimize their decisions.

Through the cognitive paradigm term, dynamic spectrum access (DSA) and spectrum sharing have been proposed as solutions to make the limited resource more accessible [5]. The term "cognitive radio" has several definitions due to different interpretations. However, there is a common defining feature: it should be aware of its environment [4,6] and learn from its observations. To allow the cognitive radio to get its "cognitive" quality, in other words capable of learning from past decisions and observations and then improving its adaptation to its environment, it must have the capacity of memorization to build the foundation of "knowledge". This brings the concept of the radio environment map (REM) [7, ch.11] from where the cognitive radio could access information about its environment to complete its own observations. The REM could be the vehicle for providing network support to cognitive radio systems by providing information on:

- spectrum policies rules applicable to where the cognitive radio is located,
- geographical information such as:
  - the location (x,y,z) for where the radio is now and for where it is heading,
  - the environment (urban, sub-urban, mountains, sea, etc),
  - current and expected pathloss and SNR,
  - current and expected multipath delay profile expected,
  - channel model to use,
- hidden nodes present in the neighbourhood,
- spectrum opportunities,
- usage patterns for primary (or licensed) users and cognitive users.

With or without the REM, the cognitive radio technology should enable the users to process four main functions: *spectrum sensing*, *spectrum management*, *spectrum sharing* and *spectrum agility* [4, 6].

*Spectrum sensing* is the process to access the knowledge of which portion of the spectrum is available when the cognitive user operates on a licensed spectrum segment and when the

spectrum segment is not available any more because of the presence of one or more primary users. In DSA, the user opportunistically takes advantage of an available portion of the spectrum band when it is unused by the licensed, or primary, user [5]. Moreover, the devices that act as opportunistic users must be capable of sensing where are the available frequencies (white spaces or spectrum holes). However, perfect knowledge of the spectrum holes is actually impossible in a wireless environment because of several factors, namely the famous hidden node problem due to shadowing, scattering effects and pathloss effect. Furthermore, at low SNR, detection of the primary user may be missed. There has been shown to be an SNR wall [8–10], which is the limit at which the receiver cannot distinguish between noise and signal. The SNR wall is dependent on noise estimation accuracy [9, 10] and noise quantization which provides robustness to the signal detection feature to a certain limit [9].

That said, acknowledging that perfect knowledge cannot be achieved, it is still possible for the cognitive radio to learn enough information about its environment to make smart decisions to access the spectrum hole opportunistically. This will imply a probability that wrong decisions would eventually be taken. However, as the name states, the cognitive sense of the cognitive radio should learn from its "mistakes" and improve its decision in the future. Therefore, the cognitive radio should not rely only on spectrum sensing but also on memorized information as per the REM concept.

The cognitive radios can gather the information on spectrum holes from their local information (their own spectrum sensing capabilities) or from cooperative spectrum sensing [11]. Cooperative spectrum sensing could be done centrally [11] or distributively [12–14]. Centrally will require a central scheduler and authority for the exchange of information about spectrum sensing and this information will be stored centrally. Distributively implies that the information is stored in a distributed manner (either locally at the cognitive radio or at least at the local network for the cognitive radio) to speed up the spectrum sensing process. As outlined in Figure 1.1, cooperative sensing provides a better performance for efficient use of the spectrum holes due to the fact that some cognitive radios might be aware of primary users that other cognitive radios might not be able to sense because of high channel attenuation or another situation. But cooperative spectrum sensing also involves more overhead communications to share the information. Even distributed spectrum sensing solutions often make the assumption that an underlay channel is available for cognitive radio to exchange the spectrum sensing information [13]. Moreover, wrong decisions may also be taken by a cog-

nitive radio based on information received from other cognitive radios; e.g.: false spectrum sensing of a spectrum hole from another cognitive radio or outdated information [13].

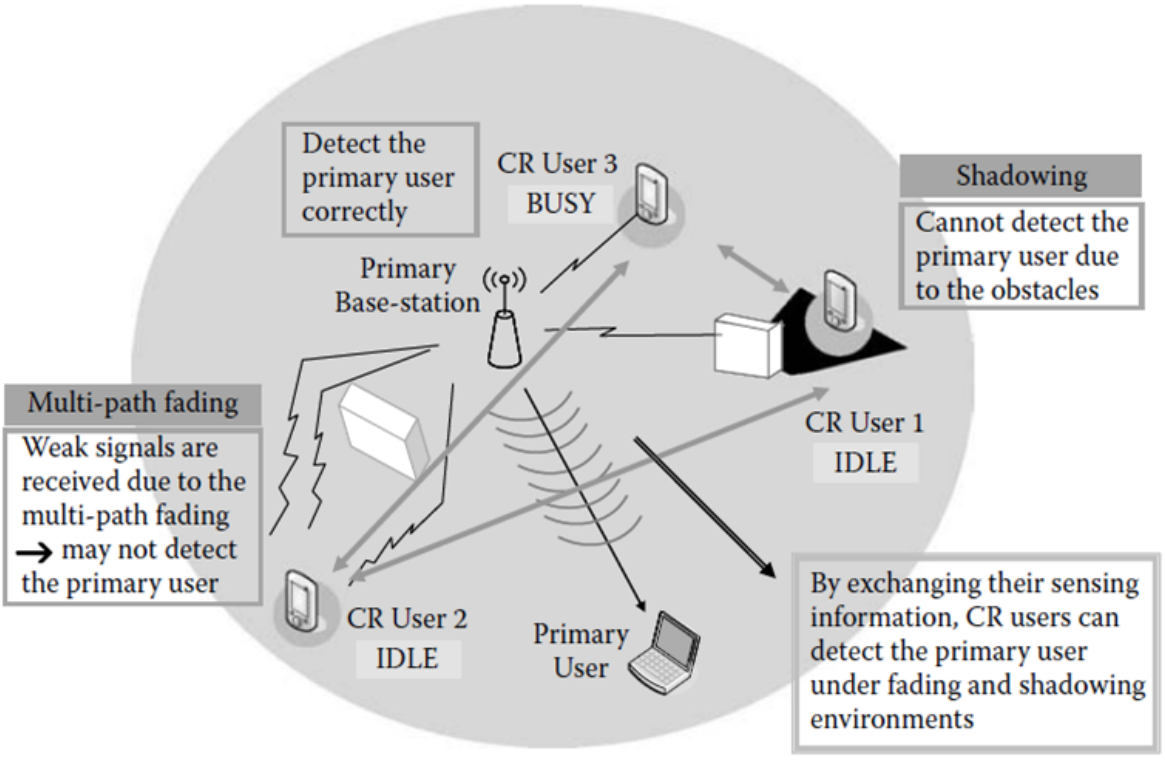


**Figure 1.1:** Cooperative spectrum sensing under faded and shadowed environment [15, ch.1]

Based on a certain probability (false detection of the primary or licensed user versus missed detection of the primary or licensed user), the cognitive radio must decide if it will or will not access the detected spectrum hole. An aggressive probability will favour the opportunity of using the white space (therefore it is more probable that there will be a missed detection of primary user) and a more conservative behaviour will increase its likelihood of leaving a spectrum hole empty. The white space might or might not be shared with other cognitive devices. This policy must be decided in the implementation of the DSA protocol [16, 17]. If it is not shared, then spectrum management is done on the principle of mutual interference avoidance, which is in accordance with the actual spectrum management allocation policies. Therefore, if it is not shared, the cognitive devices compete for the spectrum segment, and if they win the competition, they will be the only ones allowed the access until the primary or licensed user is detected or until they vacate it (when the user

does not require it anymore, the channel gains are not good enough to sustain the quality of service required by the user or under a protocol such as time limit determines that the user must vacate the spectrum segment) [6].

*Spectrum management* provides the capability to find which channel is the best for transmission based on the following considerations:

- mutual interference avoidance,
- quality of service (QoS) requirements, and
- seamless communications.

These could be affected by traffic congestion, temporal channel variations and user mobility. A mechanism must be introduced to the cognitive radios to allow them to adapt at their best advantages to these changes. Water-filling [18] and bit loading algorithms [19] which are based on a greedy algorithm have been used to optimally select power allocation for multi-carrier modulations on frequency selective channels.

Mutual interference avoidance is achieved using several techniques. On one hand, if mutual interference is not tolerated there are two main techniques. First, the physical separation specified by spectrum regulations and policies which allows only a sole source in a specific spectrum segment in a specific geographical area. Second, the signal processing techniques which allow multiple users with orthogonality separation such as: time division multiple access (TDMA) which ensures orthogonality by allowing only one user at a time, which is scheduled by a central authority; frequency division multiple acces (FDMA) which ensures only one user on a portion of the available spectrum segment; and code division multiple access (CDMA) which separates the multiple users by providing them with different pseudo-random spreading codes. But all these above techniques have not by themselves the flexibility of opportunistic spectrum sharing. One user might be given a share of the time in TDMA but it might not be the best time for the user to transmit since the channel gains are not to its advantage, it is also determined in time *a priori* and does not allow opportunistic users. The same logical thinking applies to the CDMA and FDMA techniques. On the other hand, if some mutual interference can be tolerated, then a noise temperature model [20] can be introduced where the mutual interference will be detected as noise. As long as the mutual interference is below a determined noise floor, the users in this spectrum segment will be capable of operating and satisfying their QoS requirements.

The quality of service requirements will determine the utility function that will be used for a specific system to decide which channel is best for it. The utility function provides the ability for a system to measure the reward/payoff it should obtain by selecting a specific strategy (transmit power, spreading factor, modulation rate, channel selection). There exist an infinite number of utility functions since the users are heterogeneous; e.g: delay critical system, interference tolerant, etc.

The seamless communication consideration will take into account the system QoS requirements to decide when it should select another channel to transmit. A system can seldom tolerate an abrupt interruption in the communication link but switching to another channel increases the probability of a communication interruption. This increase in probability is due to the fact that both receiver and transmitter must be aware of the new channel selection, which involves communications overhead, time to adequately choose the new channel, handshake and handoff time. Careful thought must be given prior to changing the channel for a specific user to allow appropriate time for spectrum handoff and handshake.

*Spectrum sharing* is the tool to coordinate access with other users. In other words, in spectrum sharing users must deal with and take into account other users sharing the same spectrum segment [16]. Spectrum sharing is well known for the unlicensed bands [21] which were created to promote new technology development without the burden of acquiring a spectrum licence. It has been very successful in meeting the goal of encouraging technology innovation. However, the unlicensed spectrum bands may become the victim of their own success since these bands now support a tremendous amount of new devices. Efficient algorithms must be implemented to take full advantage of the spectrum resource in minimizing the mutual interference.

There are several ways to share spectrum: the architecture could be either centralized or decentralized, sharing could be horizontal (sharing among equals) or vertical (primary and secondary user concepts), the spectrum allocation could be based on cooperative or non-cooperative behaviour and the technique used for spectrum sharing could be overlay or underlay [5].

Sharing among equals is horizontal sharing: all the devices have equal rights in sharing the available spectrum. There is usually no concept of primary/secondary users. The unlicensed bands are a good example [21]. It could also be when there is no primary user detected and the secondary users share the available spectrum holes with equal rights. The available

frequencies can be merged into a common spectrum pool from where, through a distributed protocol, the users compete either cooperatively or non-cooperatively for the spectrum.

Primary and secondary concepts are vertical sharing: usually, there is no necessity to create a spectrum pool. An agreement is in place to allow secondary users who must keep below a certain value the interference generated to the primary users. Therefore, it is often limited to low power transmission, hence short range transmission.

Cooperative spectrum sharing [17,22–24] considers the effect of the user's communications on other users' communications. Interference measurements are shared among the users and are considered by the spectrum allocation algorithm. Cooperative solutions could be either centralized or decentralized [11].

In non-cooperative spectrum sharing [21, 22, 24–26], the users consider only their best interests and do not take into account the interference generated by their action to the other users. This kind of spectrum sharing (referred to as selfish) usually involves a reduced spectrum footprint reutilization because of the selfish behaviour of the users. But alternatively, minimal overhead communication exchanges between the users are required which is an important tradeoff to consider in practical systems.

Cooperative and non-cooperative spectrum sharing have been compared in the literature through their spectrum utilization, fairness and throughput [22–24, 27]. For both kinds of spectrum sharing, the use of optimization min-max fairness criteria [27] and more specifically game theory [11] have been recently studied for this resource allocation problem.

Game theory is a set of mathematical tools that is used to analyze the outcome of a resource sharing conflict. It was first introduced in economics and then has been used extensively in several areas such as socio-political science and biology. Recently, it has been introduced to examine the outcome of resource allocation in the wireless network [17, 22, 28].

The users that will opportunistically take advantage of the available spectrum are most likely selfish (aiming only to optimize their own performance) and rational (capable of strategizing). They have conflicting objectives in competing for the limited resource (spectrum segment). Therefore, the spectrum sharing problem can be modelled as a game [22, 26, 29]. The formal form of a game framework requires three main components:

- the set of users which are normally called players,
- the set of strategies for each user. In wireless resource allocation, it could be for example

the set of possible transmit powers, modulation levels, spreading factors, channels bands, and

- the set of reward/payoff given to the user when selecting a specific strategy.

For non-cooperative games where the users do not exchange information to influence their decision on their next strategy, there must be a point for which the spectrum allocation problem will converge. The point is referred to as an equilibrium. The Nash equilibrium is usually used in the spectrum sharing non-cooperative game [22,25,26]. The Nash equilibrium is defined as a point where a user has no incentive to change its strategy any more if all other users are keeping the same strategy. The well-known water-filling algorithm for spectrum sharing is a flavour of the non-cooperative game. The convergence to the Nash equilibrium is often fast but on the other hand, due to the greedy behaviour of the users, often leads to a sub-optimal solution [22–24].

A price-based spectrum management was proposed in [30], where the utility function of the waterfilling algorithm is modified to take into account the price a user is ready to pay to obtain a specific strategy. In this context [30], a higher price factor should prevent a user from using a large amount of transmission power on a channel. The introduction of the pricing factor forces the selfish users to work toward a social optimal solution. However, the improvement in the outcome comes with the cost of an increased amount of information exchanged in order to get the channel estimates of the interference paths with neighbouring users.

In cooperative games, the users exchange information through an established protocol to bargain an agreement on their parameters. One proposed solution is the Nash bargaining solution [24, 31] which is completely different than the Nash equilibrium. Here, the users agree a point of discord before the game, letting the others know the minimum outcome they deem acceptable for their QoS requirements. If through the game they cannot strike a bargain, then the outcome for every user will be the point of discord.

Game theory was used in [22] to compare the cooperative and non-cooperative approaches in a distributed adaptive channel allocation. Two utility functions that measure the incentive for a user to choose a specific channel were considered. The first utility function represents the selfish behaviour and calculates the interference that will be measured at its receiver if that channel is selected. The second utility function is based on the cooperative be-

haviour of a user and takes into account the interference generated to the other users when selecting a specific channel. To converge to a Nash equilibrium, a learning algorithm was introduced. The results of [22] show that the non-cooperative behaviour brings a degraded fairness among the users compared to the cooperative behaviour and a slightly worse performance for the throughput. However, the exchange of communications required between the non-cooperative users is significantly lower.

*Spectrum overlay* would allow a user to access opportunistically a portion of the spectrum that has not been used by the primary user or the licensed user. Therefore, minimal interference is generated to the primary system. This was the original motivation for cognitive radio [3]. The assumption made for this type of spectrum sharing technique is that the cognitive users possess knowledge of the spectrum holes in space, time, or frequency when the primary user (noncognitive user) is not using these holes. Simultaneous communications on the same channel by both primary user and cognitive users are avoided and will happen only in the event of a false spectral hole detection. The cognitive user's transmit power is limited by the capacity of its spectrum sensing capability [6]. An overlay example that uses the OFDM-based cognitive radio system is presented in [32]. The opportunistic user uses the OFDM waveform to notch the carriers on which a licensed user is transmitting, reducing the mutual interference on the licensed user. As the main drawback of OFDM is its high sidelobes that are interfering with the neighbouring bands, the authors in [32] present techniques to mitigate this unwelcome effect.

*Spectrum underlay* would use advanced signal processing techniques to exploit spread spectrum techniques such as direct sequence spread spectrum (DSSS), frequency hopping and multiple access approaches such as code division multiple access (CDMA). Hence, the interference generated by the user will be considered as noise by the primary system and simultaneous communications on the same channel band of both primary users and cognitive users is allowed as long as the cognitive radio does not create interference higher than a certain noise floor. This brought the concept of the interference temperature model [33].

*Spectrum agility* provides the capability to change spectrum segment in a seamless manner when the spectrum segment used is not available any more to the cognitive user (a primary user has been detected, for example) or when the pathloss on this spectrum segment cannot offer the required quality of service for this user.

A problem that is commonly considered is that the available spectrum is subdivided into

$N$ channels with different channel gains. In this problem, the users compete selfishly for their share of the spectrum band by strategically allocating their total transmit power among the $N$ channels that can be either shared or not. In the problem of interest in this thesis, the $N$ channels are to be shared among the users.

When users share the same spectrum and try to transmit simultaneously on the same frequency, it becomes an interference channel problem (IFC) as represented by Figure 1.2. The capacity of the IFC has been an open problem for the last three decades because it is not completely understood, but it has been researched in the literature for example in [6, 21, 34, 35]. A nice survey of the Gaussian interference channel is provided in [6]. The best known inner bound for the IFC capacity has been given in [35] but this is difficult to work with. A looser bound is shown in [34] where the IFC capacity is bound to 1 bit/s/Hz. In [21], it is argued that a more tractable inner bound than the one provided in [35] is achieved by treating the received interference at the receiver as noise. The latter inner bound will be used for the remainder of this thesis.

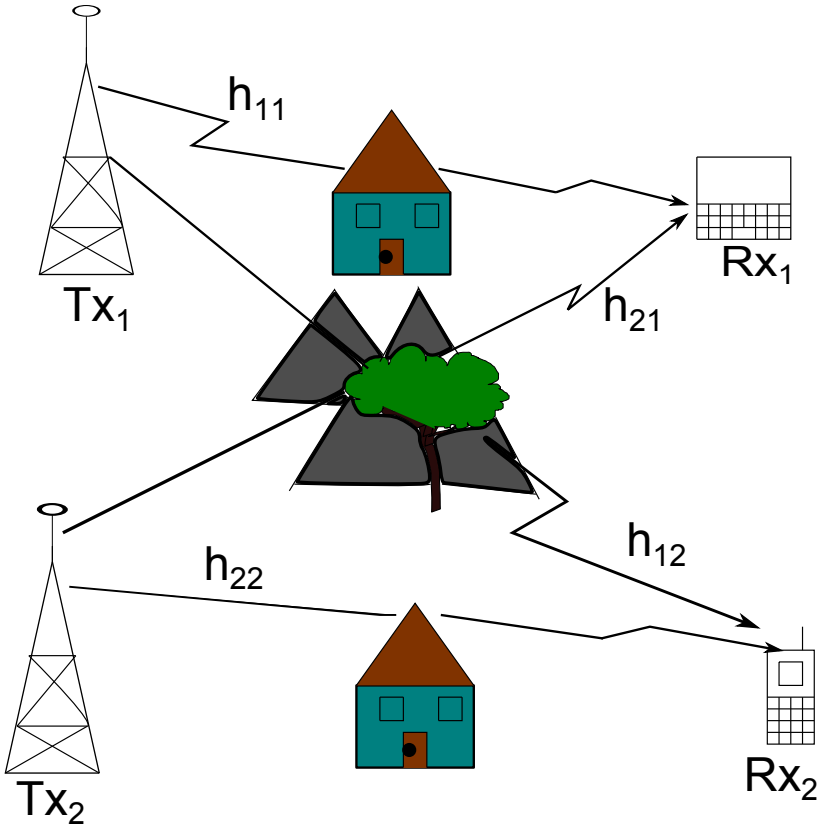


**Figure 1.2:** The interference channel.

## 1.2 Thesis Contributions

The main contribution of this thesis is to assess the effectiveness of the utility function based on the Shannon capacity for non-Gaussian signalling for a non-cooperative spectrum sharing environment. The non-cooperative spectrum sharing environment considered in this thesis has $N$ non-contiguous channels where two users determine the required transmit power allocation over the $N$ channels to maximize selfishly their sum rate. It is shown that the proposed greedy algorithm can provide better performance when the utility function is based on the knowledge of the signals characteristics. It is also shown in this thesis that not only are higher rates achieved but also total transmit power is minimized, an important factor for the reduction of mutual interference, reduction of spectral footprint, saving battery life and allowing neighbourhood users to opportunistically access the spectrum. Furthermore, it is demonstrated that when the channel attenuations change, the spectrum sharing users can choose to adapt also their waveforms in addition to the rate adaptation, transmit power adaptation and spectrum agility to meet their system's QoS requirements.

## 1.3 Thesis organization

This thesis is organized as follows. Descriptions of the water-filling and greedy algorithms are provided in Chapter 2. In Chapter 2, the system model is first presented for a narrowband scenario in Section 2.2 and performance of the two algorithms are discussed and compared in a flat Rayleigh fading environment to provide a comprehensive insight on their behaviours and rate/transmit power allocation outcomes in Section 2.6. Based on the results presented in Chapter 2, the work is then extended in a wideband environment simulated with multiple Rayleigh fading paths. The system model for the wideband scenario is first presented in Section 3.1 and the performance of the two algorithms in that environment are discussed in Section 3.6. A discussion of future spectrum management is provided in Chapter 4 with a study-case based on the results obtained in Chapter 3 and where waveform adaption is proposed as a new option to the well-known spectrum agility and rate and transmit power adaption while performing spectrum sharing. Conclusions are drawn and further work in this area is discussed in Chapter 5.

# Chapter 2

# Frequency Non-Selective Environment

## 2.1 Problem definition

The spectrum sharing environment considered here consists of two users transmitting in the same band in the same geographic area. The available spectrum is divided into $N = 3$ Rayleigh fading quasi-static channels of bandwidth $B_c$ Hz. The problem for each user is to allocate the total power, $P_{tot}$, among the channels to maximize their rates, while achieving a specified target symbol error rate (SER). The total power available for each user is the same and there is no cooperation between the users.

## 2.2 System model

There are two transmitter-receiver pairs operating in the same $N$ channels. The received signals at the two receivers on channel $k$ are modelled as

$$\begin{aligned} y_1(k) &= \mathcal{Q}_1(k) + \mathcal{I}_1(k) + w_1(k) \\ y_2(k) &= \mathcal{Q}_2(k) + \mathcal{I}_2(k) + w_2(k) \end{aligned} \tag{2.1}$$

where $y_i$ is the received signal for user $i$ and $w_i$ is the additive white Gaussian noise with power spectral density $N_0$. $\mathcal{Q}_i(k)$ is the desired signal and $\mathcal{I}_i(k)$ is the interference at receiver $i$. The transmitted signal from user $i$ on channel $k$ is $x_i(k)$, which has an average power of $E_x = \mathcal{E}\{|x_i(k)|^2\} = 1$ for $i = 1, 2$ and $k = 1, \ldots, N$.

The desired signal from transmitter $i$ to receiver $i$ on channel $k$ is

$$\mathcal{Q}_i(k) = \sqrt{P_i(k)} h_{ii}(k) x_i(k) \tag{2.2}$$

with an average power $Q_i(k) = \mathcal{E}\{|\mathcal{Q}_i(k)|^2\} = P_i |h_{ii}(k)|^2$ where $P_i(k)$ is the transmit power allocated by user $i$ on channel $k$.

The interfering signal arriving from transmitter $j$ is

$$\mathcal{I}_i(k) = \sum_{j \neq i} \sqrt{P_j(k)} h_{ij}(k) x_j(k) \tag{2.3}$$

with an average power $I_i(k) = \mathcal{E}\{|\mathcal{I}_i(k)|^2\} = \sum_{j \neq i} P_j |h_{ij}(k)|^2$.

The complex channel response from the transmitter of user $j$ to the receiver of user $i$ is denoted $h_{ij}$. In this work, there are two users. For each realization, the direct path responses $h_{11}(k)$ and $h_{22}(k)$ are drawn independently from the complex normal distribution $\mathcal{CN}(0, 1)$ while the interfering path responses $h_{12}(k)$ and $h_{21}(k)$ are independent and distributed as $\mathcal{CN}(0, \beta)$, where $\beta$ is the cross-talk factor. It is also assumed that users have perfect channel state knowledge and that they are able to measure the levels of noise and interference.

The target performance for the frequency non-selective fading channel case is a SER of of $10^{-3}$.

### 2.2.1 Cross-talk $\beta$

Cross-talk $\beta$ is the factor representing the strength of interference between the two users due to the distance separating them (Figure 1.2). Increasing the value of $\beta$ means in this case that the two users get closer and have stronger interference effect while decreasing the value of $\beta$ has the reverse effect. The cross-talk $\beta$ is defined as:

$$\beta = \frac{\mathcal{E}\{|h_{ij}(k)|^2\}}{\mathcal{E}\{|h_{ii}(k)|^2\}} \tag{2.4}$$

The cross-talk $\beta$ considered in this thesis is $\beta \leqslant 1$. The main results in this thesis are obtained for $\beta = 0.1$. The effects of changing $\beta$ are discussed in Section 2.6.3 for the quasi-static flat Rayleigh fading case and in Section 3.6.1 for the frequency selective environment.

## 2.3 Waveforms

Two waveforms are considered in this thesis, the OFDM and the DSSS waveforms; these waveforms will be further discussed in Section 2.3 for the frequency non-selective case and in Section 3.1 for the frequency selective case. The OFDM and the DSSS waveforms are used typically in a frequency selective environment. It is noted that the frequency non-selective environment does not provide a realistic environment but it will prepare the stage for the frequency selective case presented in Chapter 3.

The OFDM waveform uses $U$ frequency tones on each spectrum sharing channel and the modulation level it will transmit on each of these channels is selected by the resource allocation algorithms discussed in Section 2.4. A simplified diagram of the OFDM transmission over the $N$ channels is shown in Figure 2.1. To avoid the requirement of continuous feedback of the channel conditions, the same power and data rate are allocated on all $U$ frequency tones of one channel.

The spreading factor for the DSSS waveform each on spectrum sharing channel [36] is selected by the resource allocation algorithms discussed in Section 2.4. A simplified diagram of the DSSS transmission over the $N$ channels is shown in Figure 2.2.

The OFDM and DSSS waveforms are used in two different scenarios in a frequency non-selective environment and then in a frequency selective environment. It is assumed that both users have perfect knowledge of the waveform used by the other user.

**Scenario A** will investigate the case of two different real signals adapted to their environment to maximize the rate - the OFDM user will choose to adaptively modify its modulation level while the DSSS user will choose adaptively its spreading factor.

**Scenario B** will consider the case where the users use the same signalling, OFDM, and both have the same strategy sets. Note that 'user' refers to the transmitter and receiver pair together.

As in [37], in scenario A the case where one user uses DSSS signalling, while the other uses OFDM is considered. However, in the current work, it is not assumed that a user is designated as a primary spectrum lessee but rather, the users compete for access to the spectrum.

User 1 transmits using OFDM and adjusts its modulation level depending on the received power of the desired signal $Q(k)$, the interference $I(k)$ and the noise $N_0$ that it measures

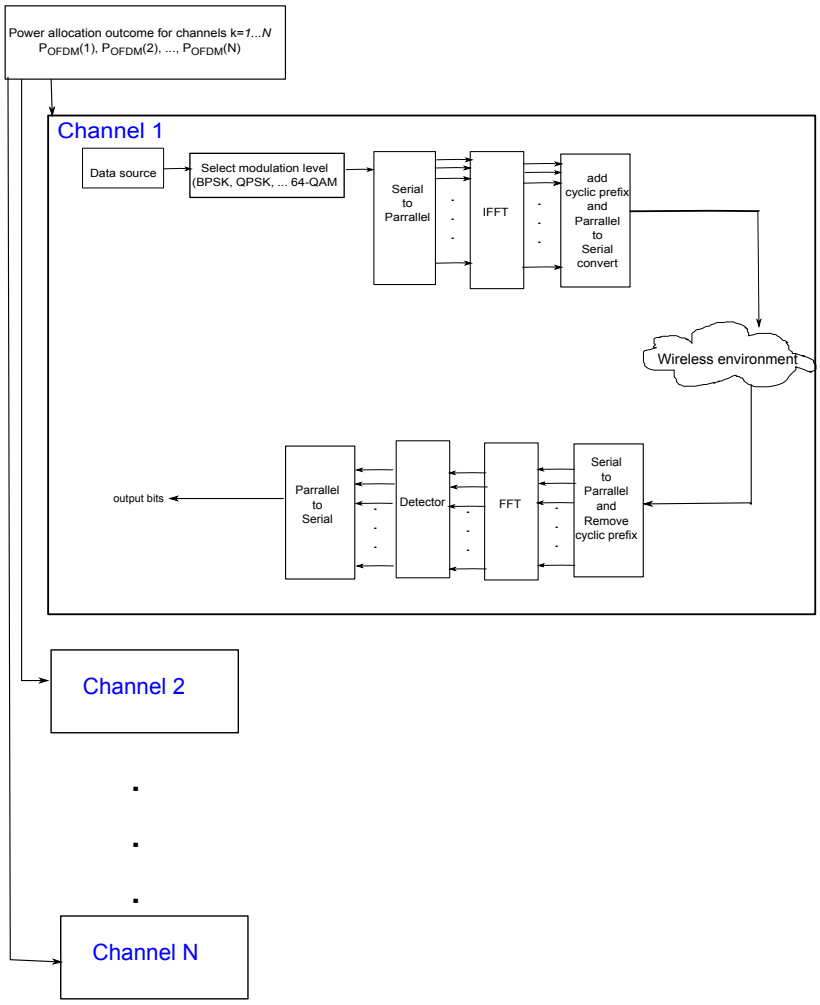


**Figure 2.1:** OFDM transmission over $N$ spectrum sharing channels.

on each of the $N = 3$ channels. The set of modulation level strategies is $R_1 = \{$BPSK, QPSK, 8-PSK, 16-QAM, 64-QAM$\}$. The OFDM signal has 200 frequency tones within the bandwidth $B_c$ and the ratio of the guard interval to the symbol duration is 0.184. The total symbol rate obtained is then $0.816B_c$ sps on each channel.

The second user uses DSSS signalling with BPSK on each channel [36] and its set of strategies is based on the spreading factor (SF): $R_2 = \{SF = 1, 3, 7, 15\}$. The spreading is achieved using a pseudo-random sequence, in this case, an m-sequence of order from 1 to 4. The DSSS signal is passed through a root raised-cosine filter with a rolloff factor of 0.22, giving a data rate of $0.82B_c/SF$ sps per channel.

In scenario B, both users use OFDM signalling and have the same set of strategies as explained for the OFDM user in scenario A. OFDM is typically used in the case where the

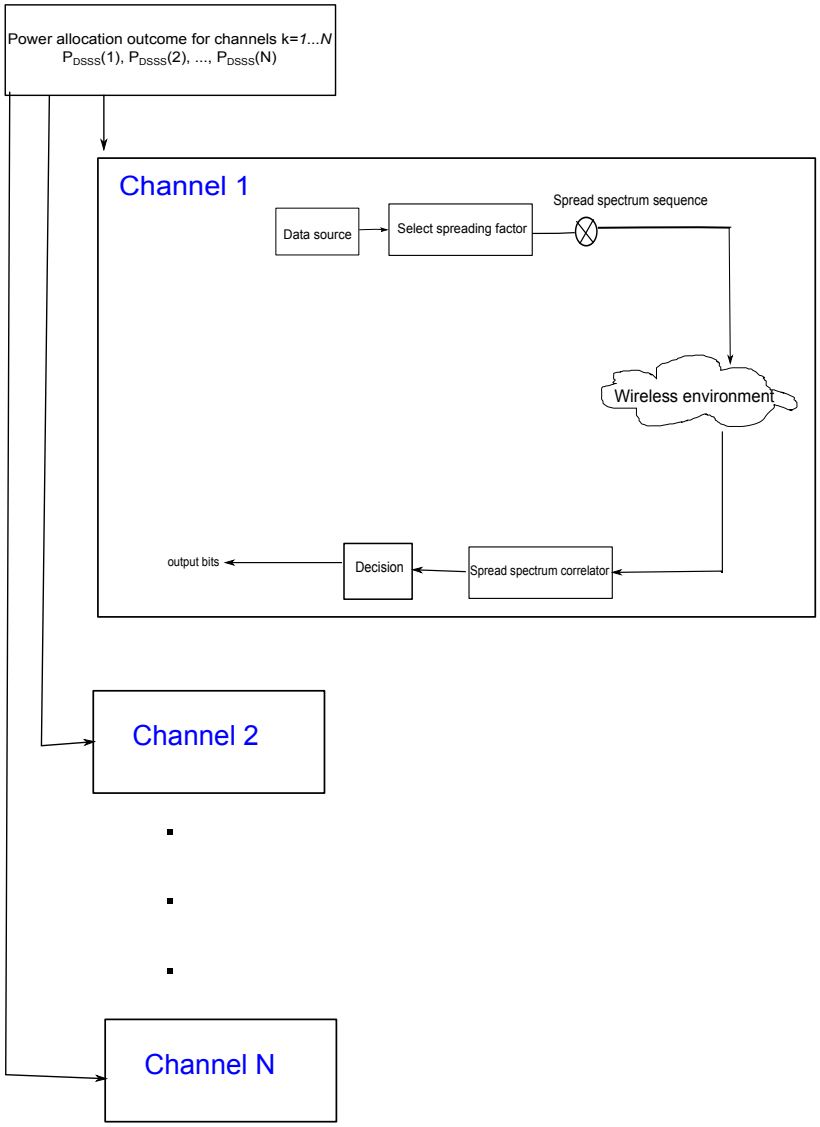


**Figure 2.2:** DSSS transmission over $N$ spectrum sharing channels.

user has only one tone per channel and maximizes its throughput by allocating power on the tones that offer the smallest channel attenuations [38]. However, in this thesis work, OFDM is thought of as a multicarrier OFDM modulation. In other words, OFDM has 200 frequency tones per channel. DSSS is also thought of as a multicarrier DSSS modulation [36] where independent DSSS signals are transmitted on each channel. Note that quasi-static flat-fading channels are considered in this chapter, even though both OFDM and DSSS are generally used for frequency selective fading channels. The flat-fading channel assumption reduces the number of parameters required in the simulations, which will more easily reveal the performance characteristics of the resource allocation algorithms. The work of this chapter

will serve as the basis for the analysis in Chapter 3, where frequency selective channels will be studied.

## 2.4 Allocation algorithms

In this section the algorithms used to allocate resources are described. The first is the well-known iterative water-filling algorithm. A second algorithm is proposed, which takes into account the characteristics of the real signal waveforms described in Section 2.3. This is a greedy algorithm which is designed to allocate the user's power in the most efficient way, such that the target symbol error rate (SER) is achieved.

### 2.4.1 Iterative water-filling power allocation algorithm

When the users do not cooperate, the iterative water-filling algorithm is commonly used to optimally allocate user power among the $N$ available channels. With this algorithm, the users will use the outcome of their utility functions, in this case, the Shannon capacity, to modify their transmission parameters (power, modulation scheme, coding, etc.) to maximize their sum rate [26].

The water-filling strategy has been long studied in the literature. Initially, the water-filling algorithm was designed for a single pair of transmitter-receiver trying to maximize the rate on multiple channels subject to a power constraint [39].

In [26], three types of water-filling are discussed: sequential, simultaneous and asynchronous. The least complex version of water-filling is the sequential algorithm where all users compete for the resource in a pre-defined order.

A sequential water-filling algorithm to distributively and optimally allocate the power for two users in the Gaussian frequency selective interference channel has been studied in [18] for the digital subscriber line. The users update their own information rates one after the other in a predefined order (this is an example of the Gauss-Seidel scheme). To update their information rate, each user performs the single-user water-filling solution sequentially according to the interference generated by the other users. The interference created by the other users is seen as additive (coloured) noise.

Although its low complexity and its distributed quality are appealing, a big disadvantage of this simplified version is that with increasing number of users, the convergence to a Nash

equilibrium tends to get very slow [26]. Another disadvantage for this water-filling version is that it requires a central scheduler to determine the order of updating strategies.

The simultaneous water-filling technique has been proposed where the users select their strategy at the same time. This is an example of a Jacobi scheme: the users update simultaneously their rate information with the single water-filling solution at each iteration based on the interference generated by the other users in the previous iteration. This version of water-filling resolves the slow convergence but it still requires some form of a central scheduler to synchronize the update timings. In a totally non-cooperative game, the requirement of a central scheduler should be removed since it does imply some form of cooperation.

The asynchronous water-filling algorithm resolves both the slow convergence and the requirement of central scheduler. In this water-filling version, each user still updates their strategy with the single water-filling solution but there is no order predefined. Some users can perform their updates more often than others. Furthermore, the users can update their strategies based on outdated information on interference caused by others. More information on this form of asynchronous principle involved in this version of water-filling can be found in [40].

The assumption that the channel information on the direct path impulse response is known at all users' receivers is often made in the literature [18, 22, 26, 40]. This assumption simplifies the scenarios and allows a reduction in the number of parameters to take into account while studying the behaviour of an algorithm. However, in real systems, perfect knowledge of the channel impulse is not possible as noise will always corrupt the estimate. Moreover, the channel state information (CSI) received would have to be computed instantaneously to ensure an up-to-date equalization. Delays and modification of the CSI packets are expected in wireless communication. Therefore systems require some level of robustness to this kind of error to ensure a similar performance from a perfectly known environment to degraded conditions. Robust iterative water-filling has been explored in [25] to allow imperfect CSI at both receivers on the direct path channel impulse of the interference channel.

Since in this thesis, there are only two users competing for their share of the spectrum, there is no issue with the convergence being slow. It is also not a large issue for central scheduling: in this case it could be pre-defined in the protocol that both parties must agree to before starting the game. Furthermore, the assumption of perfect channel state information is made to reduce the complexity of the studied problem and to get a better insight from

the presented results. Because of these assumptions, the sequential version of water-filling has been chosen for the purpose of this thesis and there is no requirement for a robust form of water-filling.

Assuming Gaussian distributed signals, the maximum achievable rate for user $i$ on channel $k$ is given by the Shannon capacity

$$R_i(k) = \log_2 (1 + \Upsilon_i(k)) \tag{2.5}$$

and the maximum sum rate for user $i$ is

$$R_i = \sum_{k=1}^{N} \log_2 (1 + \Upsilon_i(k)) \tag{2.6}$$

where the SINR $\Upsilon_i(k)$ is defined as

$$\Upsilon_i(k) \triangleq \frac{Q_i(k)}{N_0 B_c + I_i(k)} \tag{2.7}$$

where $N_0$ is the power spectral density over the channel bandwidth $B_c$ Hz.

According to [26], to obtain a Nash equilibrium the water-filling solution profile of one user must satisfy the water-filling solution of the other user. The water-filling power allocation for user $i$ on channel $k$ is then

$$P_i^{WF}(k) \triangleq \left( \mu_i - \frac{N_0 B_c + I_i(k)}{|h_{ii}(k)|^2} \right)^+ \tag{2.8}$$

where $\mu_i$ is the water-filling level that satisfies $\sum_{k=1}^{N} P_i^{WF}(k) = P_{tot}$, and $(a)^+ = \max(0, a)$. From the transmit powers found in (2.8), the received power for user $i$ on channel $k$ is calculated as $Q_i(k) = P_i(k)|h_{ii}(k)|^2$ and the interference power is $I_i(k) = \sum_{j \neq i} P_j(k)|h_{ij}(k)|^2$.

The water-filling algorithm for allocating resources is summarized as follows:

1. Initialization: set transmit powers $P_i^{WF}(k) = 1/N \cdot \ P_{tot}$

2. Iterations: repeat $N_{it}$ times

   (a) for user 1, compute the interference power $I_1(k)$ on each channel for $k = 1, ...N$

   (b) sort channels in increasing order by their level of received interference plus noise

   (c) initialize $R_{1,max} = 0$

   (d) repeat until convergence:
   for $k = N : -1 : 1$ do:

i. compute waterfill level $\mu$ for channels $1, \ldots, k$

ii. set $P_{1,temp}^{WF}(n) = 0$ for $n = k+1, \ldots, N$

iii. compute $P_{1,temp}^{WF}(n)$ from (2.8)

iv. compute received power $Q_{1,temp}(n)$ for $n = 1, \ldots, k$

v. compute rate $R_{1,temp}$ from $Q_{1,temp}(n)$ using (2.6) for $n = 1, \ldots, k$

vi. if $R_{1,temp} > R_{1,max}$

- $R_{1,max} = R_{1,temp}$
- $P_1^{WF}(n) = P_{1,temp}^{WF}(n)$ for $n = 1, \ldots, N$

(e) for user 2, compute the interference power $I_2(k)$ on each channel for $k = 1, \ldots, N$

(f) repeat steps (b), (c), (d) for user 2

3. End

Then the maximum achievable rates using real signals can be found from the lookup tables which will be discussed in Section 2.5.

### 2.4.2 Iterative greedy power allocation algorithm

Most of the literature on game theory for spectrum sharing uses the Shannon capacity as a utility function [18, 25, 26, 39–41]. This necessitates that the following two assumptions are made: Gaussian signalling and long codebooks (infinite length sequence of data information) [6]. Gaussian signalling refers to the fact that theoretically the signal could take on an indefinitely large number of different voltage levels, with each of them having a different meaning. To account for finite-order constellations, the gap approximation has been proposed to deal with reduced rate expectations [26]. However, it was shown in the case of multicarrier transmission that the water-filling solution is not optimal for realistic considerations such as these [19]. In fact, the power allocation obtained using water-filling does not maximize the data rate. As an alternative, a greedy algorithm was used in [19] using a utility function that favours allocating transmit power on tones where it can increase the rate in the most power efficient way.

A similar approach for the utility function in the spectrum sharing context was proposed in [22], in which the authors consider coding with Gaussian signalling. The utility function used in [22] will select a channel on which the receiver would achieve the greatest signal

to interference ratio. In this thesis, the suitability of the water-filling utility function is investigated for non-Gaussian signalling signals.

For non-Gaussian signalling, an iterative greedy algorithm, which aims to find a global optimal solution by making locally optimal decisions, has been developed in this work. The power allocation starts with zero power on every channel and then calculates which channel will require the least transmit power to increase its data rate by one step in the rate strategy set. The greedy algorithm continues in this manner until all the total power for the user has been allocated to the $N$ channels or until no more improvement can be made to the data rate on all channels.

The greedy algorithm for allocating resources for real signals is summarized as follows:

1. Initialization:
   (a) set transmit powers $P_i^{Gr}(k) = 0$ and rate strategies $R_i(k) = 0$, for $i = 1, 2$, $k = 1, .., N$
   (b) set remaining available power $P_{rem} = P_{tot}$
2. Iterations: repeat $N_{it}$ times
   (a) for user 1, compute interference power $I_1(k)$ on each channel
   (b) initialize $P_1^{Gr}(k) = 0$, $R_1(k) = 0$, $k = 1, .., N$
   (c) repeat until convergence:
      i. find $\Delta Q(k)$, increase in received power required to support increasing rate strategy by one on channel $k$, $k = 1, .., N$, to achieve given SER, using look-up table
      ii. compute $\Delta P(k)$, increase in transmit power required to support increasing rate strategy by one on channel $k$, $k = 1, .., N$
      iii. find $\tilde{k} = \arg\min_k \Delta P(k)$
      iv. if $\Delta P(\tilde{k}) < P_{rem}$:
         - increase rate strategy on channel $\tilde{k}$: $R_1(\tilde{k}) = R_1(\tilde{k}) + 1$
         - increase transmit power on channel $\tilde{k}$: $P_1^{Gr}(\tilde{k}) = P_1^{Gr}(\tilde{k}) + \Delta P(\tilde{k})$

- set $P_{rem} = P_{rem} - \Delta P(\tilde{k})$

(d) for user 2, compute interference $I_2(k)$ on each channel

(e) repeat step (b) and (c) for user 2

3. End

Simulations show that convergence for the greedy algorithm is typically achieved in six to eight iterations. For the simulation results presented here, the number of iterations for the competitive games has been chosen as $N_{it} = 8$. While the water-filling solution will reach a Nash equilibrium [26], the greedy algorithm may not, in which case the allocations will alternate between two different solutions until the maximum number of iterations has been reached. A flow-chart of how the simulations were performed in Matlab for the power resource allocation problem studied in this thesis is shown in Appendix A.

## 2.5 Symbol error rate

For scenario A, Monte Carlo simulations were performed for every modulation level strategy for the OFDM signal, to determine the received power required to achieve a SER of $10^{-3}$ or better in an AWGN channel over a range of interference levels created by the DSSS signal. The same Monte Carlo simulations were performed for every spread factor strategy for the DSSS signal with an OFDM interferer. A flow-chart on how the simulations were performed in Matlab is shown and described in Appendix A.

The same Monte Carlo simulations were done for scenario B with an OFDM signal with an OFDM interferer. These results were used to generate the lookup tables required in the implementation of the algorithms described in Section 2.4 to determine the real rate obtained with the power allocation for each user on each channel. Figures of the required received power for a specific level of interference power are shown in Appendix B. The lookup tables used in this thesis are given in Appendix B.

### 2.5.1 OFDM SER with a DSSS interferer

The BPSK OFDM user with a $SF = 3$ BPSK DSSS interferer SER curves for selected signal-to-interference ratio (SIR) obtained in the simulations are shown in Figure 2.3. The

selected SIRs shown in Figure 2.3 are 5 dB, 6 dB, 7 dB, 7.5 dB, 8.5 dB, 9 dB, 9.5 dB, 10 dB, 10.4 dB, 10.8 dB, 11 dB and 11.5 dB. Note that these simulations were done for each OFDM constellation with the same $SF = 3$ BPSK DSSS interferer. From these results, SIRs were obtained for the lookup table shown in Figure B.1. The performance may change slightly for other DSSS spreading factors due to the repeated spreading sequence, however, simulations suggest that theses differences are quite small, as demonstrated in Figure 2.4. Therefore in this work, the interference effects of all spreading sequences are assumed to be equal.

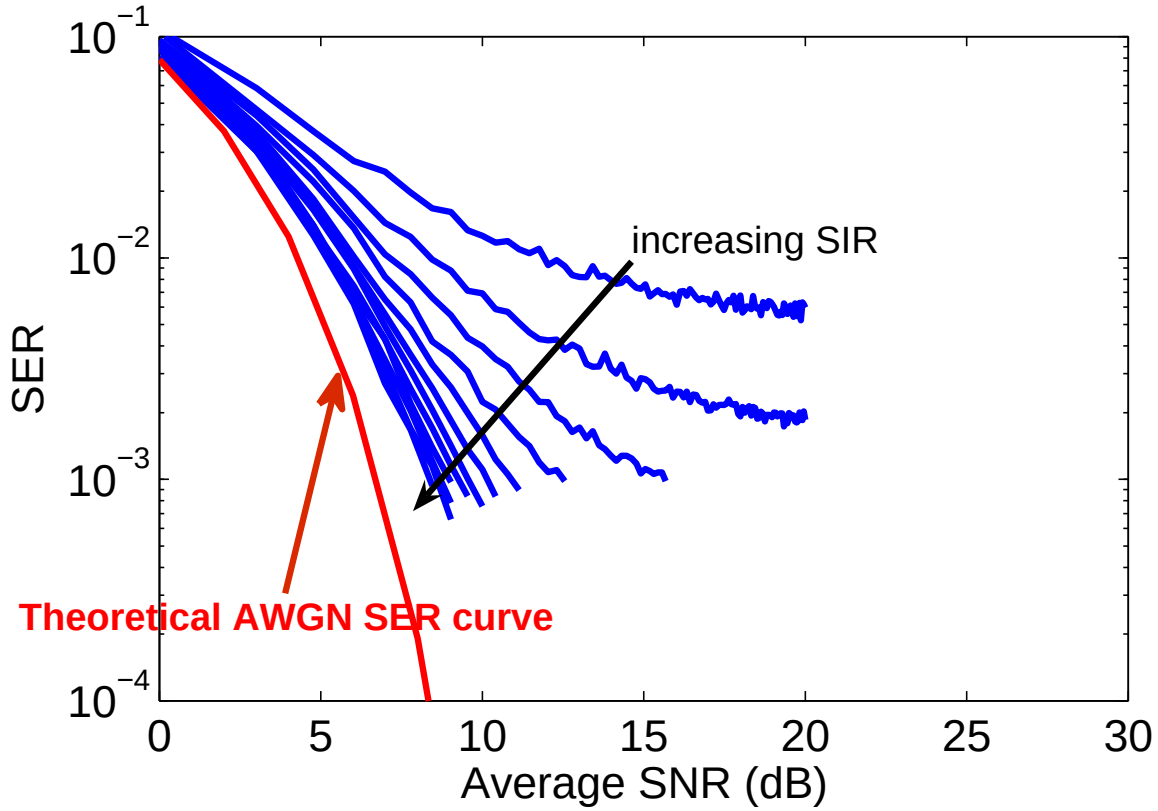


**Figure 2.3:** SER curves for the BPSK OFDM user with BPSK $SF = 3$ DSSS interference in AWGN channel. The selected SIRs shown in this figure are 5 dB, 6 dB, 7 dB, 7.5 dB, 8.5 dB, 9 dB, 9.5 dB, 10 dB, 10.4 dB, 10.8 dB, 11 dB and 11.5 dB.

### 2.5.2 DSSS SER with OFDM interferer

The SER curves for a BPSK $SF = 3$ DSSS user with a BPSK OFDM interferer obtained in the simulations are shown in Figure 2.5. The selected SIRs shown in Figure 2.5 are 0 dB,

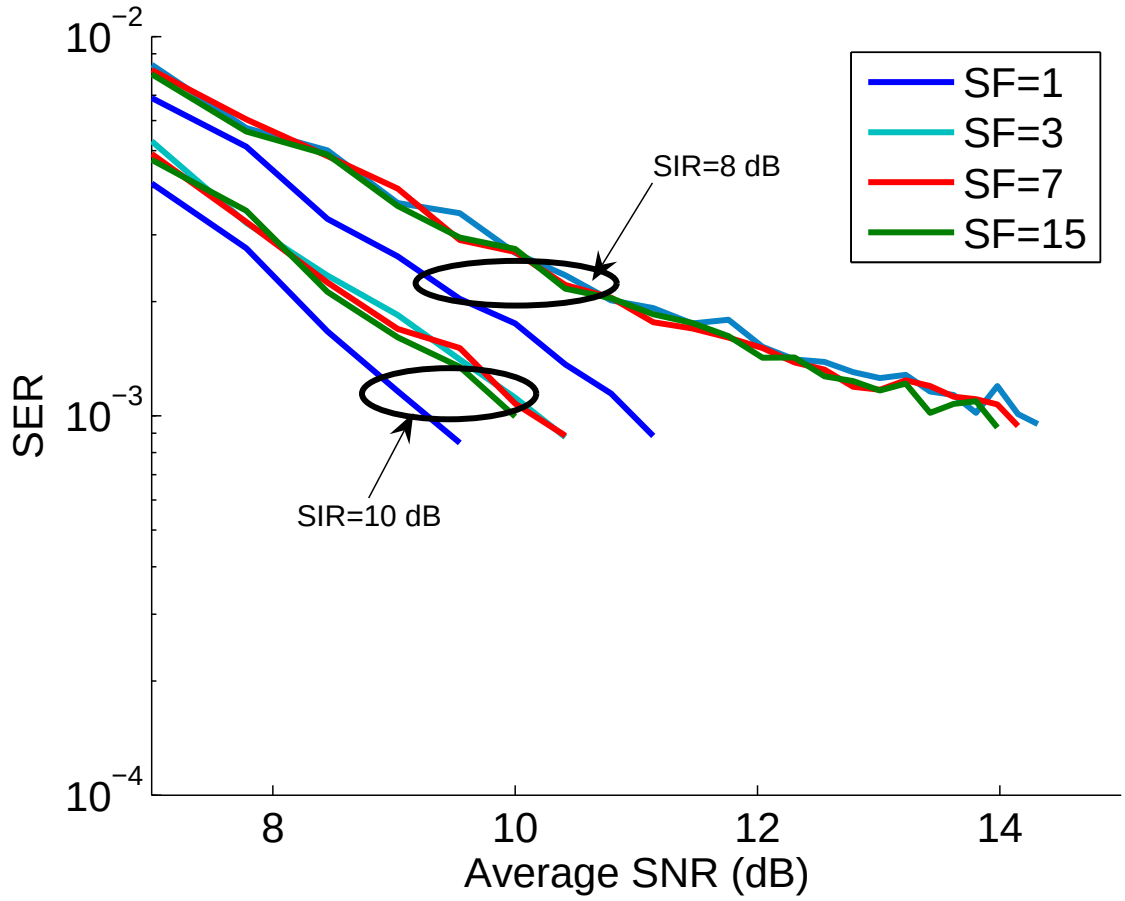


**Figure 2.4:** SER curves for the BPSK OFDM user with different spreading factor BPSK DSSS interferer in AWGN channel.

3 dB, 5 dB, and 6 dB. Note that these simulations were done for each BPSK DSSS spreading factor with the same BPSK OFDM interferer. From these results, SIRs were obtained for the lookup table shown in Figure B.3. The performance may change slightly for other OFDM constellations due to the OFDM constellation mapping, however, simulations suggest that these difference are quite small (Figure 2.6, where simulations were done for SIRs= 3 dB, 7 dB and 10 dB). Therefore in this work, the interference effects of all OFDM constellations are assumed to be equal.

### 2.5.3 OFDM SER with an OFDM interferer

The BPSK OFDM user with a BPSK OFDM interferer SER curves for selected SIR obtained in the simulations are shown in Figure 2.7. The SIRs selected for Figure 2.7 are 5 dB, 6 dB,

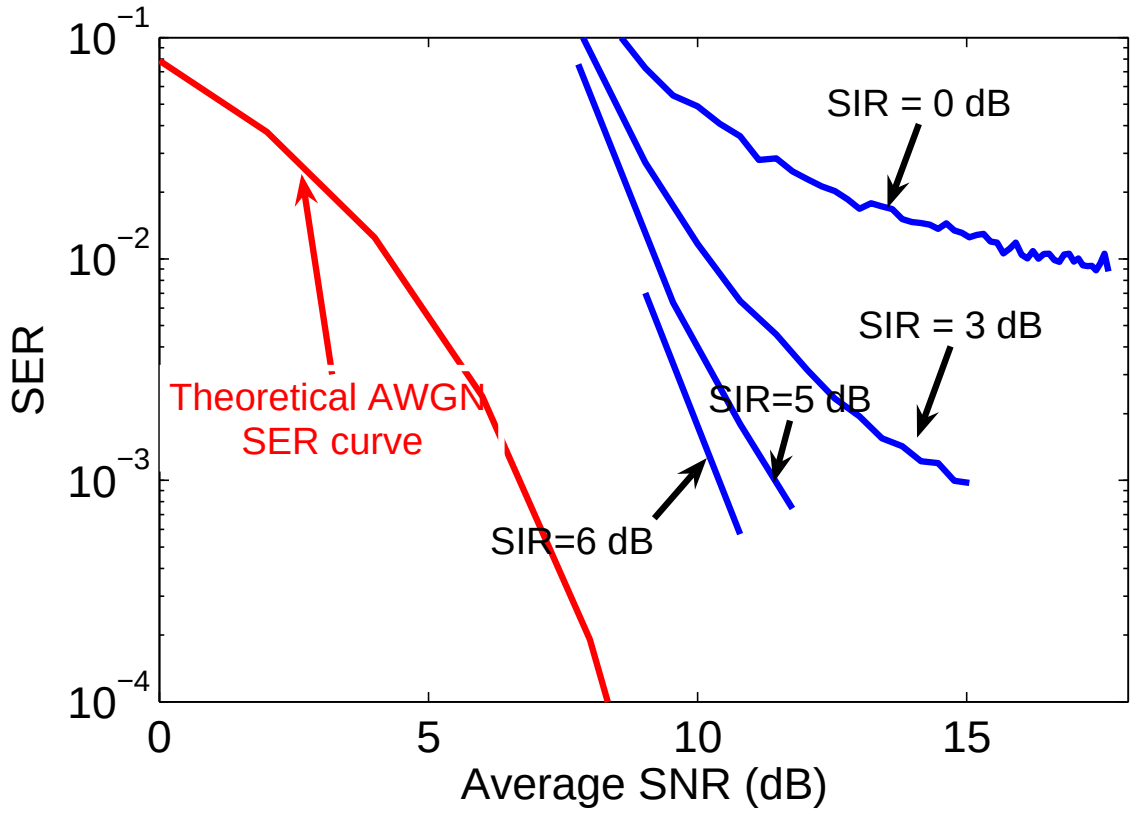


**Figure 2.5:** SER curves for the BPSK DSSS $SF = 3$ user with BPSK OFDM interferer in AWGN channel. The selected SIRs shown in this figure are 0 dB, 3 dB, 5 dB, and 6 dB.

7 dB, 7.5 dB, 8.5 dB, 9 dB, 9.5 dB, 10 dB, 10.4 dB, 10.8 dB, 11 dB and 11.5 dB. Again, the simulations for the lookup table have been done for every OFDM constellation with the same BPSK OFDM interferer, making the same assumption that the interference created by all OFDM constellations are equal based on simulations results presented in Figure 2.8. From these results SIRs were obtained for the lookup table shown in Figure B.5.

## 2.6 Results

For both scenarios, the power allocation solution can be defined as the outcome of a game theoretical problem. The users' strategies are the amounts of transmit power they allocate on each channel and their rewards are the rates at the target SER that they achieve at the end of the game.

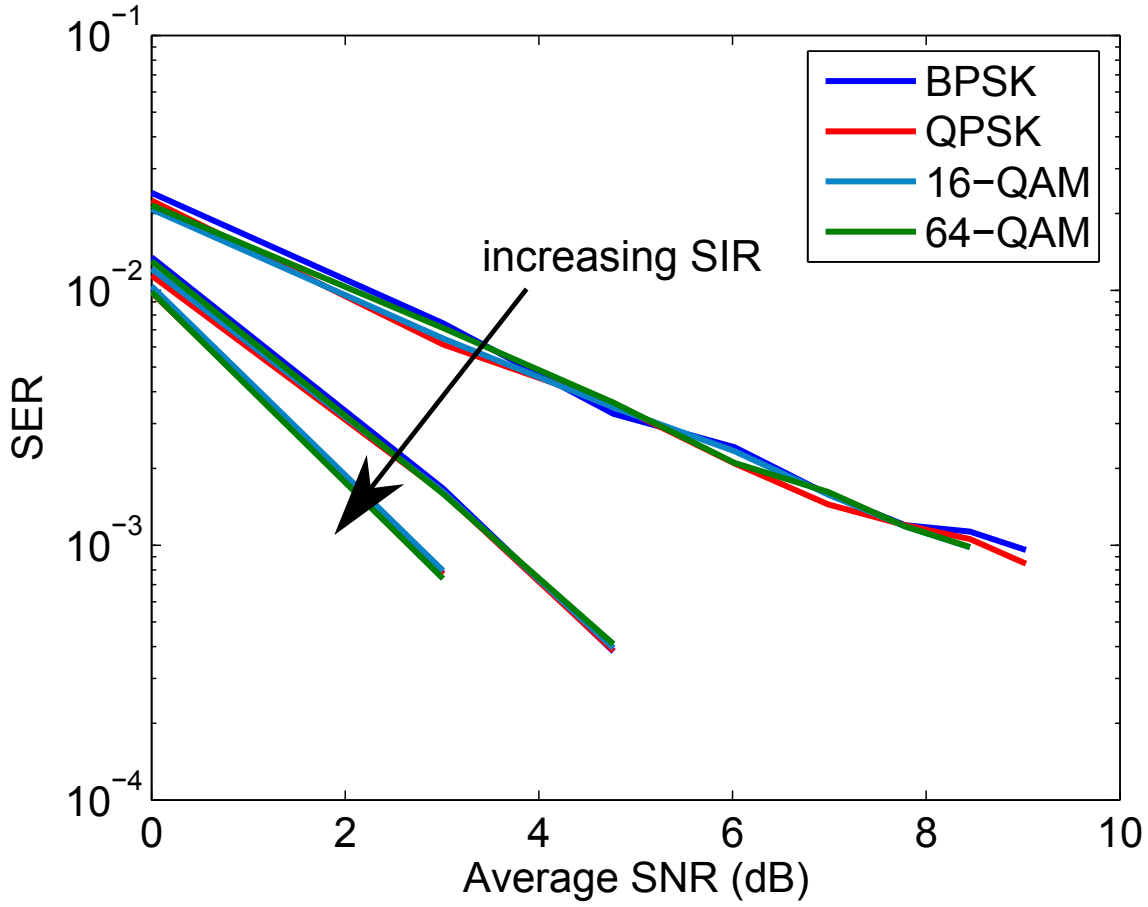


**Figure 2.6:** SER curves for the BPSK $SF = 3$ DSSS user with different constellations OFDM interference in AWGN channel. The selected SIRs shown in this figure are 3 dB, 7 dB and 10 dB.

### 2.6.1 Scenario A - Coexistence of DSSS and OFDM users

The resource allocation algorithms described in Section 2.4 have been applied to scenario A given in Section 2.3 for two users and three quasi-static frequency non-selective Rayleigh fading channels, for 10,000 different channel realizations at each SNR. The cross-talk factor was $\beta = 0.1$.

The Shannon capacity, in bits/s/Hz, given by (2.5), was computed based on the typical assumption that the transmitted signals are Gaussian distributed. This is shown in Figure 2.9, along with the rates obtained for real signals using the water-filling and greedy algorithms to allocate resources.

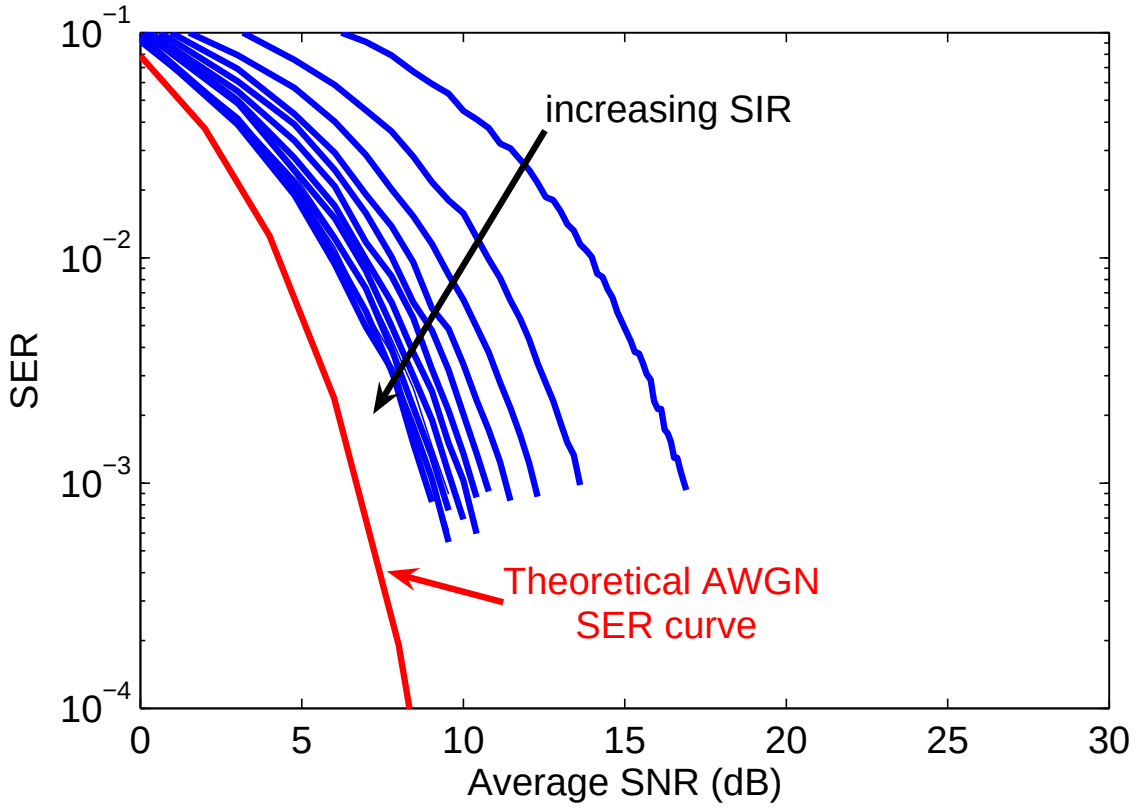


**Figure 2.7:** SER curves for the BPSK OFDM user with BPSK OFDM interference in AWGN channel. The selected SIRs shown in this figure are 5 dB, 6 dB, 7 dB, 7.5 dB, 8.5 dB, 9 dB, 9.5 dB, 10 dB, 10.4 dB, 10.8 dB, 11 dB and 11.5 dB.

The most notable observation from Figure 2.9 is that both algorithms are not close to the Shannon capacity. In fact, the OFDM user, which obtained higher rates compared to both DSSS users for SNRs exceeding 10 dB, achieved less than half the rate predicted by the Shannon capacity formula. This is expected as the assumption of Gaussian signalling and long codewords is not met.

The second noticeable observation is that the water-filling algorithm does not provide the optimal resource allocation for the real signals. The greedy algorithm, although not necessarily optimal, achieves a higher sum rate for both users over the whole SNR range.

Both users reach a plateau when the SNR is high enough: for the DSSS user this occurs at about 20 dB, while for OFDM it is in excess of 30 dB for the greedy algorithm and at about 25 dB for the water-filling algorithm. This is explained by the set of data rate strategies for each user: the set of strategies for the OFDM user includes modulation up to

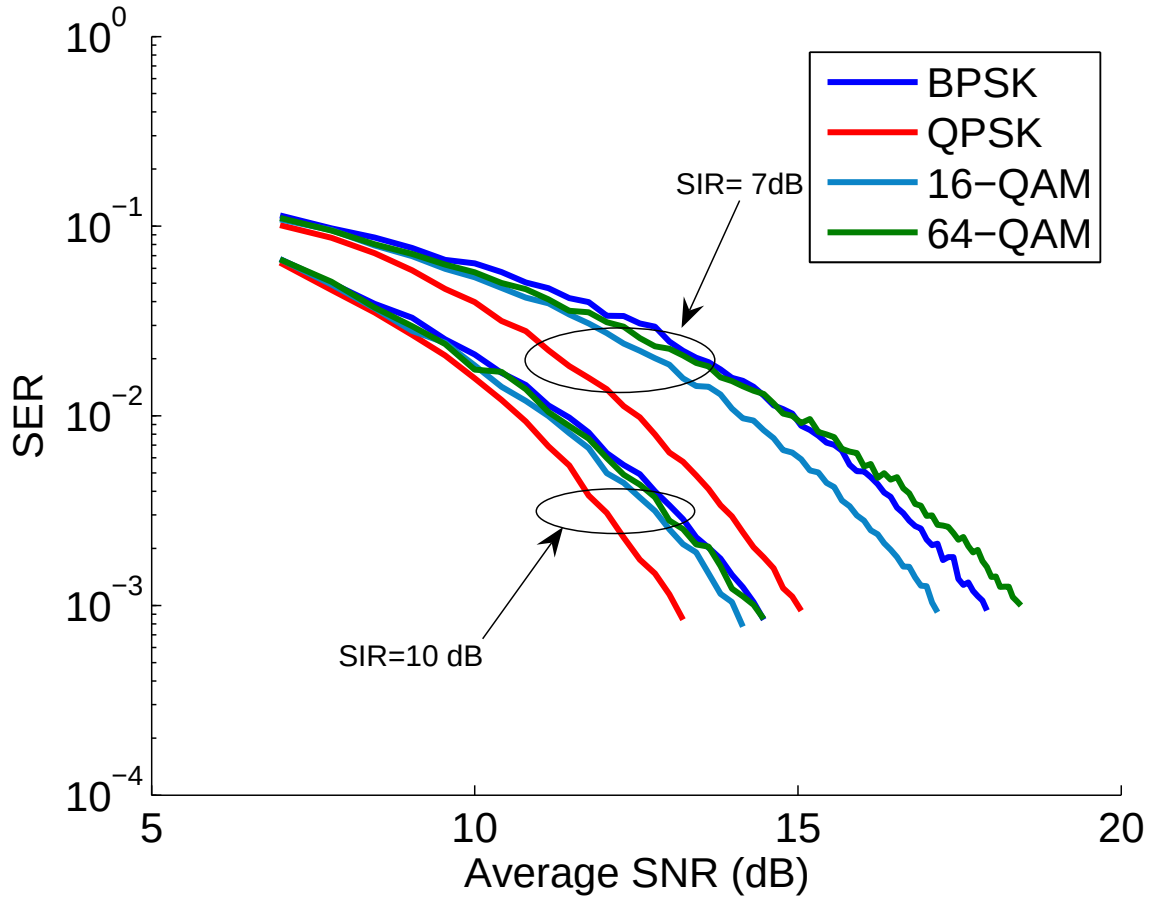


**Figure 2.8:** SER curves for the QPSK OFDM user with different contellations OFDM interferer in AWGN channel.

64-QAM, giving a maximum data rate of $6 \cdot (0.816)B_c$ sps per channel, whereas the DSSS user is limited to a maximum of BPSK on each channel, with the strategy $SF = 1$, for a maximum data rate of $0.82B_c$ sps per channel. At low average SNR, both solutions for DSSS have a higher rate than for OFDM since DSSS is more robust to interference.

In the literature, there is a discussion of the use of SNR gaps to predict the outcome of a constellation at a certain SNR while using the outcome of the Shannon capacity formula as in [26]. For example, in Figure 2.9 at average SNR 10 dB, the Shannon capacity predicts a rate of 2 bits/s/Hz. However OFDM users for both algorithms achieve only 0.5 bit/s/Hz for the same average SNR. Both algorithms achieve 2 bits/s/Hz at an average SNR of 25 dB which is 15 dB higher than predicted by Shannon capacity. Therefore, the SNR gap would be used to scale down the Shannon capacity prediction to reflect more realistically the system

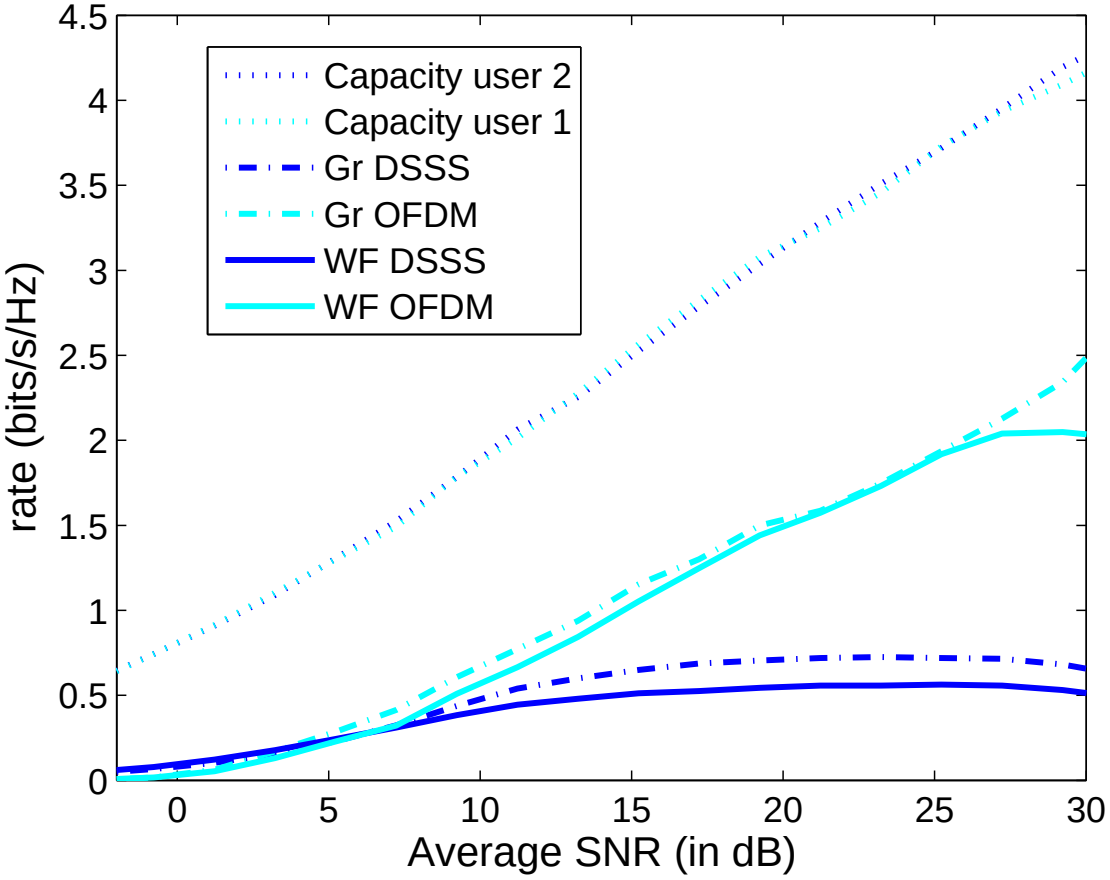


**Figure 2.9:** Rates for different resource allocation algorithms, scenario A.

outcome at that average SNR or to provide the actual average SNR required by the system to achieve the predicted rate. Up until average SNR 30 dB, an SNR gap can be estimated for the water-filling OFDM at approximately 15 dB. However, at higher average SNR, it is seen that the SNR gap would not be of any use since the rates achieved at that point start to reach a plateau due to the system limitation. The same observation on the SNR gap can be made for the greedy OFDM, but this time, the SNR gap could be used up to an average SNR above 30 dB. For the DSSS users, it is observed that SNR gaps cannot be estimated due to the limitation of the BPSK modulation, even though the rate strategy includes different spreading factors.

The distribution of rates achieved over 10,000 Rayleigh-distributed frequency non-selective channel realizations is shown in Figure 2.10 for an average SNR of 13 dB. The limitation of the set of rate strategies is clear, as the maximum sum rate achievable for DSSS is $R_i = 1$.

Thus, while the variance of the OFDM rates increases with average SNR in operational range, the variance of the DSSS rates is limited.

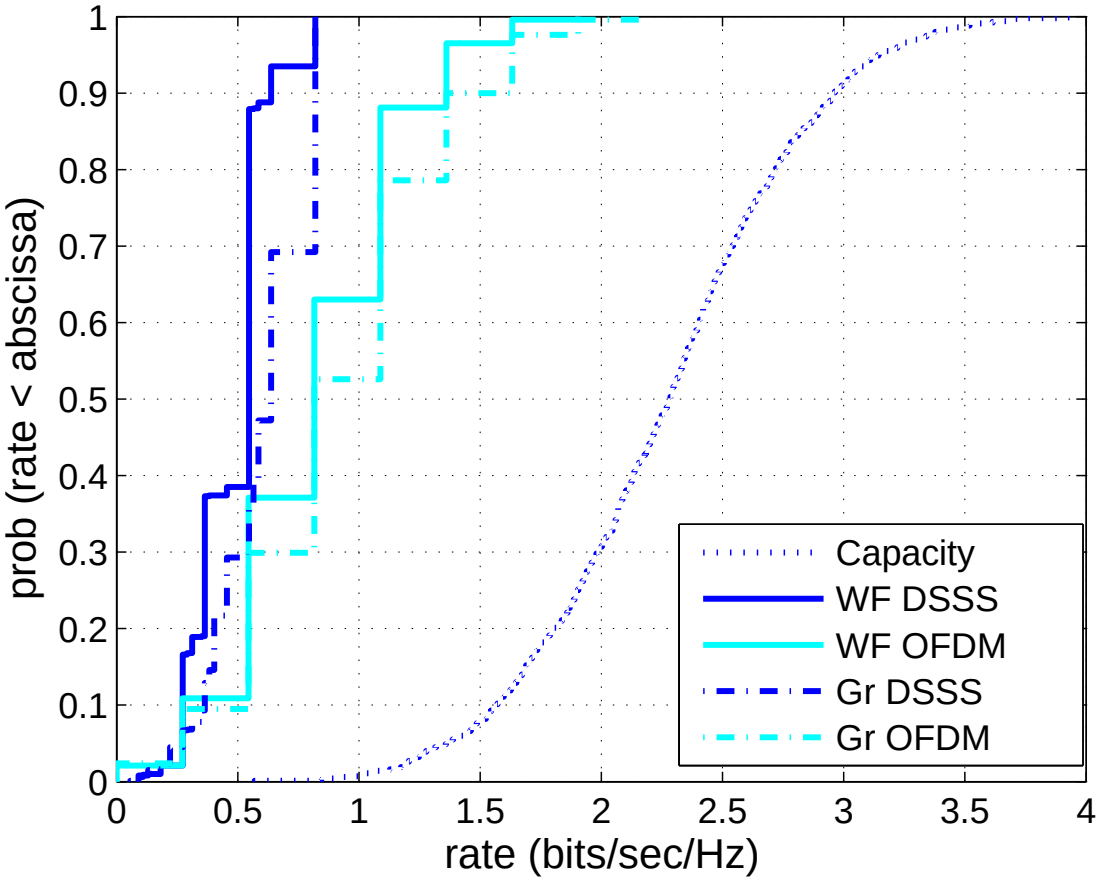


**Figure 2.10:** Cumulative frequency distribution of rates at 13 dB, scenario A.

To get further insight into the behaviour of both algorithms and to understand the impact of their strategies, two games for a specific channel realization at an average SNR of 13 dB are considered. The squared absolute channel coefficients for both users are given in Table 2.1, where the OFDM user is denoted as user 1.

Figure 2.11 shows the power allocation for the two algorithms for this channel realization and an average SNR of 13 dB. The overall bar height shows the total power allocated by the user on each channel. In Figure 2.11(a) and (b), the dark colour shows the required power to get the rate on every channel shown in the corresponding panels in Figure 2.12. The pale colour shows how much of the allocated power on each channel is wasted, i.e., over the required minimum for the rate it achieves at the target SER.

**Table 2.1:** Squared absolute channel coefficients for resource allocation example.

| | $k=1$ | $k=2$ | $k=3$ |
|---|---|---|---|
| $\|h_{11}(k)\|^2$ | 0.57 | 5.26 | 1.37 |
| $\|h_{12}(k)\|^2$ | 0.14 | 0.004 | 0.13 |
| $\|h_{22}(k)\|^2$ | 1.4 | 0.4 | 2.46 |
| $\|h_{21}(k)\|^2$ | 0.03 | 0.12 | 0.03 |

As the average SNR increases, more power is wasted, therefore more interference is created to the other user which in turn needs more power to counter the interference. Thus, the users do themselves mutual harm. Furthermore, with this kind of behaviour, other nearby users are prevented from taking advantage of the same bandwidth. This contradicts the aim of maximizing spectral usage.

It was shown in [42] that for two users, when the interference levels are high, the maximum sum-rate cannot be achieved unless at most one channel is shared. This effect can be observed in Figure 2.11(a) and (b) where only one channel is shared in the case of the water-filling algorithm. The same behaviour does occur for the greedy algorithm, but it is observed that the level of cross-talk required is much higher in the greedy case. Although the sum rates achieved in this example are relatively high for both algorithms, the behaviour observed is typical of most realizations.

As noted previously, the greedy algorithm allocates only the minimal power to achieve each rate strategy. Therefore, there is unused power, $P_{rem}$, at the end of the game. In this example, 3.8 % of the total power remains for the OFDM user, and 7.5 % for the DSSS user. In Figure 2.11, it can be seen that less transmit power is allocated to channel 3 by both greedy users compared to both water-filling users, but the greedy OFDM user still achieves a higher rate compared to the water-filling case on that channel, as shown in Figure 2.12. This is again explained by the fact that having more power on a channel creates a higher interference for the other user which consequently must increase its own power to get a specific rate.

Figure 2.13 shows the percentages of total available power that are wasted or unused. For the greedy case, only a small percentage of power for the OFDM user is wasted at

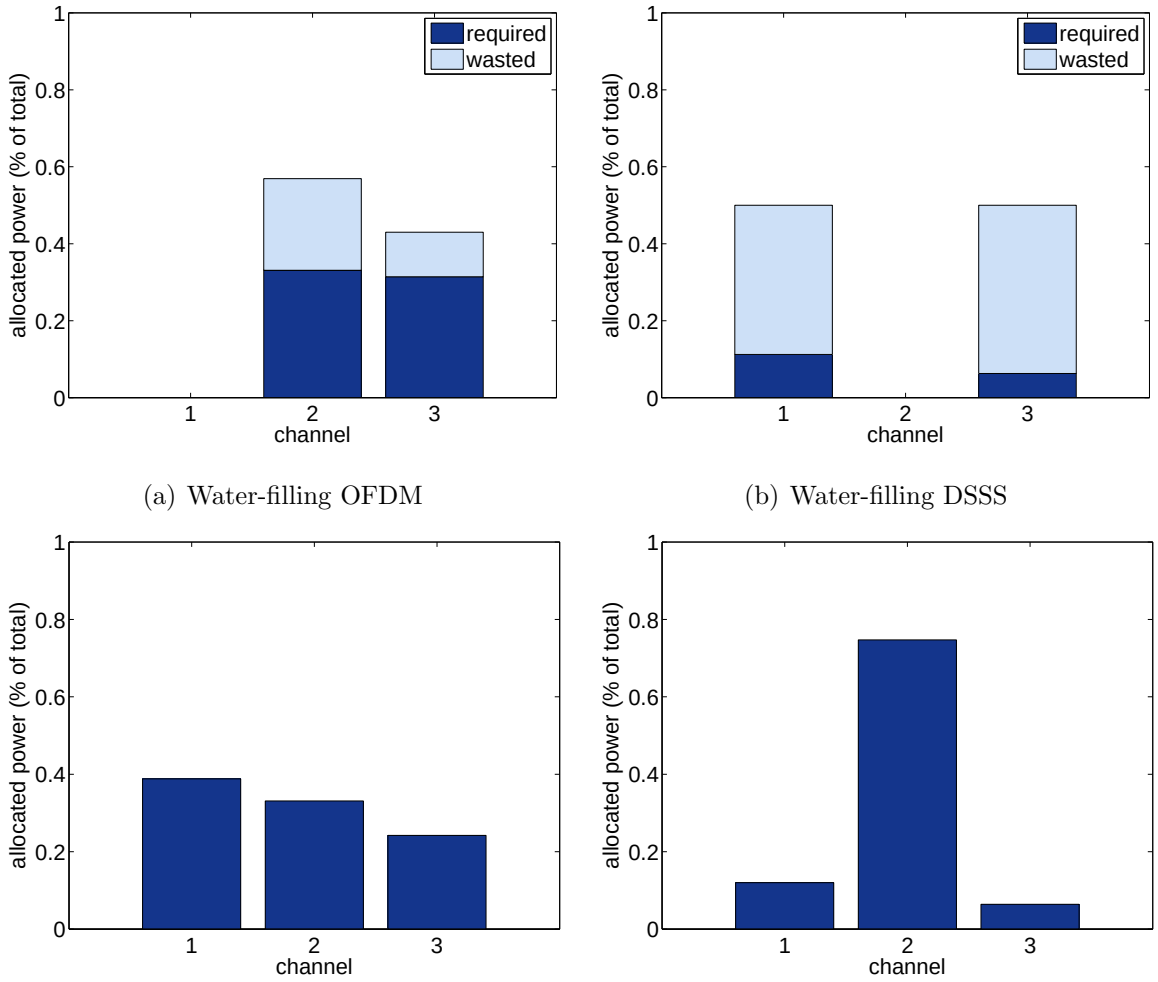


(a) Water-filling OFDM

(b) Water-filling DSSS

(c) Greedy OFDM

(d) Greedy DSSS

**Figure 2.11:** Power allocated to each channel at average SNR 13 dB, scenario A example.

SNRs above 10 dB while the DSSS user has no wasted power. This is due to the fact that the greedy DSSS user makes the last move in this game. As explained in Section 2.4.2, the greedy algorithm does not always reach an equilibrium. Therefore, the greedy DSSS user may change its power allocation at the last iteration based on the last observed power allocation of the greedy OFDM user, while the OFDM user based its power allocation on the interference level of the previous iteration. If the OFDM user were last, the DSSS user might have some wasted power while the OFDM user would have none. Simulations showed that the total power wasted is similar, regardless of the order of the users.

The percentage of power wasted for the greedy algorithm increases with SNR because

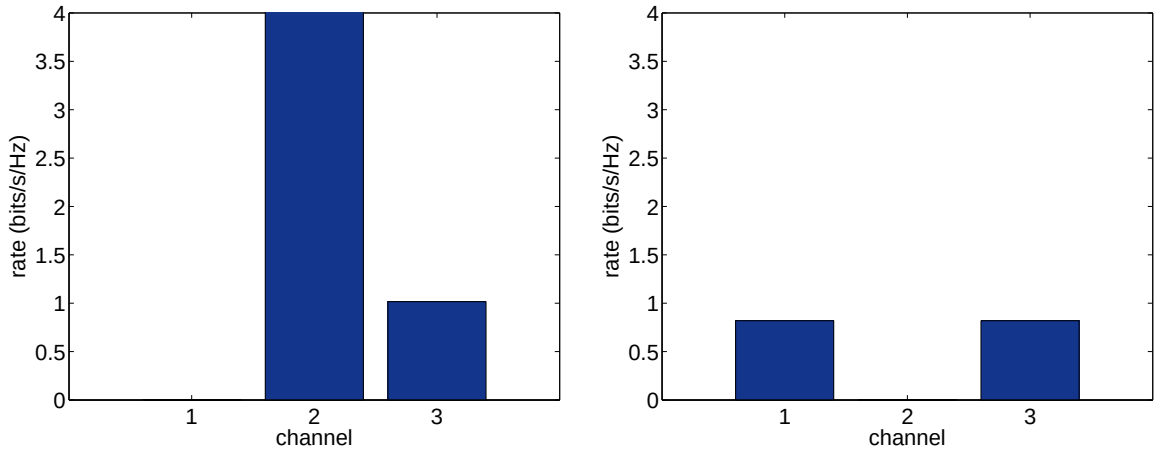


(a) Water-filling OFDM




(b) Water-filling DSSS

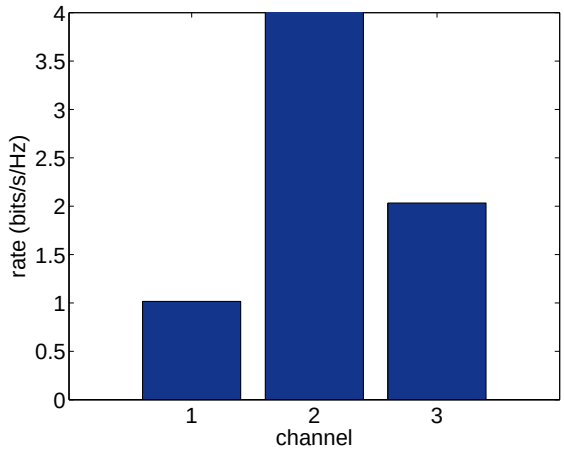


(c) Greedy OFDM

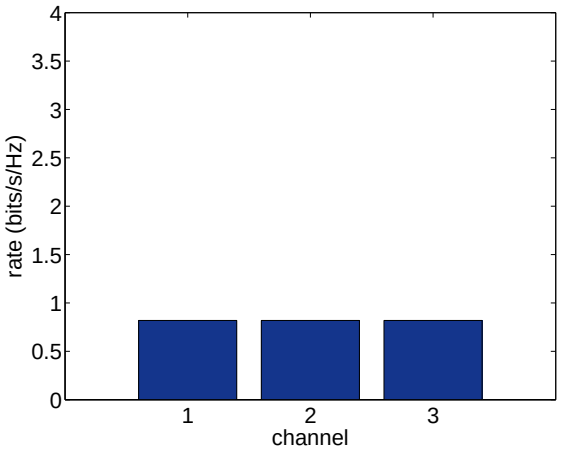


(d) Greedy DSSS

**Figure 2.12:** Rate on each channel at average SNR 13 dB, scenario A example.

interference begins to dominate the noise. The actual wasted power remains constant after reaching a peak at around 30 dB, resulting in a decreasing percentage.

It can be seen that for the greedy case, the unused power, $P_{rem}$, decreases as the average SNR increases, and then increases again at high SNR. For the DSSS user, this is explained by the fact that at low average SNR, the greedy OFDM does not allocate any power because it cannot achieve the target SER even at the lowest rate strategy, hence the DSSS user is, on average, dealing only with noise and not interference. For the OFDM user, a similar effect occurs at higher SNR when the DSSS user has achieved its maximum rate, with $SF = 1$ being selected in most realizations. At this point, the interference experienced by the OFDM user remains unchanged, hence a decreasing percentage of total power is required to combat

it.

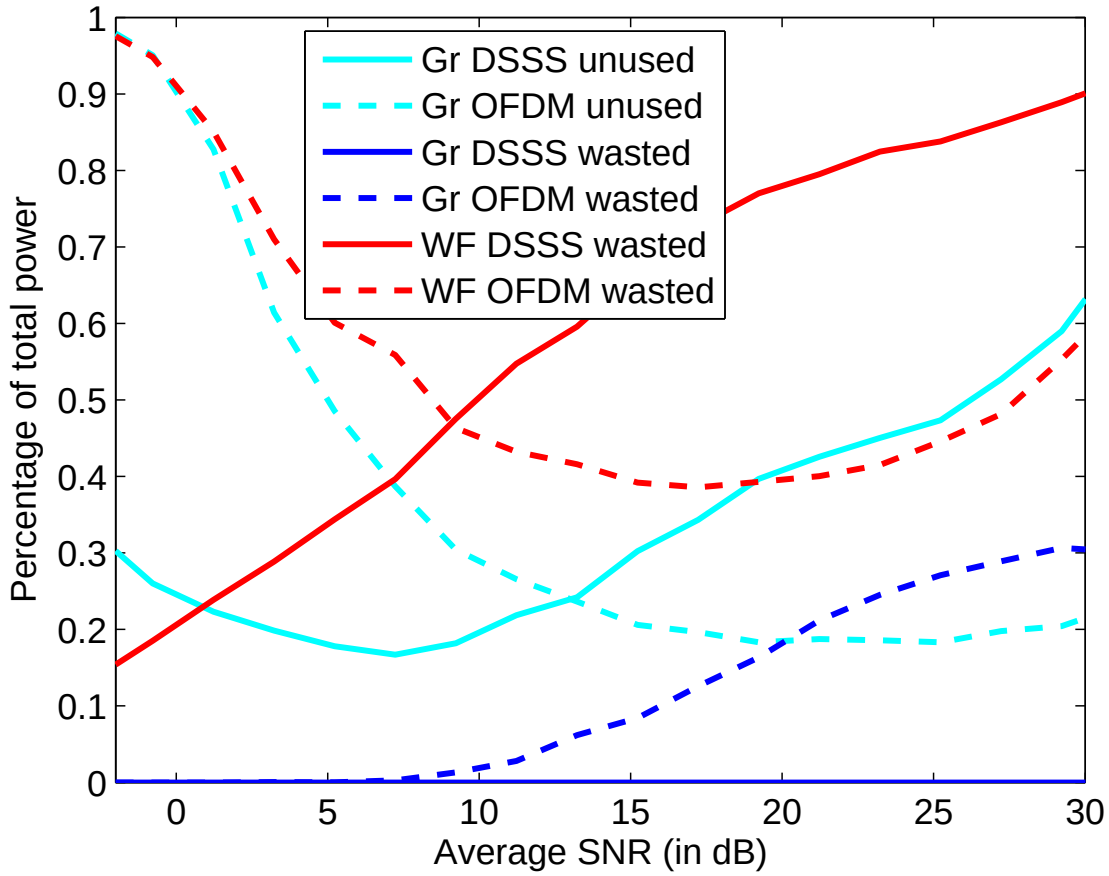


**Figure 2.13:** Power usage for different resource allocation algorithms, scenario A.

The distributions of the percentages of power that are wasted or unused, corresponding to Figure 2.10, are shown in Figure 2.14. Note that in 75% of the 10,000 realizations, no power is wasted using the greedy algorithm. This is because, in these cases, the greedy algorithm has reached equilibrium. At this SNR, 13 dB, the distributions of unused power are approximately the same for the OFDM and DSSS users: it is clear from Figure 2.13 that as the SNR increases, the DSSS user allocates less of its power to achieve its maximum rate and the unused portion increases.

Finally, note that power wasted by the water-filling solution is higher, in general, than the unused power of the greedy algorithm. This is because the greedy algorithm uses its power more efficiently as it does not create unnecessary interference on the available bandwidth. As noted above, this also reduces the spectral footprint of this pair of users, allowing other

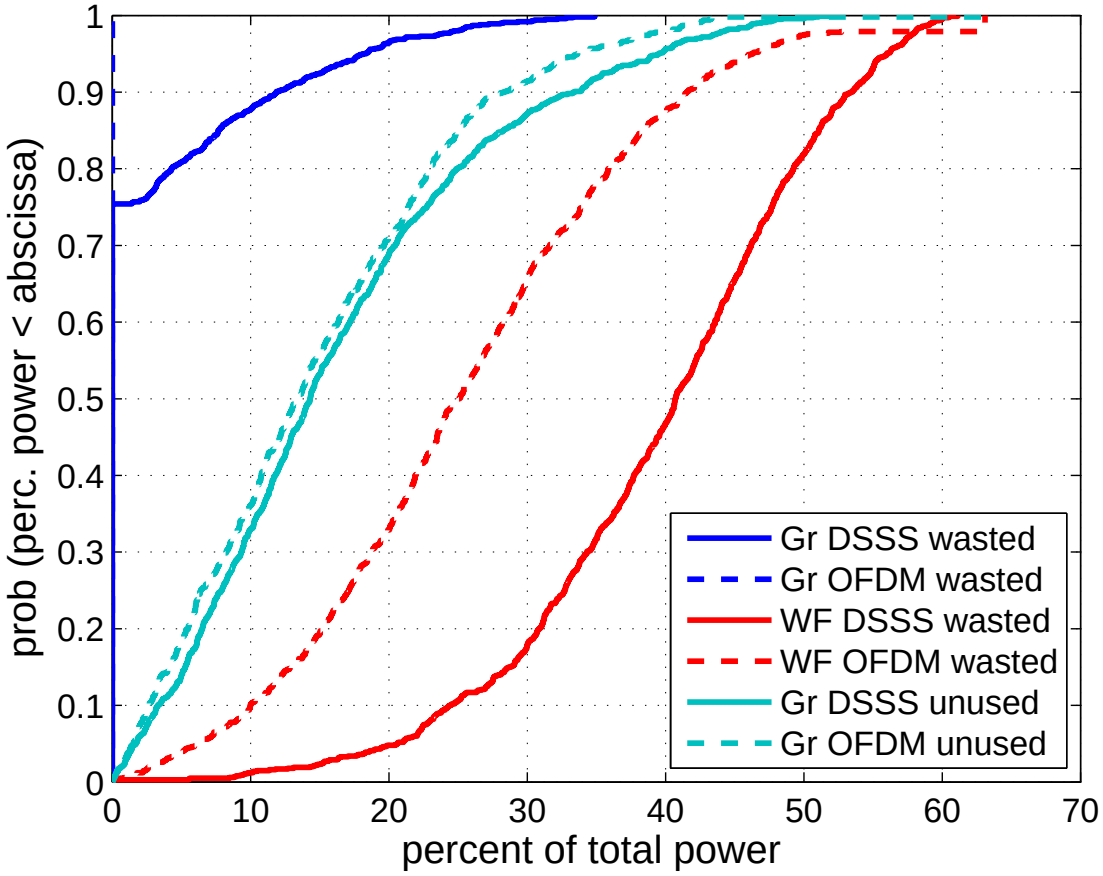


**Figure 2.14:** Cumulative frequency distribution of power usage at 13 dB, scenario A.

users to access the spectrum nearby.

### 2.6.2 Scenario B - Coexistence of two OFDM users

In this scenario, both users use the OFDM modulation. This scenario provides a view of the rate outcomes for the greedy algorithm compared to the water-filling algorithm when both users have the exact same set of strategies. When comparing Figure 2.9 from the previous scenario and Figure 2.15 with both users having OFDM as their modulation, it is observed again that the water-filling algorithm reaches a plateau at high SNR. For the greedy algorithm, the second user will reach a plateau eventually while the first user will get a decrease in its rate. This is due to the greedy behaviour of the algorithm, the second user has enough power to overcome the interference created by the first user and maximizes its rate on the three channels. Then the first user becomes limited in its power allocation on

the three channels since the interference is now so high it cannot obtain a reasonable QoS at its rate. The water-filling algorithm has chosen at high SNR to apply a solution that is equivalent to frequency division multiplexing (FDM), i.e. each channel supports only one user, which resolved this issue and allows the users to reach a plateau. It will be shown in Section 3.6.2 that the application of FDM at high SNR also resolved this issue with the greedy algorithm while still minimizing the required transmit power.

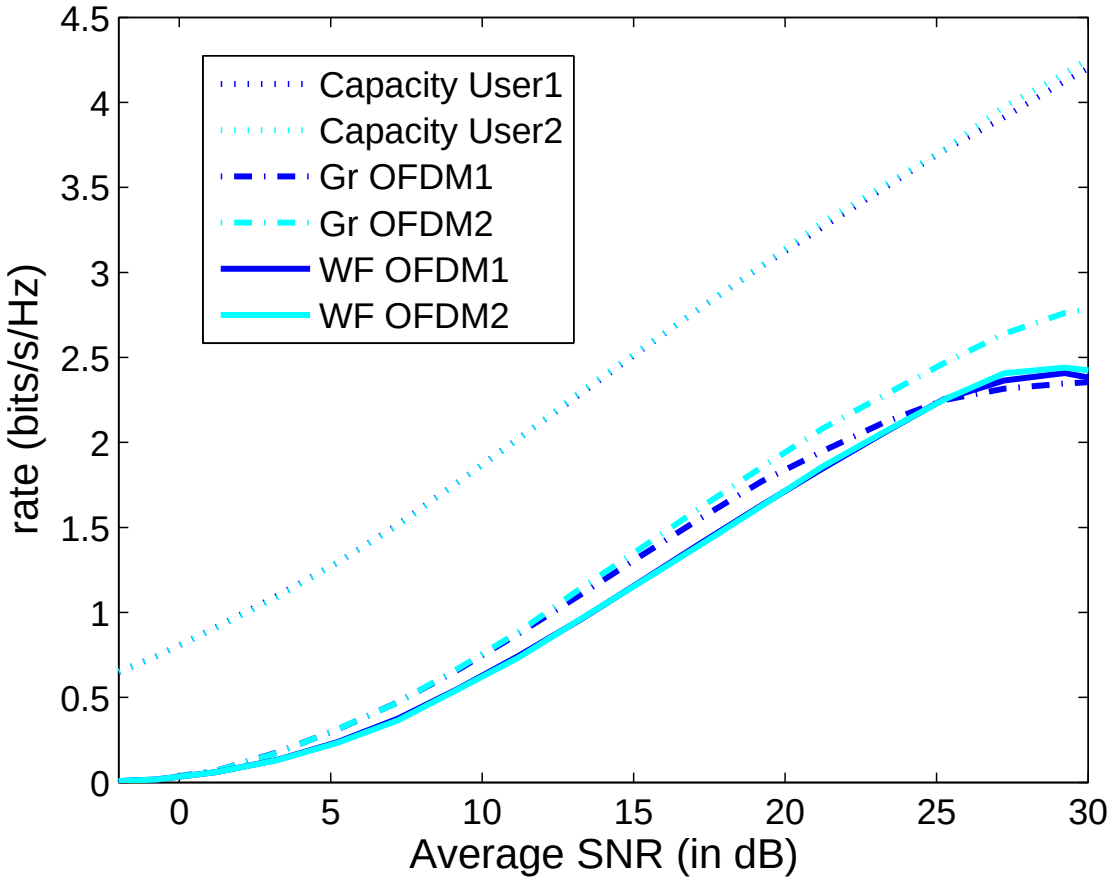


**Figure 2.15:** Rates for different resource allocation algorithms, scenario B.

Again, the greedy algorithm is capable of a higher performance (while still possibly sub-optimal) than the water-filling in that region due to the unused power by both users. In Figure 2.16, one will note that for every greedy user, a minimum of approximately 20% of the user's power is unused. The water-filling algorithm, in contrast, will waste 20% more most of the time per user than the unused power in the greedy algorithm. For example, at average SNR of 20 dB, the water-filling will waste 40% of the total power per user while the

greedy algorithm will choose to save (not use) 20% of the total power per user. This might be an important advantage when considering saving battery life, seamless communications, mutual interference, and spectrum reuse.

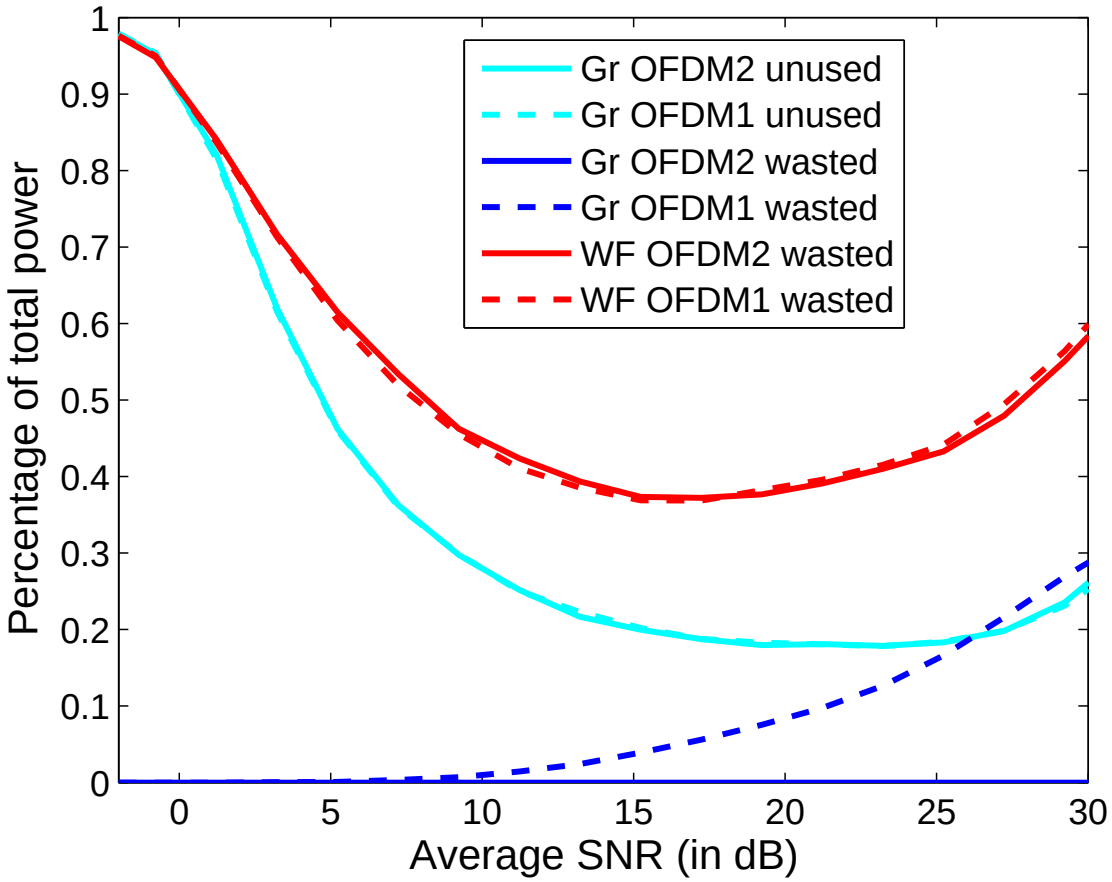


**Figure 2.16:** Power usage for different resource allocation algorithms, scenario B.

While comparing scenario A (Figure 2.14) and scenario B (Figure 2.17), it is seen that for both scenarios the greedy algorithm still saves the same amount of power. It is noted that in scenario B, 90% of the time there is no power wasted for the greedy algorithm while in scenario A (Figure 2.14), it was only 75% of the time. Meanwhile, both water-filling users in this scenario have the same amount of wasted power as the worst water-filling user (the water-filling DSSS user) in scenario A (Figure 2.14). For example, 50% of the time there is a waste for each water-filling user of 40% of the total power in this scenario while in the previous scenario, the water-filling OFDM user had a 25% waste of its total power 50% of the time and the water-filling DSSS user had a 40% waste of its total power 50% of

the time. This is explained by the fact that DSSS is more tolerant to mutual interference due to its spreading sequence strategy and requires less transmit power to reach its highest performance (due to the system modulation level limitation for DSSS set to BPSK in this thesis; if higher constellations were allowed for DSSS, higher transmit power would then be required). Therefore, adding more transmit power on that channel will only be wasted. However, the OFDM user does require more transmit power to transmit information with a higher constellation and it is less tolerant to mutual interference. Therefore, as shown in Figure 2.17, both water-filling users in scenario B will require more transmit power to combat the interference generated by the other user, which explains why there is less power wasted.

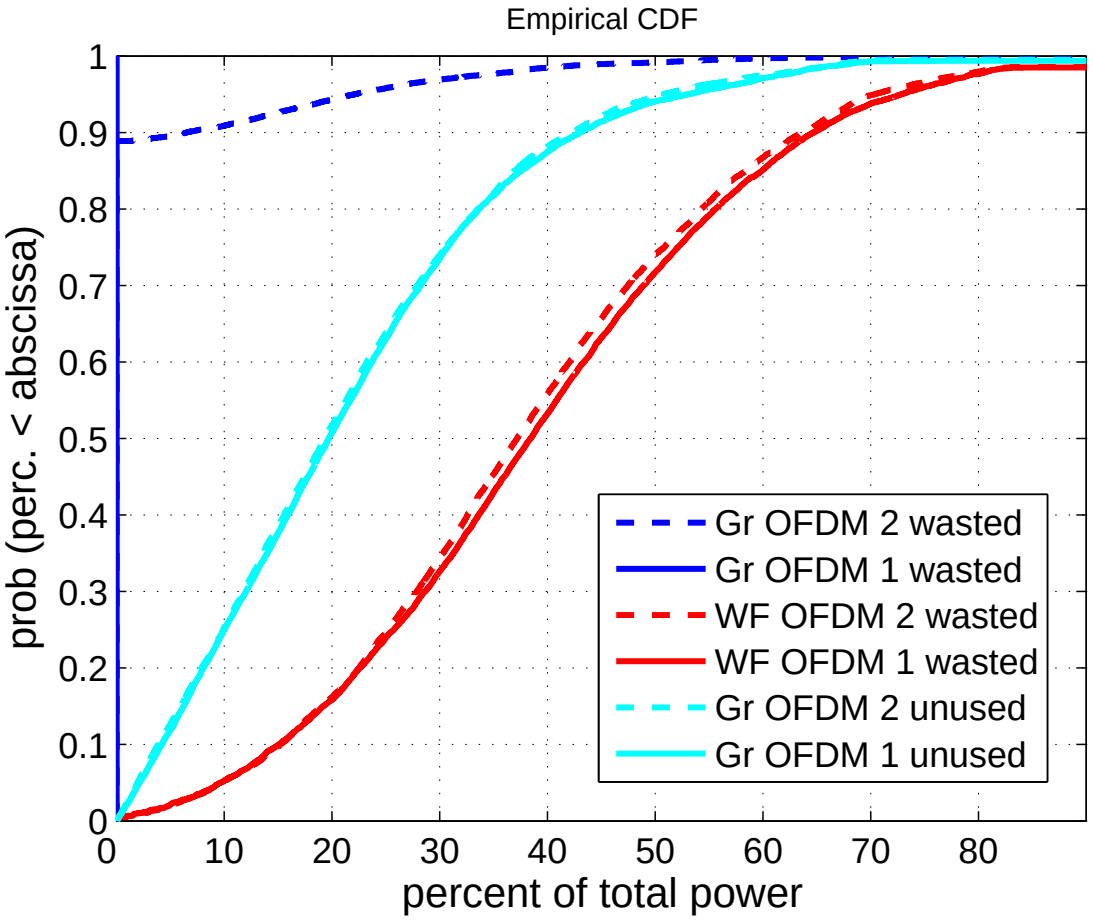


**Figure 2.17:** Cumulative frequency distribution of power usage at 13 dB, scenario B

### 2.6.3 Effect of cross-talk $\beta$

Cross-talk $\beta$ is the factor representing the strength of interference between the two users due to the distance separating them. Increasing the value of $\beta$ means in this case that the two users get closer and have a stronger interference effect while decreasing the value of $\beta$ has the reverse effect.

For scenario A, in Figures 2.18, it is noted that as $\beta$ decreases, the greedy OFDM outperforms more and more the water-filling OFDM at all average SNRs. Similarly, the greedy algorithm outperforms the water-filling for the DSSS user, except that at average SNR above 30 dB for $\beta$=0.01 (Figure 2.18 (a)), the greedy algorithm's DSSS rate performance and the water-filling rate performance converge to the same outcome. This is explained by the limitation of the DSSS user to BSPK modulation. If the DSSS had in its strategy set the option to increase also its modulation levels, it would be expected that the rate performance would be increased.

For both scenarios, decreasing $\beta$ increases the rates achieved by both users with both algorithms. From Figure 2.18 (a) and (c) when $\beta$=0.01 increases to $\beta$=0.1, there is a decrease in the rate performance for both iterative algorithms. This decrease in rate performance has the same percentage for both algorithms. For example, Table 2.2 shows the rate obtained for each user by both algorithms when $\beta$=0.01 (Figure 2.18 (a)) and when $\beta$=0.1 (Figure 2.18 (b)):

**Table 2.2:** Comparison of rate performance when $\beta = 0.01$ and $\beta = 0.1$ at average SNR 15 dB.

| | $\beta = 0.01$ | $\beta = 0.1$ |
|---|---|---|
| Gr OFDM | 1.4 bits/s/Hz | 1.2 bits/s/Hz |
| Gr DSSS | 0.7 bits/s/Hz | 0.6 bits/s/Hz |
| WF OFDM | 1.2 bits/s/Hz | 1.0 bits/s/Hz |
| WF DSSS | 0.6 bits/s/Hz | 0.5 bits/s/Hz |

As shown in Figure 2.22, the water-filling algorithm may achieve a higher rate than the greedy algorithm as the interference level increases. The $\beta$ at which this reversal takes places depends on the SNR and the order of the strategy updating.

For scenario A (Figure 2.20), it is noticed that the order of the user in the sequential iterative greedy algorithm has a considerable effect when $\beta$ is larger than 0.1. When the OFDM user is first to play the sequential iterative greedy game, i.e., the DSSS user changes its strategy last, therefore changing its power allocation. This decreases noticeably the rate achieved by the greedy algorithm as shown in Figure 2.20 (a).

This is explained by the fact that when the cross-talk is small, i.e., the users are far apart, the change in power allocation of the DSSS user has less effect on the rate achieved by the OFDM user since the measured SINR at the OFDM receiver will be minimized by the cross-talk $\beta$. For example, at $\beta = 0.1$ the interference perceived at the OFDM receiver will be 10 dB lower than if $\beta = 1$, if $\beta = 0.5$, the interference perceived at the OFDM receiver would then be 3 dB lower than if $\beta = 1$. Therefore, the OFDM user requires less transmit power to combat the interference generated by the DSSS user and will be able to achieve a high OFDM constellation. Even if it might not get the OFDM constellation it was aiming for in its last iterative strategy selection, the OFDM user will most of the time be able to get at least a lower rate at the end of the game when $\beta \leq 0.1$. However, when $\beta > 0.1$, the strategy selection for the OFDM user is smaller (due to the perceived interference at the OFDM receiver, it is seldom possible to achieve the highest OFDM constellation) as it will require more transmit power to combat the interference generated by the DSSS. Moreover, when the DSSS user changes its strategy with a larger $\beta$, the amount of mutual interference added by this change will require more transmit power from the OFDM user to combat it. Therefore, due to the fact that the interference perceived at the OFDM receiver will be much higher than predicted (effect of the cross-talk $\beta$ with the last strategy updates of the DSSS user) and the limited strategy space for the OFDM user when cross-talk $\beta$ is large, the transmit power selection will not be enough to support a BPSK signal.

In contrast, the DSSS user is less affected (Figure 2.18) because the power required from one interference level to another requires a smaller differential in transmit power (Figure 2.19). If it calculates a rate for lower interference, even if the OFDM user changes its power allocation strategy, it will be capable most of the time to get at least a lower rate with a larger SF.

When the greedy OFDM user is second (Figure 2.20), it achieves a lower rate because it is affected by the choice of the greedy DSSS user. As explained previously, when $\beta > 0.1$, it will seldom get a constellation higher than QPSK. The rate provided by the power allocation

for the greedy OFDM looks similar to that of the water-filling OFDM, just slightly below most of the time, and a few times zero rate is obtained on the three channels while the water-filling chooses a solution that is equivalent to FDM, i.e., each channel supports only one user.

The rates achieved by the greedy DSSS user are better than those of the water-filling DSSS user at lower SNR when $\beta = 1$ (Figure 2.20). However, at higher SNR, the greedy OFDM can combat the interference generated by the greedy DSSS user by allocating more transmit power, but then the greedy DSSS user has a decrease in its rate outcome (Figure 2.20).

It is noted that in Figure 2.18 when $\beta = 1$, the capacity sum rate for both users does not converge when SNR is larger than 20 dB. The reason for the change in the capacity sum rate convergence behaviour with $\beta$ is not fully understood; further investigation in this area would give more insight.

This investigation of the cross-talk effect mixed with the user order for updating their strategies study illustrates the difficulty of having just a greedy algorithm without some form of intelligence to recognize when convergence cannot be reached and to take the appropriate actions to remedy that situation.

For scenario B, as per Figure 2.23, it is seen that the greedy algorithm rate achieved outperforms more and more the water-filling achieved rates as $\beta$ decreases. However as per Figure 2.23(c), when the cross-talk gets stronger, $\beta > 0.1$, the second user in the greedy algorithm is affected by the power allocation of the first user and it cannot obtain a rate similar to the first user. It actually becomes worse than the water-filling second user at average SNR above 25 dB. This explained by the selfish behaviour of the greedy algorithm: the first user will selfishly maximize its rate objective since it can obtain high rates and its power allocation creates an interference level for the second user which it cannot combat with higher power allocation due to the limitation of the total power per user. Therefore, the second user would have difficulty obtaining a higher constellation rate, even if it still had power available. This is shown in Figures 2.24 (b) ($\beta$=0.1) and (c) ($\beta$=1) where the amount of unused power for the second user increases drastically at average SNR above 30 dB.

## 2.7 Conclusions

The iterative greedy algorithm, using power efficiency as a utility function to allocate power over several channels, provides a higher rate than iterative water-filling using the Shannon capacity for the real signals considered when the cross-talk is low to moderate. It is expected that this observation would be extended to other real signals, and other rate strategies based on parameters such as code rate. The greedy algorithm presented in this thesis will require refinements for the convergence, especially for larger $\beta$, to avoid switching between two solutions. The application of a solution equivalent to FDM at high SNR and high interference could drastically improve the rate achieved of the proposed greedy algorithm, as demonstrated in Section 3.6.2. These improvements, with the inclusion of some fairness rules, could also resolve the lowest rate outcomes when the cross-talk $\beta$ is large.

Furthermore, the greedy algorithm does not always allocate all the available power for each user. This reduces the spectral footprint associated with the two users, thereby allowing more additional users to access the spectrum in the same geographic area. This is an important characteristic, which has been overlooked in previous work, as the concept of spectrum sharing should go beyond the users in a specific game. Moreover, transmitting with a lower provides the advantage to save battery life, an important concept for user system that requires high mobility capability (small, light and portable).

The complexity of the greedy algorithm is dominated by the generation of the lookup tables necessary to compute the resources required for each rate strategy. Although this computation can be done off-line, a lower complexity solution may be preferred for real-time implementation. Some of these lookup tables could be produced at the initial setup of the system and further develop as the system, through some cognitive ability, observes its environment and the outcome of its decisions.

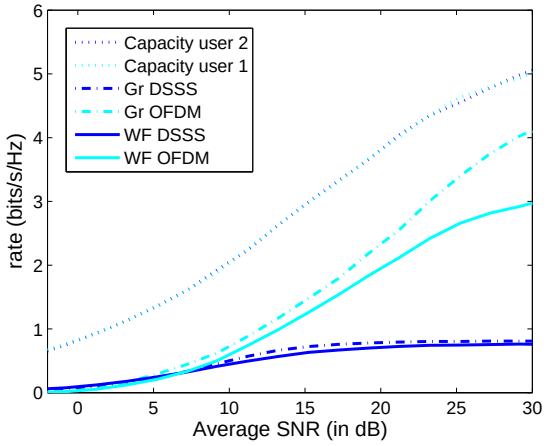


(a) $\beta = 0.01$

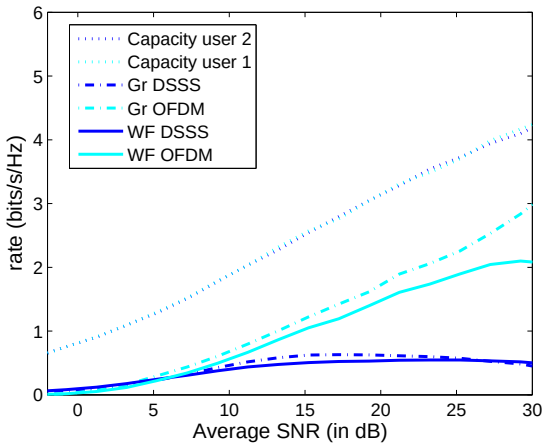


(b) $\beta = 0.1$

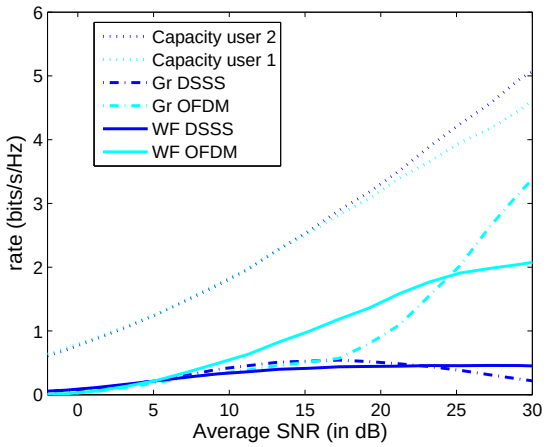


(c) $\beta = 1$

**Figure 2.18:** Effect of $\beta$ on rate for Scenario A with OFDM user first.

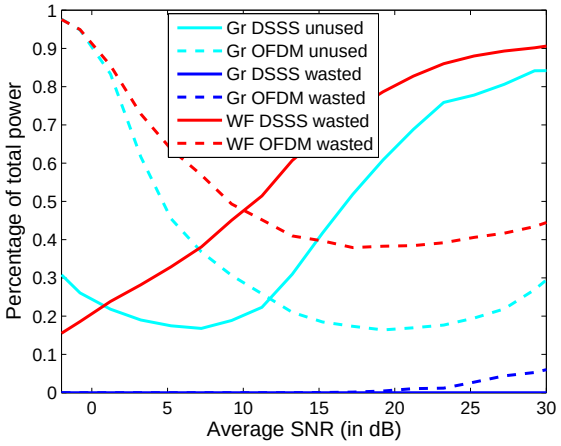


(a) $\beta = 0.01$

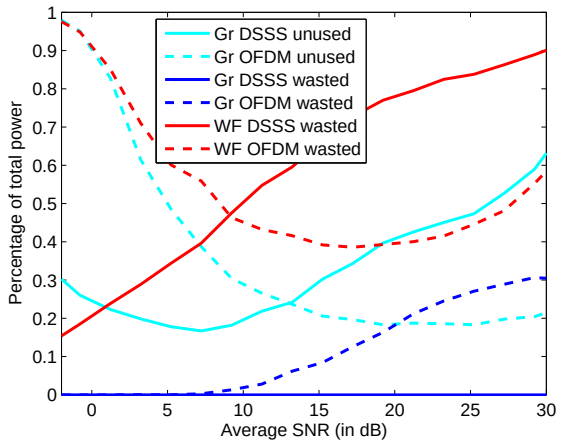


(b) $\beta = 0.1$

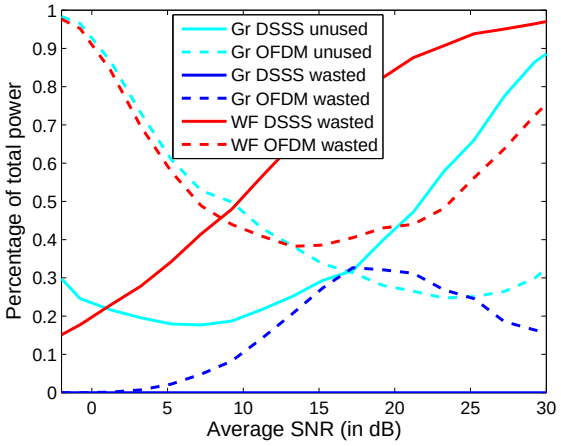


(c) $\beta = 1$

**Figure 2.19:** Effect of $\beta$ on power allocation for Scenario A with OFDM user first.

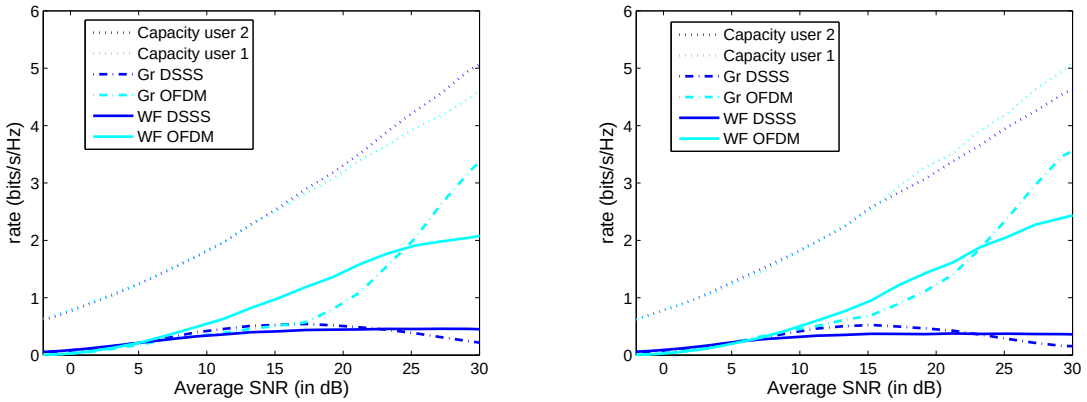


(a) OFDM user first

(b) OFDM user second

**Figure 2.20:** Rates achieved for Scenario A when the order of strategies updating is reversed, $\beta = 1$.

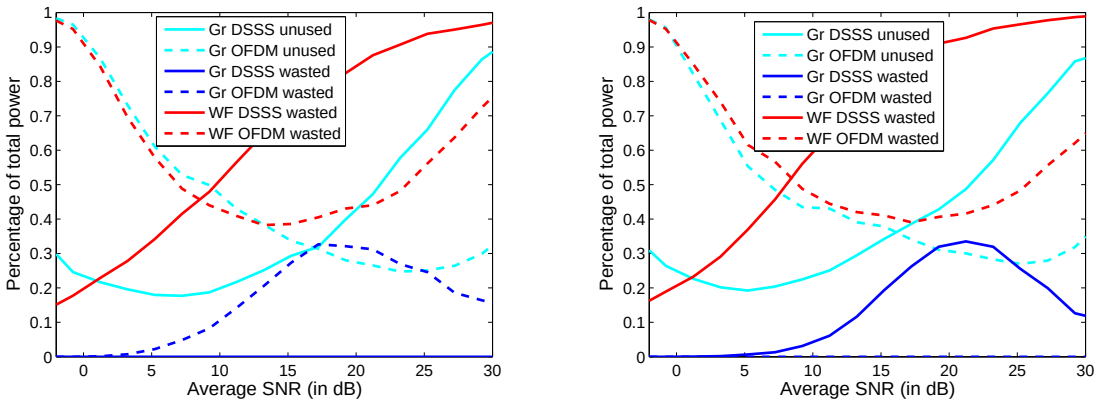


(a) OFDM user first

(b) OFDM user second

**Figure 2.21:** Power allocation for Scenario A when the order of strategies updating is reversed, $\beta = 1$.

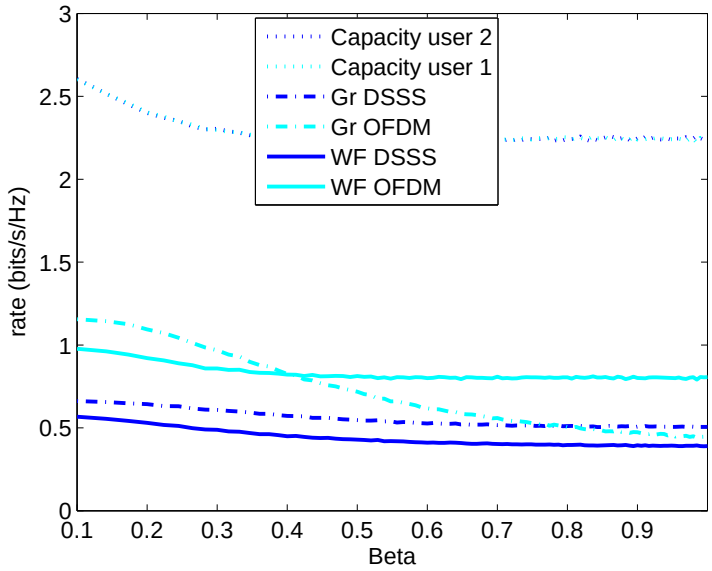


(a) OFDM user first

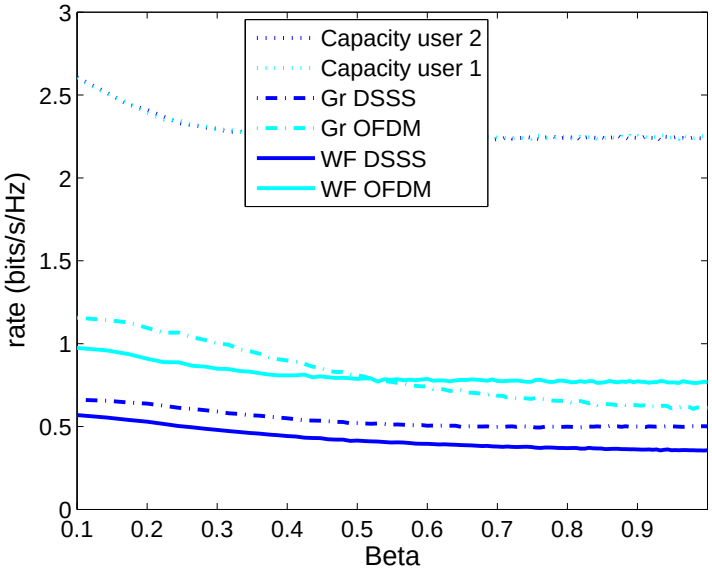


(b) OFDM user second

**Figure 2.22:** Rates achieved for Scenario A when average SNR is 13 dB and $\beta$ varies.

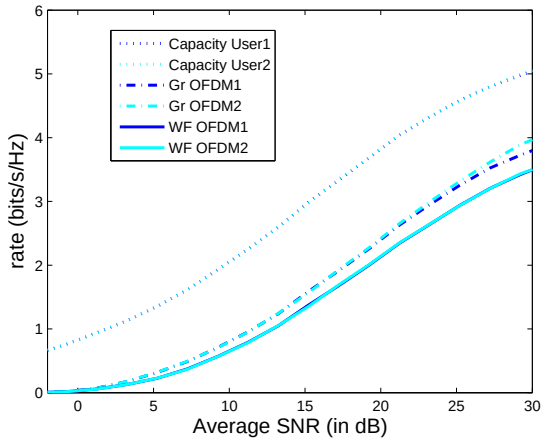


(a) $\beta = 0.01$

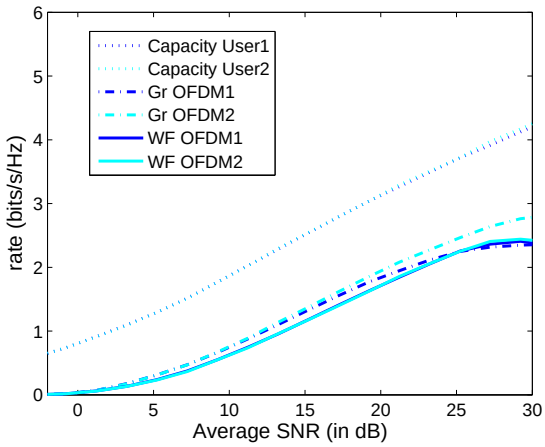


(b) $\beta = 0.1$

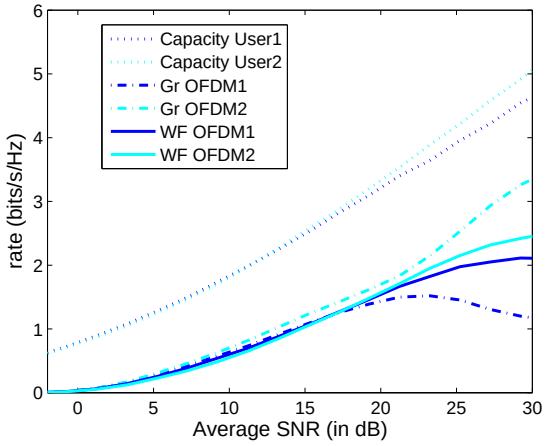


(c) $\beta = 1$

**Figure 2.23:** Effect of $\beta$ on rates for Scenario B.

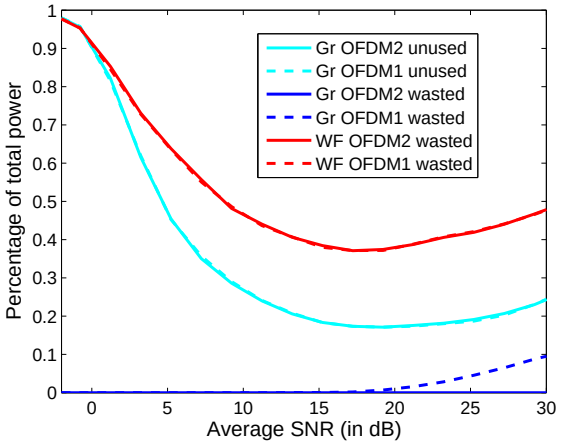


(a) $\beta = 0.01$

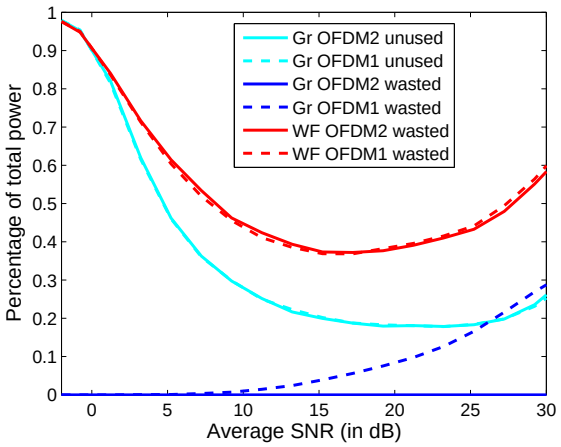


(b) $\beta = 0.1$

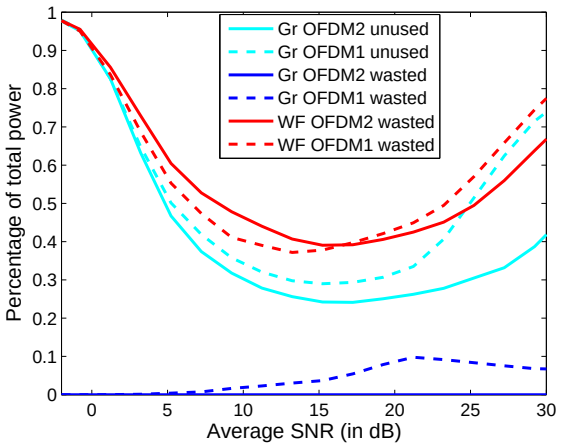


(c) $\beta = 1$

**Figure 2.24:** Effect of $\beta$ on power allocation for Scenario B.

# Chapter 3

# Frequency Selective Environment

This chapter will consider Rayleigh multipath fading channels to investigate and compare the algorithms presented in Chapter 2.4 with a simplified wideband frequency selective environment. Two real signals are considered, the OFDM and the DSSS signals used typically in a frequency selective environment. This chapter will investigate a step further the material studied in Chapter 2 to get a better insight on the spectrum resource allocation problem before discussing spectrum management in Chapter 4.

## 3.1 System model

In the frequency selective scenario, the channel will be modelled using an $M$-tap delay line to simulate a Rayleigh multipath environment. The desired signal at receiver $i$ from transmitter $i$ on channel $k$ at sampling instant $nT$ is given by

$$\mathcal{Q}_i(k, nT) = \kappa_{ii}(k)\sqrt{P_i(k)}\sum_{m=1}^{M} h_{ii}(k, \tau_m)x_i(k, nT - \tau_m) \tag{3.1}$$

with an average power $Q_i(k, nT) = \mathcal{E}\{|\mathcal{Q}_i(k, nT)|^2\}$ and the interfering signal arriving from transmitter $j$ is

$$\mathcal{I}_i(k, nT) = \kappa_{ij}(k)\sqrt{P_j(k)}\sum_{m=1}^{M} h_{ij}(k, \tau_m)x_j(k, nT - \tau_m) \tag{3.2}$$

with an average power $I_i(k, nT) = \mathcal{E}\{|\mathcal{I}_i(k, nT)|^2\}$. $P_i(k)$ is the transmit power allocated by user $i$ on channel $k$. The transmitted signal from user $i$ on channel $k$ is $x_i(k)$, which has an average power of $E_x = \mathcal{E}\{|x_i(k)|^2\} = 1$ for $i = 1, 2$ and $k = 1, \ldots, N$. The complex channel

response on the $m$th tap at delay $\tau_m$, from the transmitter of user $j$ to the receiver of user $i$, is denoted $h_{ij}(k, \tau_m)$. The variance of this coefficient is given by $\alpha_{ij}(k, m)$. The scaling factors $\kappa_{ij}(k) = \left(\sum_{m=1}^{M} \alpha_{ij}(k, m)\right)^{-\frac{1}{2}}$ are used to normalize the average received powers.

The complex channel responses are assumed constant for the duration of each resource allocation operation. For each realization, the direct path responses $h_{ii}(k, \tau_m)$ are drawn independently from the complex normal distributions $\mathcal{CN}(0, \alpha_{ii}(k, m))$ for $i = 1, 2$, $k = 1, \ldots, N$ and $m = 1, \ldots, M$. The interfering path responses $h_{ij}(k, \tau_m)$, $i \neq j$, are independent and distributed as $\mathcal{CN}(0, \beta \cdot \alpha_{ij}(k, m))$, where the cross-talk factor is $\beta \leqslant 1$. As in the frequency non-selective case, it is assumed that the users have perfect channel state knowledge and that they are able to measure the levels of noise and interference.

The total received signals at the two receivers can then be modelled as:

$$\begin{aligned} y_1(k, nT) &= \mathcal{Q}_1(k, nT) + \mathcal{I}_1(k, nT) + w_1(k, nT) \\ y_2(k, nT) &= \mathcal{Q}_2(k, nT) + \mathcal{I}_2(k, nT) + w_2(k, nT) \end{aligned} \tag{3.3}$$

where $y_i(k, nT)$ is the received signal for user $i$ at time $nT$ on channel $k$, and $w_i(k, nT)$ is the additive white Gaussian noise with power spectral density $N_0$. $T$ is the sample interval and $n$ is the index number of the transmit symbols.

To reduce the number of degrees of freedom, the number of taps for the Rayleigh multipath channel is $M = 3$ and the time delays and variance are fixed over all the simulations. To ensure that both modulations, OFDM and DSSS, are able to resolve the multipath (bandwith coherent and time coherent), the time delays are chosen to ensure they are smaller than the symbol time $T_s$ for the DSSS modulation (which is affected by the spreading) and smaller than the guard interval for the OFDM modulation. The DSSS chip interval is 0.2 $\mu$s and the smallest spreading factor for this scenario is $SF = 15$, therefore the shortest symbol time is $T_s = 15 \cdot 0.2$ $\mu$s$= 3$ $\mu$s. The guard interval for the OFDM lasts 9 $\mu s$. Based on measurements results presented in [43], the tap time delays and variance have been chosen as per Table 3.1.

It is noted that the channel model is not realistic as due to the nature of wireless channels, delays and variance are expected to change over time (user mobility, channel variation and/or wireless traffic fluctuations). It is also noted that both users in this model have the same delays and variance, which will be rarely seen in a real environment. But the path delay and variance values chosen are expected on average in a realistic environment for a conventional

**Table 3.1:** Paths delays and variance for the frequency selective channel

| | $\tau_0$ | $\tau_1$ | $\tau_2$ |
|---|---|---|---|
| Time Delay $\tau$ | 0 | 1 $\mu s$ | 2.6 $\mu s$ |
| Variance $\alpha$ | 1 | -10 dB | -20 dB |

channel as described in [43]. These assumptions are taken to simplify the problem and to focus on gaining insight into the resource allocation problem.

## 3.2 Channel equalization for OFDM

Pilot symbols are normally introduced at regular intervals among the OFDM symbols to calculate the channel variations and provide the right equalization prior to the symbol detection/decision. In this thesis, it is assumed that the OFDM user has perfect knowledge of the channel. Therefore, the pilot symbols are not simulated but are assumed to be taken care of by a prior process.

Since addition of sinusoid with a delayed version of the sinusoid does not change the frequency of the sinusoid (only the amplitude and phase are affected), the orthogonality across subcarriers is not lost even in the presence of multipath. Therefore a simple one tap equalization [44] is required to correct the amplitude and phase over the frequencies based on the CSI:

$$\breve{Q}_i(k, f_u) = \frac{Y_i(k, f_u)}{H_i(k, f_u)} \tag{3.4}$$

where $Y_i(k, f_u)$ is the received signal impulse response at the OFDM receiver on tone $u$ for user $i$ on channel $k$ and is obtained from the discrete Fourier transform of $y_i(k, nT)$ described in (3.3). $H_i(k, f_u)$ is the direct path channel frequency impulse response detected by the CSI mechanism on tone $u$ for user $i$ on channel $k$ and is given by the discrete the Fourier transform of $h_{ii}(k, nT)$. The discrete Fourier transforms of $y_i(k, nT)$ and $h_{ii}(k, nT)$ are obtained with (3.5) and (3.6).

$$Y_i(k, f_u) = \frac{1}{\sqrt{U}} \sum_{n=0}^{U-1} y_i(k, nT) e^{\frac{-j2\pi nu}{U}} \quad for\ 0 \leq u \leq U-1 \tag{3.5}$$

$$H_i(k, f_u) = \frac{1}{\sqrt{U}} \sum_{n=0}^{U-1} e^{\frac{-j2\pi nu}{U}} h_{ii}(k, nT) \quad for\ 0 \leq u \leq U-1 \tag{3.6}$$

where $U$ is the number of OFDM tones.

## 3.3 Channel equalization for DSSS

The DSSS uses the rake receiver [45, ch.13] with three fingers which are assumed to be aligned with the three strongest multipath signals received at the DSSS receiver. The rake receiver uses maximum ratio combining (MRC) to combine all signals received prior to making a decision on the received symbol. The rake MRC will ensure that more weight is given to the strongest received signal. The combining of the received signal at the rake receiver can be performed at the chip level and then the despreading of the received signal is done afterwards. The combining can also be performed after each received signal has been despread by the pseudo-noise random code (the m-sequence) which is called rake receiver symbol-combining and shown in Figure 3.1.

For the DSSS waveform, the equation of the desired received signal of (3.1) is further defined as:

$$\mathcal{Q}_i(k, nT) = \kappa_{ii}(k)\sqrt{P_i(k)} \sum_{m=1}^{M} h_{ii}(k, \tau_m) \sum_{v=1}^{V} b_i(n) a(n\frac{T_s - v}{T_c} - \tau_m) \tag{3.7}$$

where $b_i(n)$ is the $n^{\text{th}}$ information bit, $V$ is the size of the spreading factor, $T_c$ is the chip time, $T_s$ is the symbol duration for $SF = V, \quad V = \{15, 31, 63, 127\}$ and $v$ is the index of the pseudo-noise random spreading sequence. $a(n\frac{T_s - v}{T_c})$ is the pseudo-noise random m-sequence where $n\frac{T_s - v}{T_c}$ is an integer.

The rake MRC can be described as:

$$\breve{y}_i(k, nT) = \sum_{m=1}^{M} h^*_{ii}(k, \tau_m) \sum_{v=1}^{V} y_i(k, nT - \tau_m) a^*(n\frac{T_s - v}{T_c} - \tau_m) \tag{3.8}$$

where $M$ is the number of resolved multipath for the rake fingers. The path search and the channel estimation $h^*_{ii}(k, \tau_m)$ are assumed to have been taken care of by a prior process and are made available to the DSSS receiver prior to the descrambling of the received signal. $h^*_{ii}(k, \tau_m)$ and $a^*(n\frac{T_s - v}{T_c} - \tau_m)$ are the complex conjugates of $h_{ii}(k, \tau_m)$ and $a(n\frac{v}{T_c} - \tau_m)$, respectively.

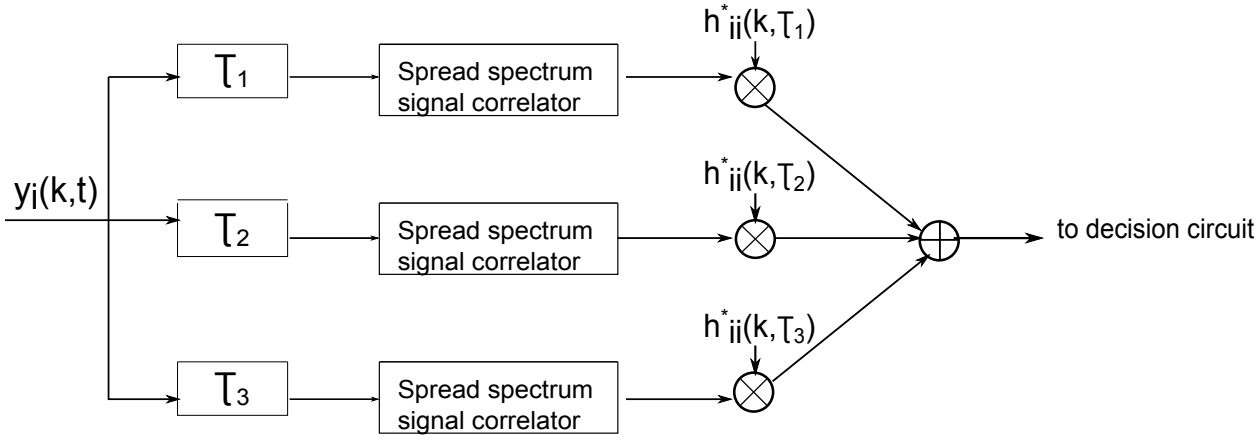


**Figure 3.1:** Rake receiver with MRC at symbol-level.

## 3.4 Resource allocation algorithms

The resource allocation algorithms used in this thesis have been described in a general format in Section 2.4. This section will redefine the equations provided in Section 2.4 to be in accordance with the frequency selective model described in Section 3.1. A flow-chart of how the simulations were performed in Matlab for the power resource allocation problem studied in this thesis is shown in Appendix A.

### 3.4.1 Iterative water-filling algorithm

Assuming Gaussian distributed signals in a frequency selective environment, the maximum achievable rate on channel $k$ is given by the Shannon capacity equation [46]:

$$R_i(k) = \sum_{n=0}^{U-1} \log_2 \left(1 + \Upsilon_i(k, f_n)\right) \quad i = 1, 2 \tag{3.9}$$

and the maximum sum rate for user $i$ is

$$R_i = \sum_{k=1}^{N} \sum_{n=0}^{U-1} \log_2 \left(1 + \Upsilon_i(k, f_n)\right) \quad i = 1, 2 \tag{3.10}$$

where the SINR $\Upsilon_i(k, f_n)$ on tone $n$ for channel $k$ is defined as

$$\Upsilon_i(k, f_n) \triangleq \frac{Q_i(k, f_n)}{N_0 B_c + I_i(k, f_n)}. \tag{3.11}$$

with transmit power $P_i(k)$ from (3.1) and (3.2) divided equally among the $U$ tones. The direct path channel attenuation on tone $n$, $H_{ii}(k, f_n)$, and the interfering path channel at-

tenuation on the same tone, $H_{ij}(k, f_n)$, are obtained from the Fourier transforms of $h_{ii}(k, \tau)$ and $h_{ij}(k, \tau)$ as defined in Section 3.1.

Therefore, the water-filling power allocation for the frequency selective environment is defined as:

$$P_i^{WF}(k) \triangleq \left( \mu_i - \frac{N_0 B_c + I_i(k)}{\sum_{n=0}^{U-1} |H_{ii}(k, f_n)|^2} \right)^+ \tag{3.12}$$

where $\mu_i$ is the water-filling level that satisfies $\sum_{k=1}^{N} P_i^{WF}(k) = P_{tot}$, $(a)^+ = \max(0, a)$, and $P_i^{WF}(k)$ is divided equally among the tones. For the wideband case, the total received power $Q_i(k)$ for user $i$ on channel $k$ is calculated as per (3.13), i.e,

$$Q_i(k) = P_i^{WF}(k) E_x \frac{1}{U} \sum_{n=0}^{U-1} |H_{ii}(k, f_n)|^2 \quad k = 1, \ldots, N \tag{3.13}$$

### 3.4.2 Frequency selective greedy algorithm

The interference power $I_i(k)$ for user $i$ on channel $k$ is calculated as described by (3.14):

$$I_i(k) = \sum_{j \neq i} P_j^{Gr}(k) E_x \frac{1}{U} \sum_{n=0}^{U-1} |H_{ij}(k, f_n)|^2 \quad k = 1, \ldots, N \tag{3.14}$$

where $P_j^{Gr}(k)$ is the transmit power allocated by the greedy algorithm of user $j$ on channel $k$. The interfering channel attenuation $H_{ij}(k, f_n)$ and the average power $E_x$ of the desired signal $x_j$ are both described in Section 3.1.

The increased transmit power to provide the required received power $Q_i(k)$ of user $i$ on channel $k$ calculated by the greedy algorithm is defined for the frequency selective environment as (3.15):

$$\Delta P_i(k) = \frac{\Delta Q_i(k)}{\frac{1}{U} \sum_{n=0}^{U-1} |H_{ii}(k, f_n)|^2} \quad k = 1, \ldots, N \tag{3.15}$$

where $H_{ii}(k, f_n)$ is the direct path channel attenuation on tone $f_n$ described in Section 3.1.

## 3.5 Symbol error rate curves simulations

For scenario A, Monte Carlo simulations were performed for every rate strategy for the OFDM signal, to determine the received power required to achieve a SER of $10^{-2}$ or better in the frequency selective channel described in Section 3.1 over a range of interference levels created by the DSSS signal, and vice versa for OFDM interference on a DSSS signal. The

chosen target SER for the frequency selective environment is larger than the frequency non-selective environment due to the increase of simulations durations to obtain the signal characteristics required for the greedy algorithm. The same Monte Carlo simulations were performed for scenario B with an OFDM signal with an OFDM interferer. The Monte Carlo simulations were done over 1000 channel realizations for each interference level. These results were used to generate the lookup tables required in the implementation of the algorithms described in Section 2.4 to determine the real rate obtained with the power allocation for each user on each channel. The figures of the required received power for a specific level of interference power are shown in Appendix B. The lookup tables used in this thesis are also shown and described in Appendix B.

### 3.5.1 DSSS signal with an OFDM interferer SER curves

The SER curves for a BPSK $SF = 15$ DSSS user with a BPSK OFDM interferer obtained in the simulations are shown in Figure 3.2. The selected SIR shown in Figure 3.2 are -3 dB, -2.5 dB, -2 dB, and -1 dB. Note that these simulations were performed for each BPSK DSSS spreading factor with the same BPSK OFDM interferer. As mentioned previously in Section 2.5.2, the performance may change slightly for other OFDM constellations due to the OFDM constellation mapping, however, simulations suggest that these difference are quite small. Therefore in this work, the interference effects of all OFDM constellations are assumed to be equal.

### 3.5.2 OFDM signal with a DSSS interferer SER curves

The SER curves for a BPSK OFDM user with a $SF = 15$ BPSK DSSS interferer in the simulations are shown in Figure 3.3 for selected SIR obtained. The selected SIRs shown in Figure 3.3 are 13 dB, 14 dB, 15 dB, and 16 dB. Note that these simulations were performed for each OFDM constellation with the same spreading factor $SF = 15$ BPSK DSSS interferer. As mentioned in Section 2.5.1, the performance may change slightly for other DSSS spreading factors due to the repeated spreading sequence, however, simulations suggest that these difference are quite small. Therefore in this work, the interference effects of all spreading sequences are assumed to be equal.

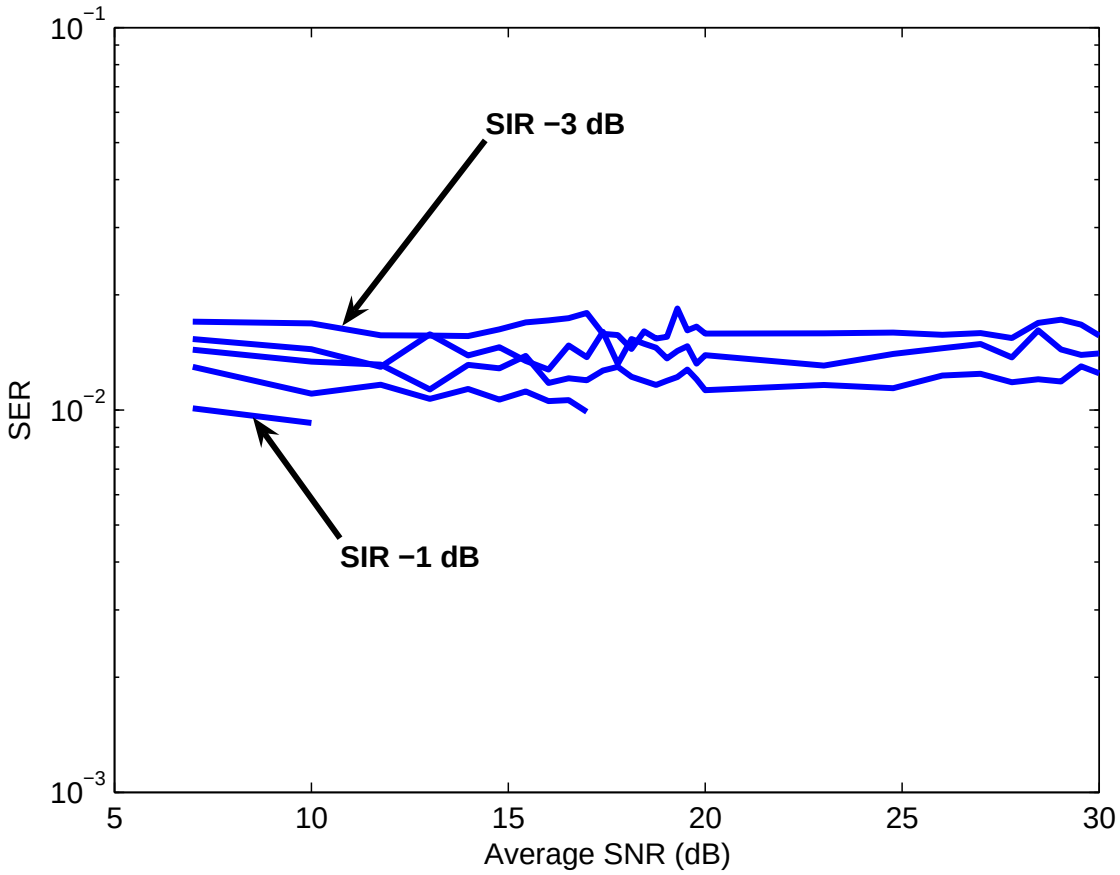


**Figure 3.2:** SER curves for BPSK $SF = 15$ DSSS with BPSK OFDM interference. The selected SIRs shown in this figure are -3 dB, -2.5 dB, -2 dB, and -1 dB.

### 3.5.3 OFDM signal with OFDM interferer SER curves

The SER curves for a BPSK OFDM user with a BPSK OFDM interferer obtained in the simulations are shown in Figure 3.4 for selected SIR. The SIR selected for Figure 3.4 are 14 dB, 15 dB, 16 dB, 17 dB, 18 dB and 22 dB. Again, as mentioned previously in Section 2.5.3, the simulations for the lookup table have been done for every OFDM constellation with the same BPSK OFDM interferer, making the same assumption that the interference created by all OFDM constellations are equal.

It is seen in Figure 3.5 that changing the delays of the multipath Rayleigh channel model has a small impact on the SER curves. In Figure 3.5, the same SIR values were simulated with the fixed delays described in Section 3.1 and with random delays which are smaller than the guard interval of the OFDM waveform. In this model, the fixed delays provide a

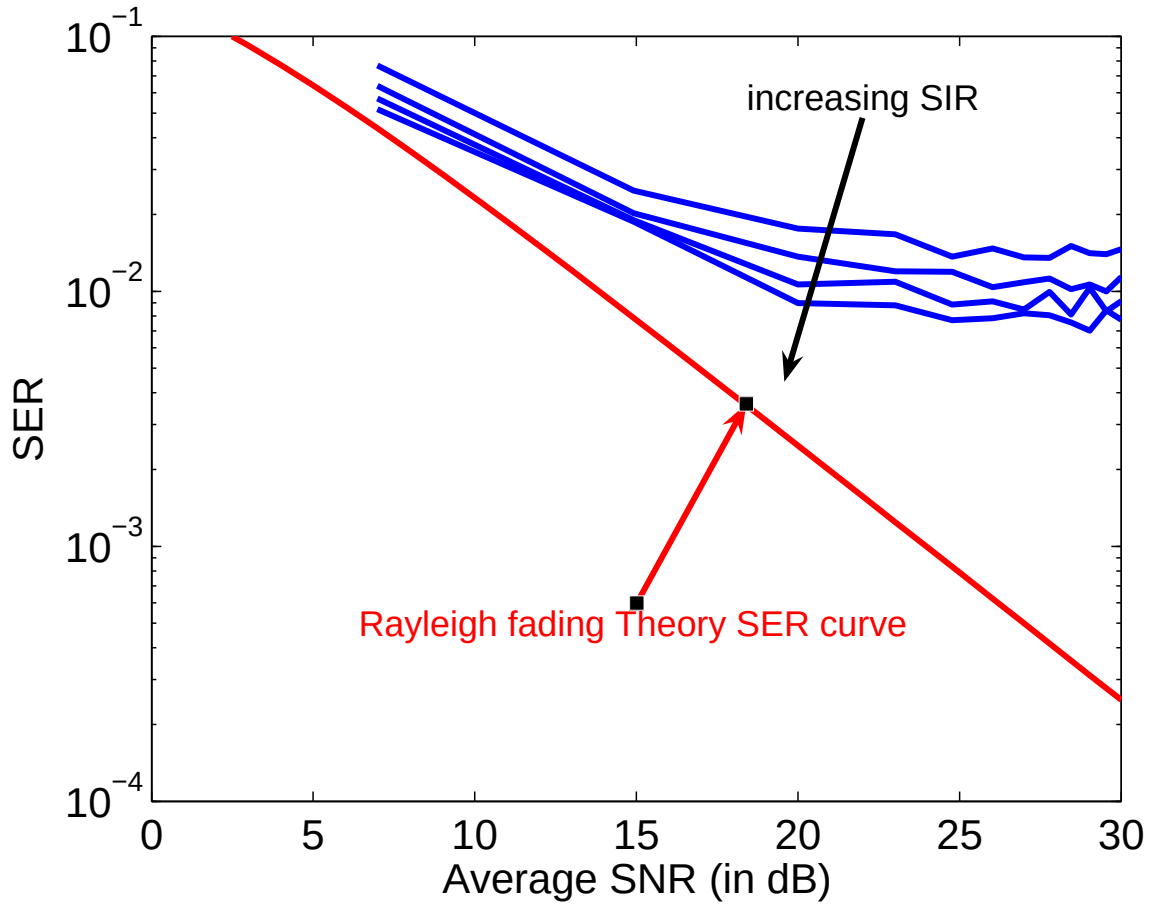


**Figure 3.3:** SER curves for BPSK OFDM with $SF = 15$ BPSK DSSS interference. The selected SIRs shown in this figure are 13 dB, 14 dB, 15 dB, and 16 dB.

SER $10^{-2}$ with at a slightly lower SNR than the random delays, all differences appear to be quite small. Further work would be required to investigate more precisely the impact of the delays and power variance of the multipath channel on the greedy algorithm.

## 3.6 Results

As per Section 2.6, the same non-cooperative spectrum sharing resource allocation problem over 3 channels of $B_c$ Hz is considered with two users with the same total power $P_{tot}$. Each channel is modelled as Rayleigh multipath fading with $M = 3$ multipaths. The simulations were performed for both scenario A (coexistence of a DSSS user with an OFDM user) and scenario B (coexistence of two OFDM users) for 10 000 different channel realizations. The

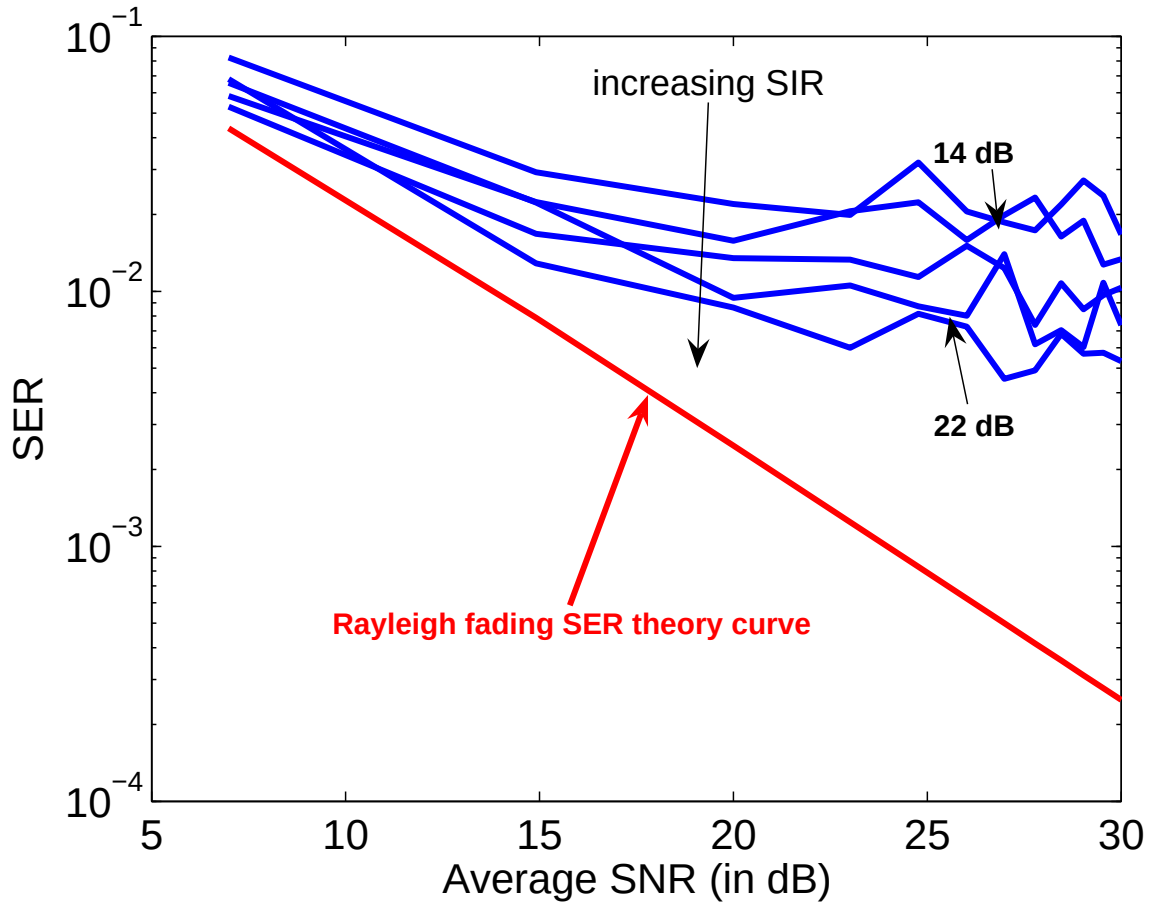


**Figure 3.4:** SER curves for BPSK OFDM with BPSK OFDM interference. The selected SIRs shown in this figure are 15 dB, 16 dB, 17 dB, 18 dB and 22 dB.

cross-talk $\beta = 0.1$ unless it is stated otherwise.

### 3.6.1 Scenario A - Coexistence of DSSS and OFDM users

In the results obtained for scenario A in Section 2.6.1, it was shown that at low SNR, DSSS users obtained higher rates than OFDM users since they are more tolerant to interference. From these results and from the SER curves in the wideband scenario discussed in Sections 3.5.1 and 3.5.2, it was expected that DSSS users would achieve higher rates than the OFDM users below a certain SNR. In Figures 3.6 and 3.7, it is shown that both DSSS users achieve higher rates than both OFDM users when the SNR is below 10 dB. Both algorithms provide the same behaviour as per the narrowband scenario (Figure 2.9) but both users are more limited in the outcome rates due to their strategy sets. The DSSS users are limited to

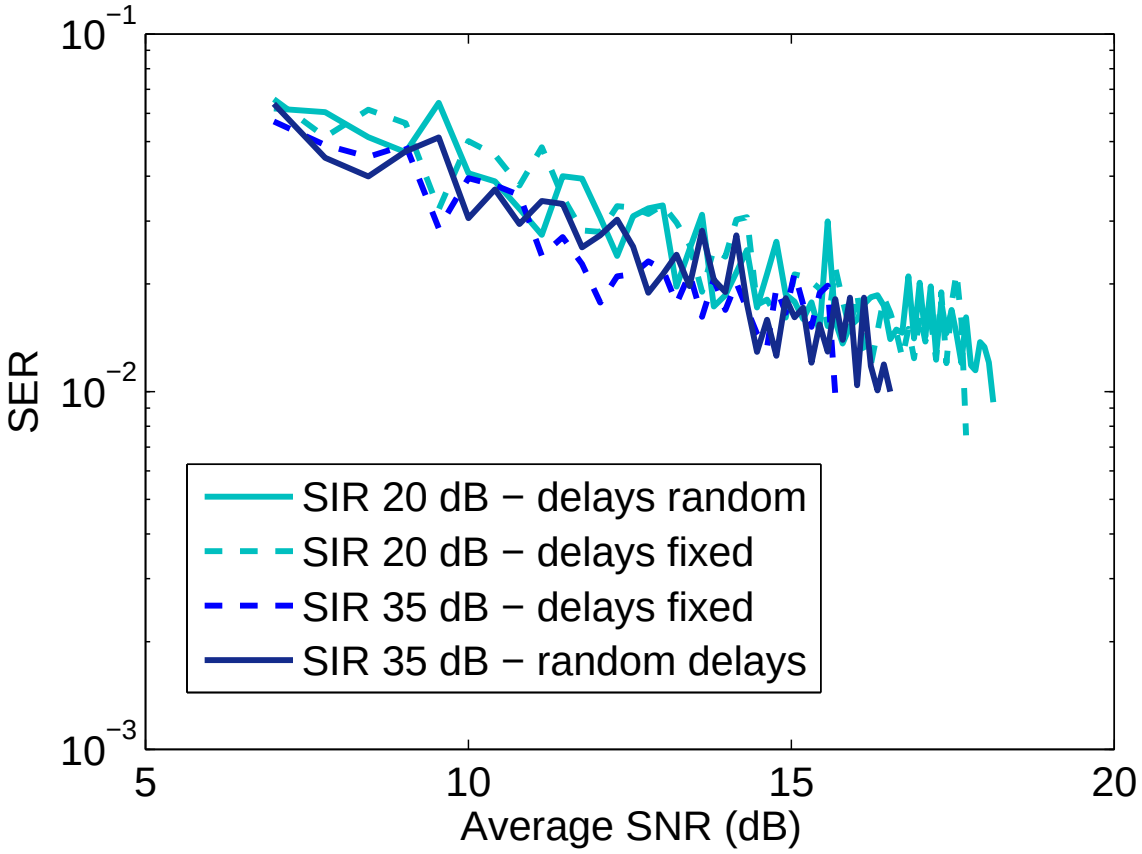


**Figure 3.5:** SER curves for BPSK OFDM with BPSK OFDM interference for fixed and random multipath delays

a BPSK modulation with the smallest spreading factor being $SF = 15$, giving a maximum rate of $1/15 \cdot (0.82)B_c$ sps per channel. The OFDM users are limited to 16-QAM as the highest constellation achievable under that model, giving a maximum rate of $4 \cdot (0.816)B_c$ sps per channel.

The OFDM waveform requires more average SNR to combat the interference under the frequency selective Rayleigh fading than under the frequency-flat Rayleigh fading. This is shown in Figure 3.8 in which the greedy OFDM user needs a higher SNR to allocate power on the channels compared to the frequency non-selective environment (Figure 2.13). Above 25 dB, the greedy OFDM is able to achieve higher constellations by allocating more power into the channels, to which the greedy DSSS user reacts by choosing a higher SF to combat the increased interference. The counter-action of the greedy DSSS user is shown by the slow descent of the greedy DSSS rate curve above 25 dB in Figure 3.7 and the increased amount

of unused power of the greedy DSSS user above 25 dB in Figure 3.8 which indicates that only the highest SF strategy is available to the greedy DSSS user at that point.

When comparing Figure 2.13 and Figure 3.8, it is seen that the water-filling OFDM user wasted much more of its power resource in the wideband scenario than in the narrowband scenario. The smallest amount of wasted transmit power for the water-filling OFDM is 40% in the frequency non-selective environment while it is 65% in the frequency selective environment. This amount of transmit power does not provide for the user higher rates and has a disadvantageous effect on battery life, spectral footprint and allowing other opportunistic users access on the spectrum resource. However, this increase of the amount of wasted transmit power is not as noticeable for the water-filling DSSS user since it is more tolerant to the interference due to its different spreading factor strategy set.

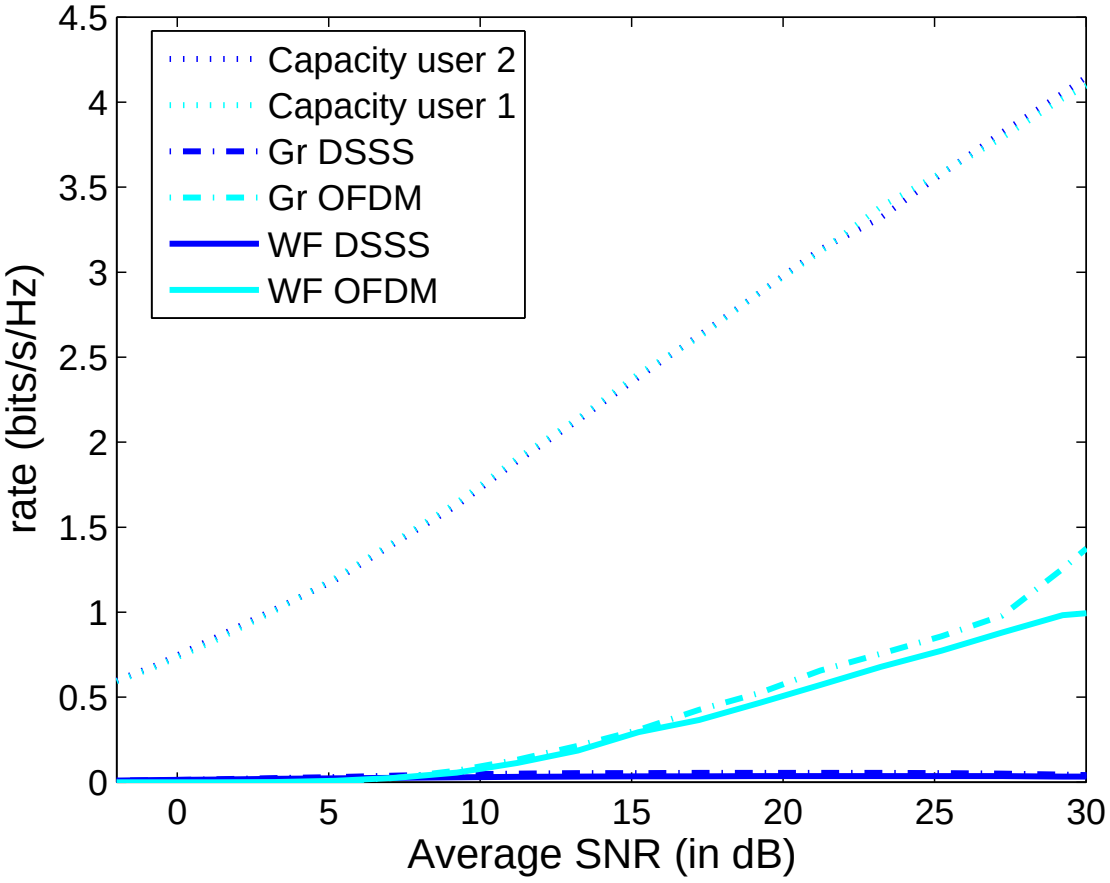


**Figure 3.6:** Rates for different resource allocation algorithms, scenario A.

The effect of the cross-talk $\beta$ discussed in Section 2.6.3 is similar in the wideband scenario.

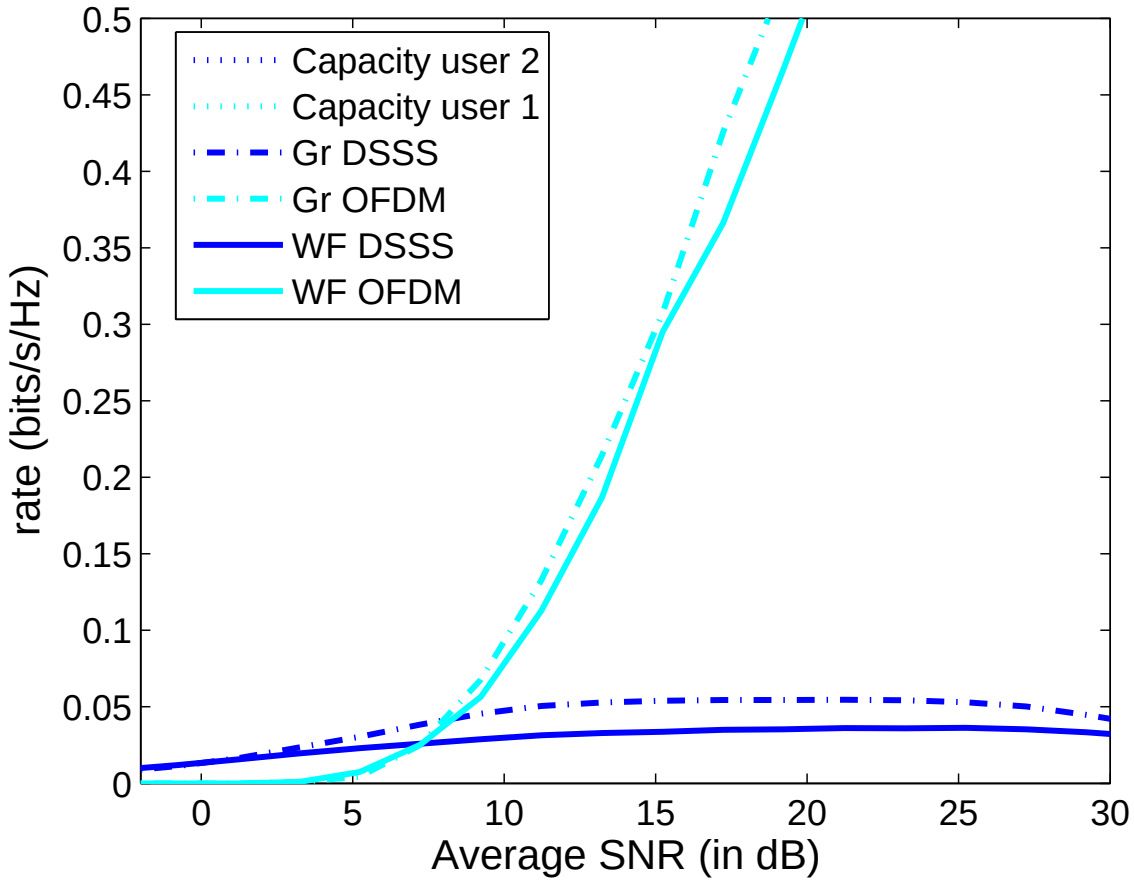


**Figure 3.7:** Rates for different resource allocation algorithms, scenario A. Close-up of Figure 3.6.

The order of the users is still important for the rate outcome of the greedy algorithm (see Figure 3.9); it is better for a user to play second in the proposed greedy iterative resource allocation algorithm if a solution equivalent to FDM is not applied. A demonstration of how a FDM equivalent solution could improve the greedy algorithm is shown in Section 3.6.2.

### 3.6.2 Scenario B - Coexistence of two OFDM users

One observation about the rates achieved in scenario B in the wideband model (Figure 3.10) is that the greedy OFDM user 1, the first user to play the iterative game, has a steep descent above an SNR of 20 dB before reaching a plateau at 30 dB while this behaviour is not observed in the frequency non-selective environment (Figure 2.15). It is observed, however, in the frequency non-selective environment when the cross-talk $\beta$ is increased (Figure 2.23(c)).

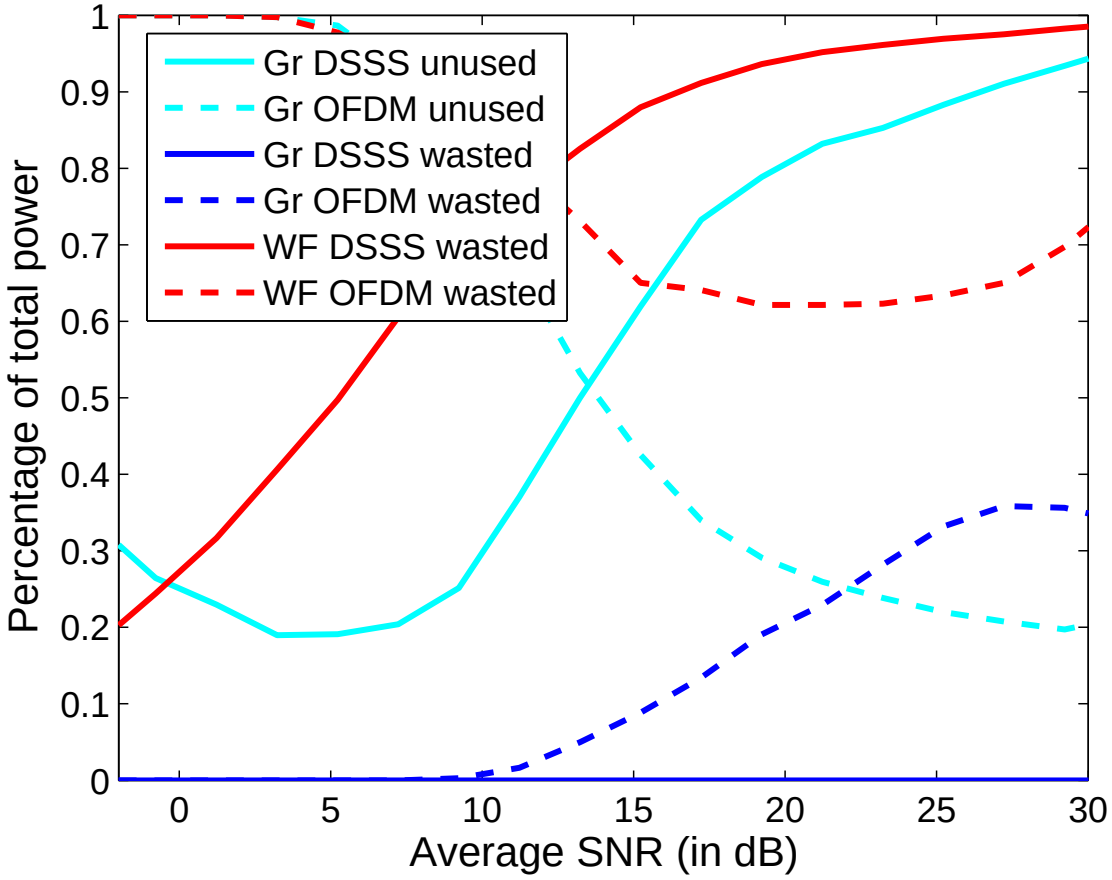


**Figure 3.8:** Power usage for different resource allocation algorithms, scenario A.

This is explained by the increased interference caused by the change of strategy of the second user. At high SNR, the second user is still able to achieve the higher constellations since it has the required transmit power. But this addition of transmit power creates a larger interference to the first user which it did not foresee. As discussed in Chapter 2, adding 'intelligence' in the greedy algorithm to observe when both users are switching back and forth between two solutions might improve the rate achieved by the greedy algorithm. One solution could be the application of a FDM equivalent solution at high SNR (in this case, SNR above 20 dB). This is shown in Figure 3.12 where the first user is forced to use only the first two channels while the second user is forced to use only the third channel. This solution could be further improved in allowing the users to choose the channels based on their attenuations while allowing only one user per channel when above a target SNR.

A second observation on Figure 3.10 is that once again the SNR gap cannot be usefully

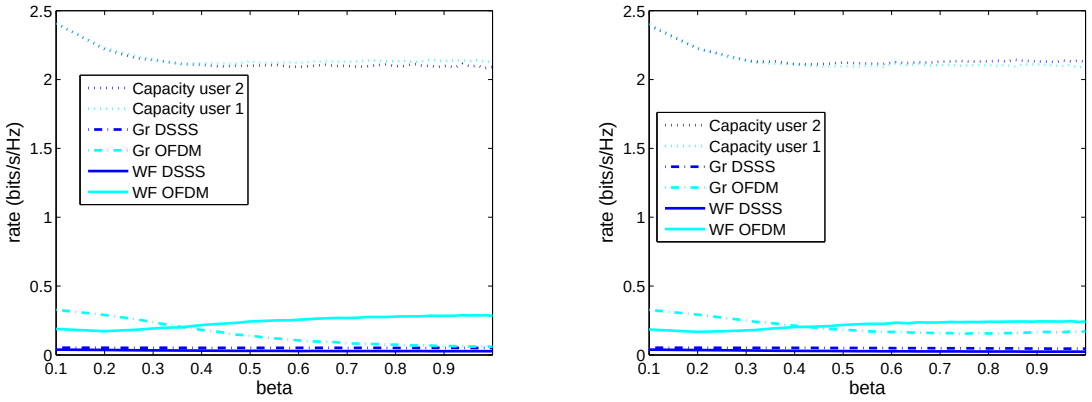


(a) OFDM user first

(b) OFDM user second

**Figure 3.9:** Rates achieved for Scenario A when average SNR is 13 dB and $\beta$ varies.

applied to this scenario. For both algorithms, the slopes of the curves are almost constant for an SNR below 15 dB. Above an SNR of 30 dB, the water-filling users reach a plateau; the greedy users also reach a plateau with the first user having practically no achievable rate and the second the maximal rate achievable under these conditions. Obviously, the latter observation is changed when the FDM equivalent solution is applied at high SNR (Figure 3.12); both users reach a plateau, the second greedy user reaches the same level as the water-filling users while the first user has a higher achievable rate because it accesses two channels compared to the single channel of the second user.

As discussed in Section 3.6.1, in comparing Figures 2.16 and 3.11, it is shown that the water-filling algorithm wastes more transmit power in the frequency selective environment and the greedy algorithm decreases the amount of unused transmit power due to the multipath effect. At high SNR, the greedy second user shows a larger decrease in the amount of unused transmit power than the first user due to the increase of transmit power required to achieve a higher constellation rate. This was not observed in the frequency non-selective environment because at high SNR, both users could achieve the highest constellations which requires, in the frequency non-selective environment, a smaller differential in transmit power from one constellation to another constellation; therefore, the mutual interference generated by the last change in strategy of the second user has less impact on the rate outcome of the first user in the frequency non-selective environment than in the frequency selective environment.

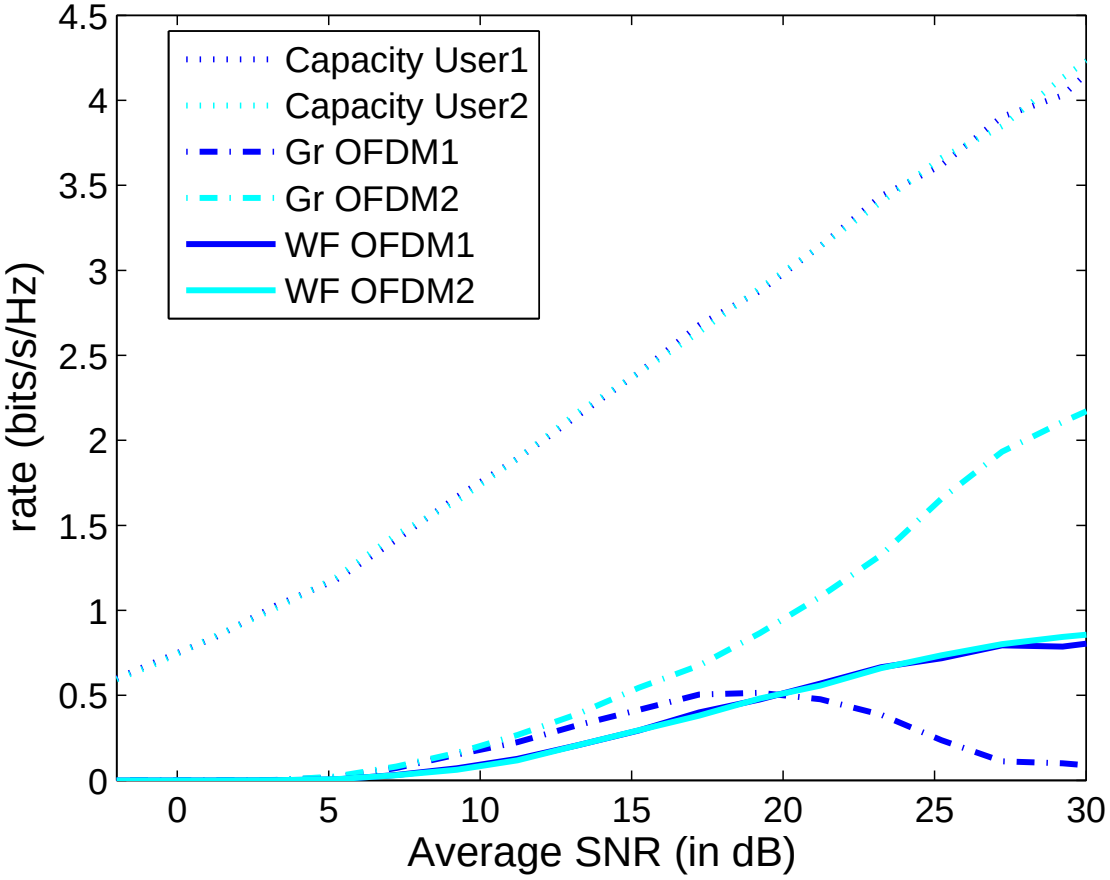


**Figure 3.10:** Rates for different resource allocation algorithms, scenario B.

While comparing Figure 3.11 without the prescribed FDM equivalent solution enforced at high SNR; and Figure 3.13 where the FDM is enforced for high SNR above 20 dB, it is observed that while the greedy algorithm achieves higher rate than the water-filling, less transmit power is required in the enforced FDM equivalent solution.

## 3.7 Conclusion

Although not a realistic scenario because of the assumptions taken to simplify the problem and focus on the greedy and water-filling algorithms' behaviour, the wideband scenario provides insight that in a frequency selective environment, the iterative greedy algorithm still provides a higher rate than iterative water-filling using the Shannon capacity for the real signals considered when the cross-talk $\beta$ is low. The same conclusions as Section 2.7 can

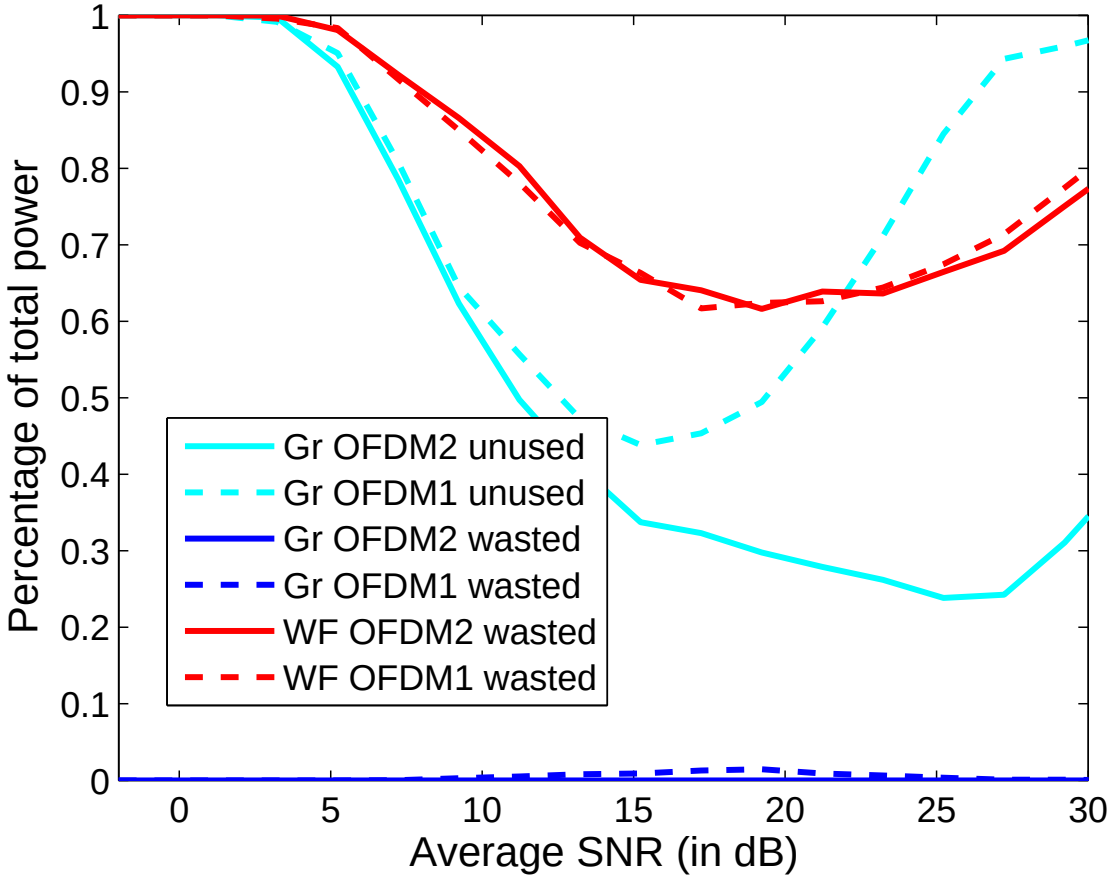


**Figure 3.11:** Power usage for different resource allocation algorithms, scenario B.

be drawn about the convergence of the greedy algorithm and the inclusion of fairness rules to improve the rate outcome.

It has been also shown that similarly to Section 2.6, the greedy algorithm does not always allocate all its transmit power, therefore reducing the mutual interference and reducing the spectrum footprint. The same advantages mentioned in Section 2.7 about this feature also apply with this scenario.

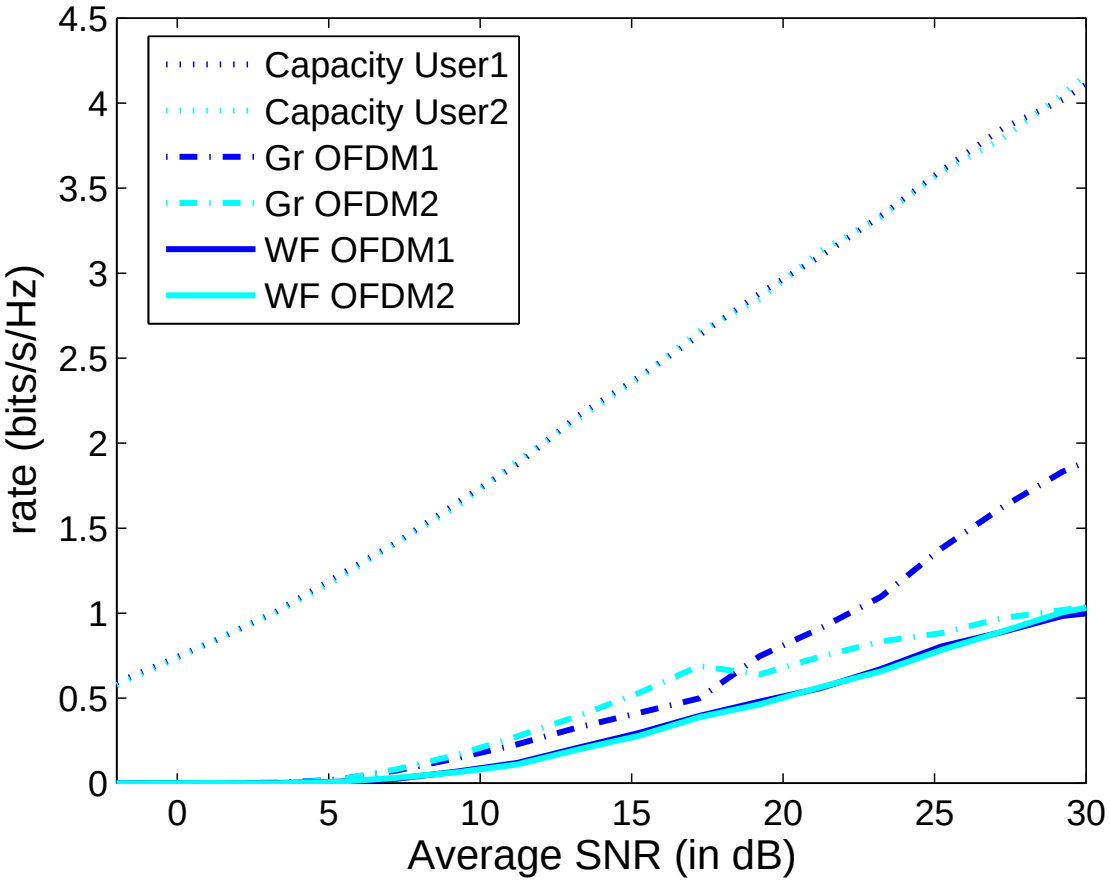


**Figure 3.12:** Rates for different resource allocation algorithms when FDM is applied at high SNR, scenario B.

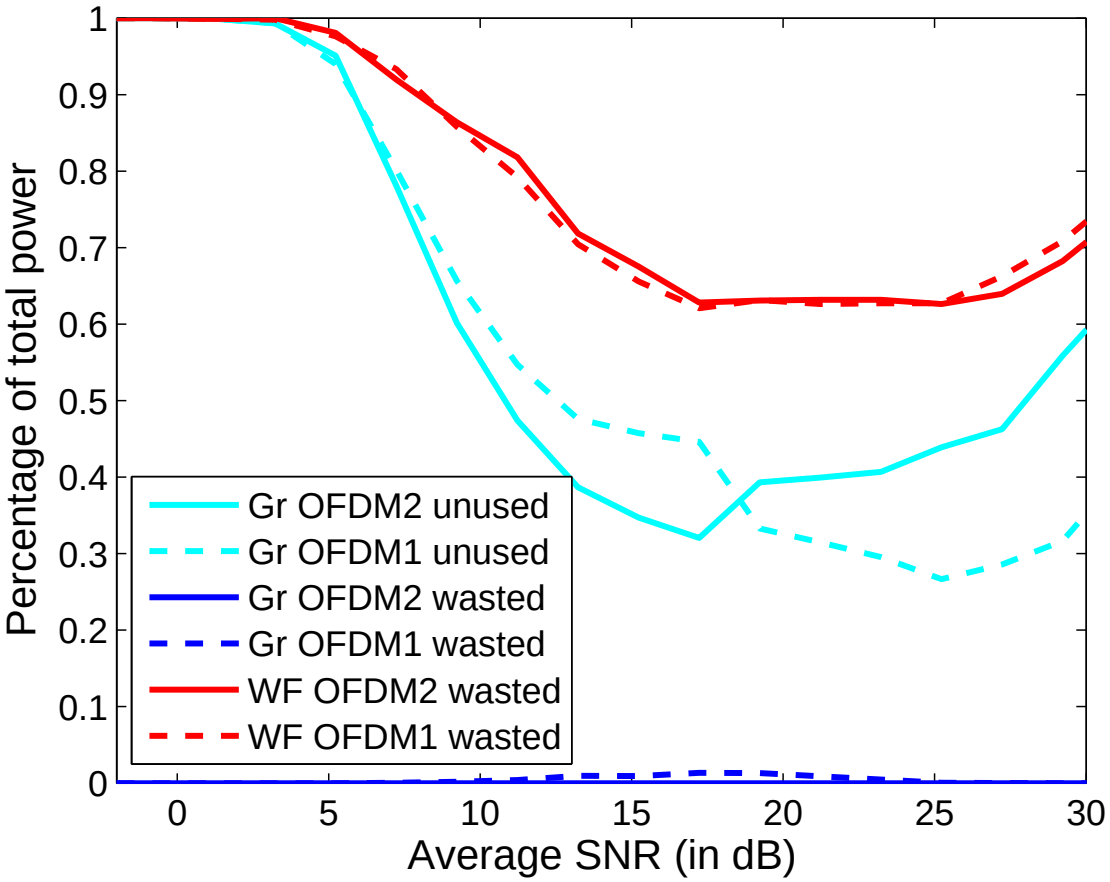


**Figure 3.13:** Power usage for different resource allocation algorithms when FDM is applied at high SNR, scenario B.

# Chapter 4

# Future Spectrum Management

In Chapters 2 and 3, two scenarios have been explored with the first having two users using different waveforms and the second both of them using the same waveform. It has been shown in this thesis that knowing the signal waveform and having a utility function that takes into account the actual signal characteristics and the minimal transmit power required achieves a higher rate outcome. However, only two waveforms have been explored in this thesis: DSSS and OFDM. Other waveforms are used in real systems such as continuous phase modulation (CPM) [47] and the hybrid use of both waveforms, OFDM-CDMA [37, 48]. For a more complete study, this work should be extended to other waveforms.

In this thesis, two channel models have been used, the Rayleigh flat-fading channel for the frequency non-selective environment and the multipath Rayleigh fading channel for the frequency selective environment. In the case of the multipath Rayleigh fading channel, the number of paths, delays and fading variance have been fixed. Further work should analyze the impact that other channel models (Rician for example), delays and fading variance have on the greedy algorithm.

This thesis has studied the case of a two users sharing the same spectrum segments. Based on the central limit theorem, it is expected that increasing the number of users on the spectrum segment, the interference plus noise will more closely resemble additive white Gaussian noise. The work of this thesis could be extended to study the behaviour of the greedy algorithm when the number of spectrum sharing users increases to verify if the AWGN hypothesis made above is realistic. Furthermore, the work of this thesis could be extended to analyze the behaviour of the greedy algorithm when the users do not have the same

limitation on transmit power.

The size of the database is not really an issue as the hardware required for the storage of these databases is available as an enabling technology. Moreover, the cost of the hardware will be much more lower and accessible than the cost of spectrum licence. However, building databases that will contain lookup tables for all expected scenarios could be time-consuming, although it only needs to be done once. The REM discussed in Section 1.1 could be the network support providing these databases where initial lookup tables could be stored. As mentioned in Section 1.1, the cognitive radios must be capable of observing their environment and learning from these observations. Learning algorithms could take advantage of these observations and complete the knowledge of the signal characteristics in building or modifying the information in the lookup tables. Data mining techniques could be used by the cognitive radio to recognize a pattern concerning the temporal, spatial and frequency characteristics of the spectrum band in a geographical region. When a cognitive radio wants to access a spectrum hole opportunistically, the signal characteristics lookup tables could be pre-computed based on the patterns related to that spectrum hole before starting the resource allocation algorithm.

Spectrum agility is a challenge and must be considered carefully. Most real systems have seamless communications as a quality of service requirement. Prior to changing the frequency, spectrum sensing must be done ahead of time to ensure a good quality decision on the opportunistic use of the detected spectrum hole. The longer the spectrum sensing is done, the more accurate it is on the probability of detecting spectrum holes and primary users [12]. One must consider that while doing spectrum sensing, there is no transmission on that channel, i.e., connectivity is broken temporarily, so a proper balance must be determined in the allocation of spectrum sensing time and information transmission time. In addition to spectrum sensing time, spectrum management as discussed in Section 1.1, i.e., spectrum quality analysis, must be done to compute which spectrum holes offer the best channel conditions. Since the channel conditions are not static in a wireless environment, the cognitive radio ideally have access to the REM to get the expected pathloss and channel attenuations for this specific spectrum hole. This requires overhead communication, which uses bandwidth and time. Furthermore, an agreement protocol must be exchanged between the user receiver and user transmitter prior to switching frequency to allow proper handoff on the vacating frequency and handshake on the new frequency. Therefore, switching frequency

should be considered the last option; that is, it should only be considered when the channel conditions no longer provide the level of QoS required by the system.

The work in this thesis suggests two other solutions before considering switching frequency. The first is the use of non-contiguous spectrum holes [5]. Using non-contiguous spectrum holes might increase the probability of getting seamless communications since different spectrum holes would not have the same pathloss. Also, if one of the non-contiguous channels gradually provides decreasing QoS quality required by the user, the user could gradually switch into the other non-contiguous channels until the QoS of that channel increases again or until the user decides to drop it. The second solution is waveform adaption. Rate and power can be modified adaptively to adjust to temporal changes in the characteristics of the spectrum holes. Systems can also adapt to their environment by changing their waveform.

To illustrate waveform adaptation, a basic scenario of two users sharing the same spectrum segment is proposed in Figure 4.1. Only one multipath Rayleigh fading channel is considered and the parameters are the same as in Chapter 3. The two users share a spectrum segment of 5 MHz at 2 GHz (wavelength = 0.15 m) frequency bands. Each user keeps its transmitter and receiver pair the same distance apart so an average SNR of 20 dB is assumed. Also, the distance between the transmitter of user 1 and the receiver of user 2 is the same as the distance between the transmitter of user 2 and the receiver of user 1. The standard pathloss model is used to compute the received interference from transmitter $j$ at receiver $i$ at distance $d$ is defined as:

$$P_{loss} = P_j(\frac{4\pi}{\lambda})^2 d^{-\alpha} \tag{4.1}$$

where $\lambda = 0.15$m, $d$ is the distance between transmitter $i$ and the receiver $j$ and $\alpha$ is the pathloss exponent. The pathloss exponent used for this scenario is 3. The maximum distance between transmitter $i$ and receiver $j$ is $D = 1$ km.

As demonstrated in Figure 4.1, when the distance $d$ is equal to $D = 1$ km, both users can use the OFDM waveform and achieve a QPSK constellation rate. As the distance $d$ reduces, both users are increasing first their transmit power to continue to transmit with a QPSK OFDM rate. Then one user has to change its modulation level to BPSK OFDM; it is noted that the power allocation of both users are adapted (decrease amount of transmit power) to that user's constellation change because it also adapts its transmit power. Again,

as the distance $d$ continues to decrease, both users increase incrementally their transmit power until $d = 460$ m which becomes, in this scenario, a transition zone to change the waveform of at least one user. Both users can decide to keep OFDM as their waveform and the impact is that they have both to get the lowest OFDM constellation, i.e., BPSK, or one user (dark blue user at distance $d = 460$ m in Figure 4.1) might switch to BPSK DSSS waveform with a spreading factor $SF = 15$ which will allow the other user (pale blue user at distance $d = 460$ m in Figure 4.1) to achieve QPSK OFDM. Then increase in transmit power and change in OFDM constellation level is performed until the OFDM user reaches a point where it must also adapt its waveform (pale blue user at distance $d = 90$ m in Figure 4.1). The green line in Figure 4.1 demonstrates that for this scenario at $d = 210$ m, if both users were transmitting all their transmit power, the OFDM user would not be able to continue its communication any more on that channel unless it changes its waveform.

Spectrum sharing users may not have the same priority on the spectrum band. For example: the primary or licensed user should have priority over opportunistic users. Other priority levels might be considered such as military systems in an operational environment or medical systems in an emergency situation. There may be also a social agreement protocol that an opportunistic user must adhere to before transmitting on the spectrum band. Therefore, the utility function might be modified to reflect such a priority requirement. The scenario illustrated for the waveform adaption can also be modified to incorporate priorities which might force a user to adjust its waveform to minimize the mutual interference on a higher priority user.

It has been suggested in the literature that a price-based utility function [30] may improve the outcome of a non-cooperative game by approaching the Pareto optimal solution. The Pareto optimal solution is described as an operational point where no further change in the players' strategies can improve at least one player's outcome without decreasing the other players' outcomes [30]. It is slightly different from the Nash equilibrium where only one user is trying to improve its outcome in changing its strategy while the others keep the same strategy. In the Pareto optimal solution, more than one user can get their strategy set changes as long as at least one user improves its outcome and none have their outcome decreased. This has been shown for the iterative water-filling algorithm proposed in [30]. Future work could modify the greedy algorithm to include a price-based utility function and compare the improvement with other price-based algorithms.

Other algorithms for the spectrum resource allocation problem have explored the power minimization utility function. It could be interesting to compare the throughput and power allocation of the greedy algorithm with these. For effective spectrum management, power control is important to minimize the effect of mutual interference, especially in the spectrum sharing environment. The hardware may not be capable of adaptively adjusting its transmit power; however a spectrum manager might provide access to a spectrum segment to a user with the condition of a maximum transmit power.

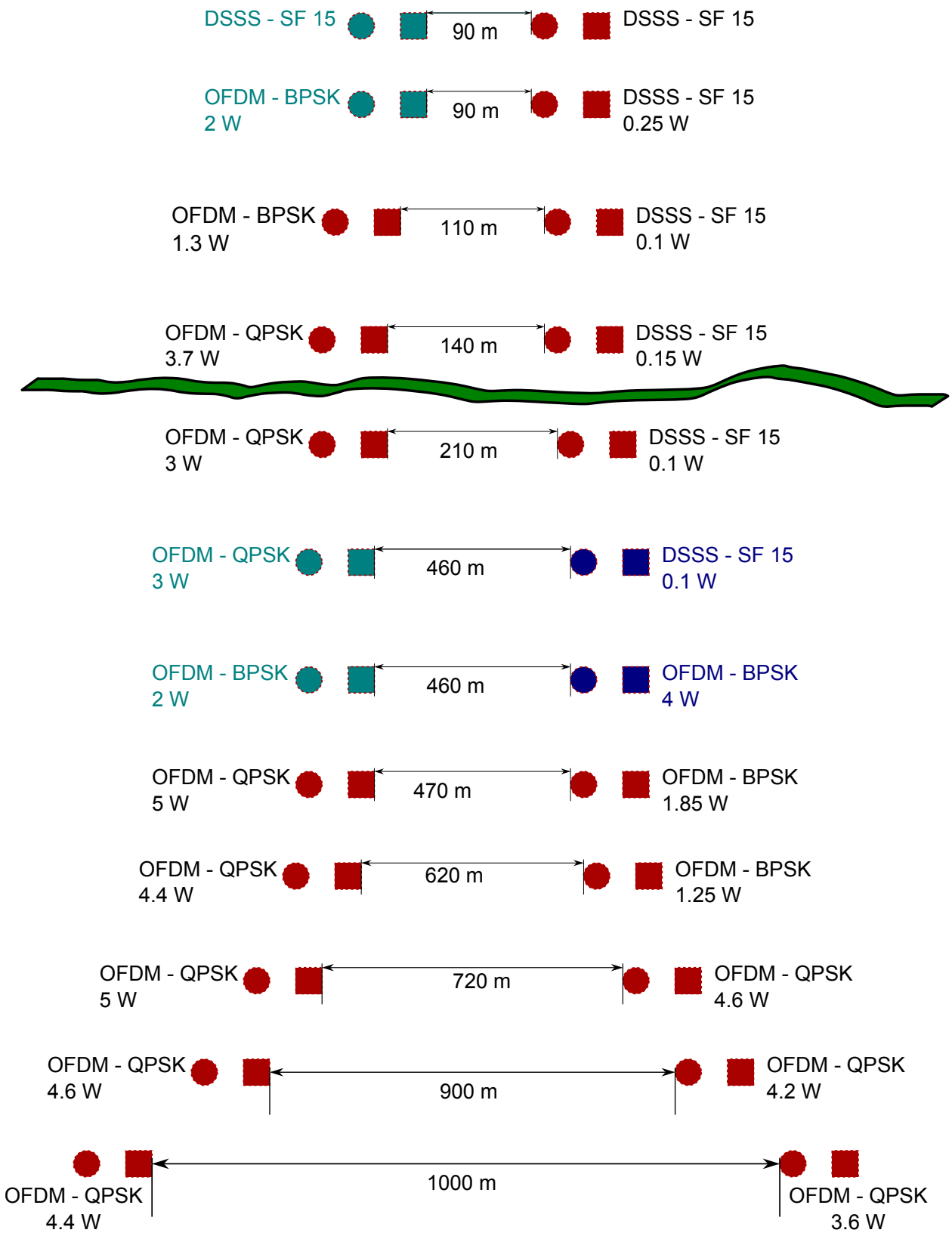


**Figure 4.1:** Spectrum management for two users sharing the same spectrum segment versus the distance.

# Chapter 5

# Conclusions

In this thesis, spectrum sharing resource allocation has been studied for a two user case. Two algorithms with different utility functions have been presented and compared. The first one is the well-known water-filling algorithm, which uses Shannon's capacity formula as its utility function to allocate transmit power on three different channels. The algorithm proposed in this thesis is a greedy algorithm that uses knowledge of the signal characteristics to adapt its rate while minimizing the power allocation on the three channels.

In Chapter 2, the two algorithms have been studied in a Rayleigh flat-fading channel. It has been shown that both algorithms provide solutions far below that of Shannon's formula, even for a $10^{-3}$ SER target. It is expected that worse outcomes would be provided by both algorithms if the SER target were below $10^{-3}$. The Shannon's capacity requires long codebooks and Gaussian constellations. The waveforms studied in this thesis, OFDM and DSSS, go against this assumption by being limited in their constellations and their bandwidth.

It has been also shown in Chapter 2 that while not always converging to an equilibrium, the greedy algorithm provides higher rates than the water-filling solution except when the cross-talk is strong. The higher rates obtained are due to the knowledge of the required transmit power for a certain level of received power of an interfering signal. The fact that the greedy algorithm minimized the transmit power on the channels reduced the mutual interference to both users. The effect of the cross-talk when it is strong is partly due to the non-convergence of the presented greedy algorithm.

Chapter 3 presents the frequency selective environment where the path fading and delays have been fixed for the purpose of simplicity. The behaviour of both algorithms has been

shown to be similar to that for the frequency non-selective environment.

Other than improved rate outcome provided by the greedy algorithm, the minimization of transmit power on the channels is an important advantage provided by the greedy algorithm. Minimizing transmit power on spectrum segments offers opportunities to others users to take advantage of the surrounding spectrum holes, saving battery life and reducing the spectral footprint.

Chapter 4 provides a discussion on future spectrum management challenges and some leads for future research. Spectrum agility, rate adaptation and power minimization are often discussed in literature but another solution could also include waveform adaptation. Spectrum agility might be inevitable when channels do not provide the required quality of service expected by a user's system but it must be done carefully to avoid a discontinuity in communication. Along with power minimization and rate adaptation, waveform adaptation may avoid the necessity of switching frequency and provide the advantage of more time to prepare the system if switching frequency is unavoidable. A scenario of a two-user case sharing the same spectrum segment has been discussed in Chapter 4 to illustrate the different options a user could have in its strategy set prior to switching into a different spectrum segment.

## 5.1 Further work

Spectrum sharing is an exciting area that could provide solutions to the limited access to spectrum resource induced by the present spectrum management policy. This thesis has studied the spectrum resource allocation through a non-cooperative environment to minimize the communications between users; an important feature often found in real systems. The insight provided by this thesis could be further developed in several areas.

The transmit power allocation and rate strategy choice of the greedy algorithm might be improved if refinements to the greedy algorithm were provided to recognize the symptoms of non-convergence and remedy to this situation in taking the proper steps. Moreover, learning algorithms could be added to the greedy algorithm to let it learn from its past decisions and improve in the future its choice strategy. Furthermore, fairness rules could be studied to modify the greedy algorithm to approach the Pareto optimal solution; this study will require investigation also of the cost of the additional overhead communication between the users

and compare it with the benefits obtained from the fairness rules.

This work could be modified to include additional spectrum sharing users and verify that the interference plus noise seen by all users' receivers will resemble additive white Gaussian noise.

Further analysis under different channel models and without perfect CSI would allow a deeper understanding of the impact the channel variations might have on the greedy algorithm's performance. This could be extended to be compared with other available spectrum resource allocation algorithms other than the water-filling algorithm.

The work proposed in this thesis could be extended to other waveforms. This involves prior knowledge of the signal characteristics before the spectrum resource allocation begins which can be provided by a central spectrum management authority, the local cognitive spectrum sensing and/or the REM. Further work could investigate the impact on all parties involved if one or more users have the wrong information about other users' signalling usage.

Spectrum agility is challenging; it requires overhead communication for knowledge spectrum holes and handoff/handshake between the receiver and transmitter. Waveform adaptation could be further studied as it might be easier and preferable for the user than spectrum agility. Moreover, as not all users might have the same priority on a spectrum segment or require the same quality of service requirements, priority hierarchy can be implemented to force a sharing user to change its waveform to minimize the mutual interference on a higher priority user.

# Appendix A

# Flow Charts

The simulations in this thesis were done in Matlab. The following flow charts show the process on how the simulations were done for the lookup tables and for the non cooperative spectrum resource sharing allocation algorithms. The initial transmit power for each rate strategy was determined based on the simulation results obtained to that point.

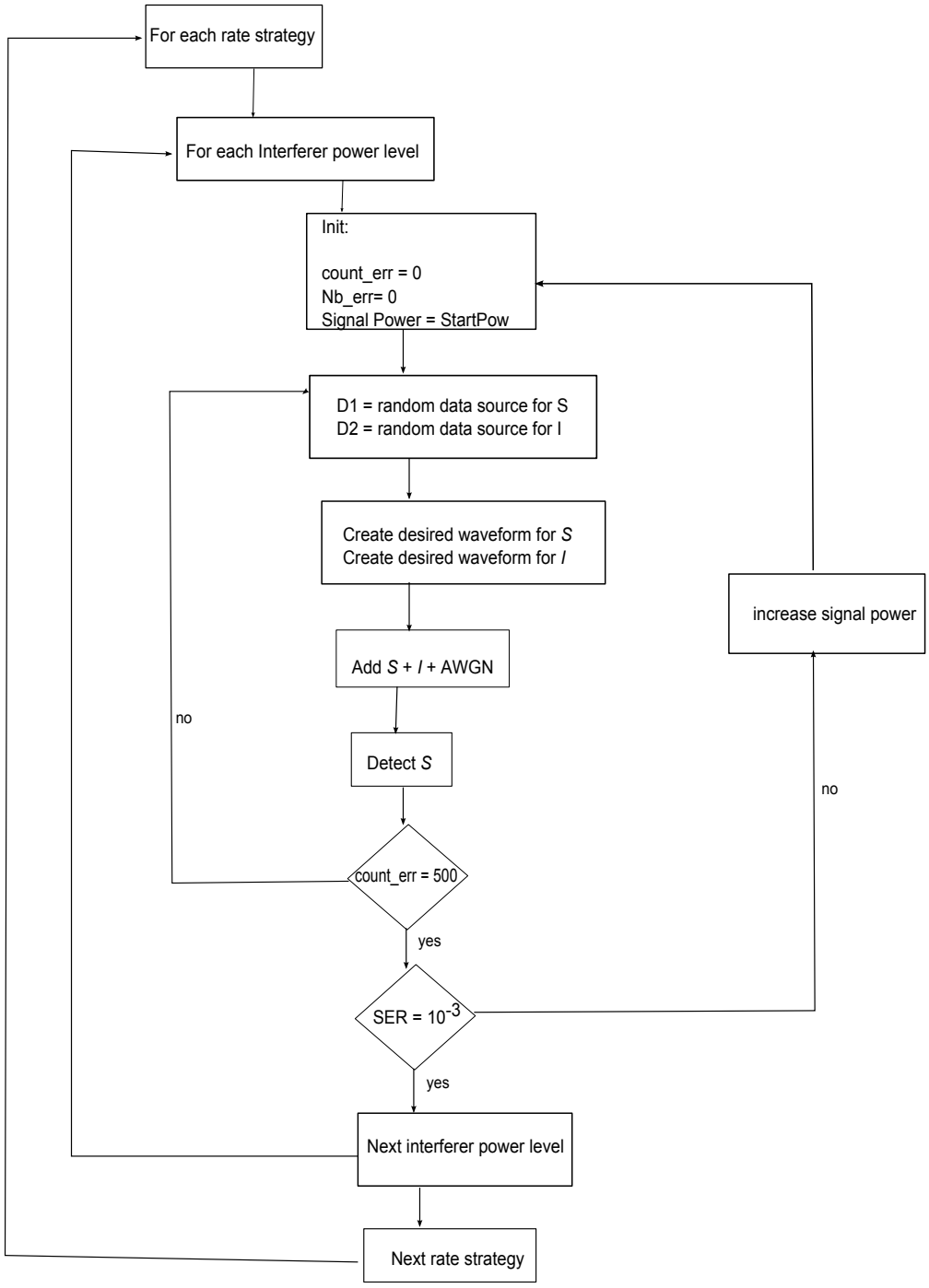


**Figure A.1:** Flow chart for the lookup table simulations for each waveform for the narrowband case.

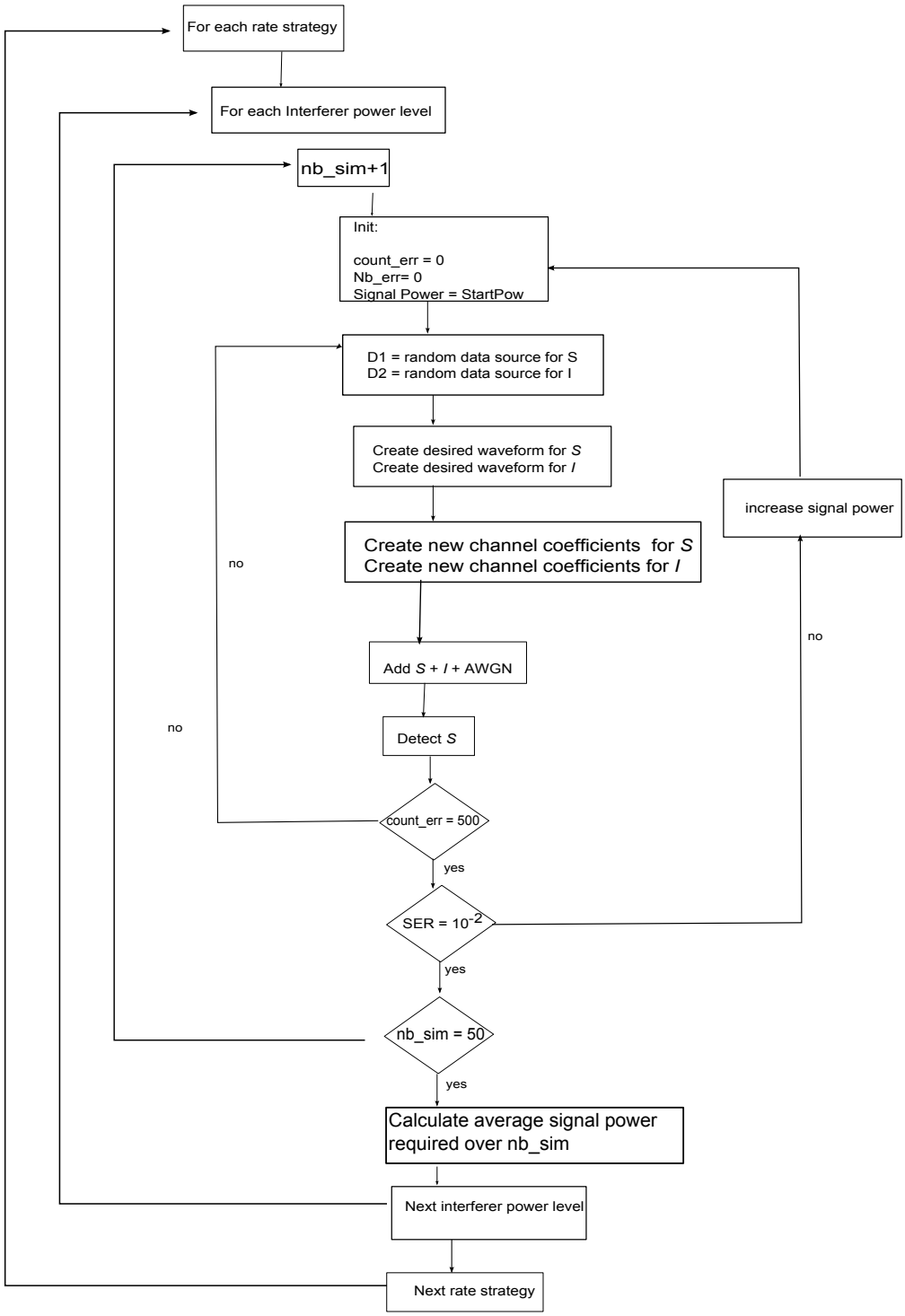


**Figure A.2:** Flow chart for the lookup table simulations for each waveform for the wideband case.

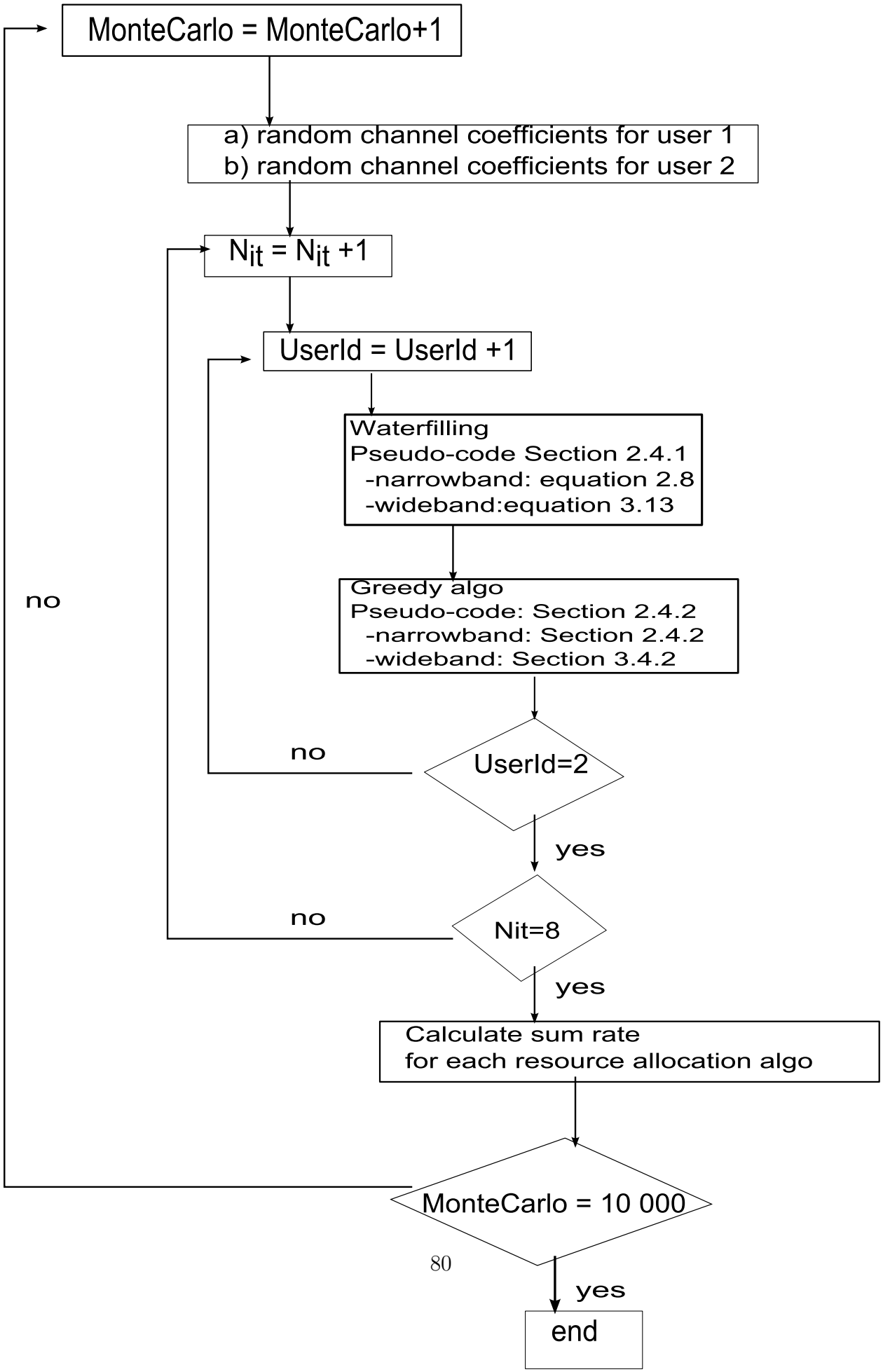




**Figure A.3:** Flow chart for the resource allocation algorithms.

# Appendix B

# Lookup tables

This appendix provides the lookup tables used in this thesis for the greedy algorithm utility function based on the signal characteristics. Each lookup table has been built through Monte Carlo simulations in Matlab for each user rate strategy with different interferer power levels. For the OFDM user, the set of rate strategies is based on the available modulation levels given by $R_1 = \{$BPSK, QPSK, 8-PSK, 16-QAM, 64-QAM$\}$. For the DSSS user, the set of rate strategies is given by the choice of a spreading factor and defined as $R_2 = \{SF = 1, 3, 7, 15\}$ for the frequency non-selective environment and $R_2 = \{SF = 15, 31, 63, 127\}$ for the frequency selective environment.

The lookup tables are built for an interference power $I$ and a received signal power $Q$ compared to a noise power equal to unity. The value in the lookup tables provides for each rate strategy the minimal required received power $Q$ under a specific level of interference $I$. For example, in Figure B.1 at a DSSS interferer power of 0 dBW, the OFDM user could not obtain any achievable rate for received power below $Q = 10$ dBW. For the same interferer, it could obtain a BPSK rate with a received transmit power above 10 dBW, a QPSK rate for a received transmit power of 13.4 dBW, a 8-PSK rate for a received transmit power of 18.8 dBW. This is further shown with the figures following the lookup tables (e.g., Figure B.2) where the region of an achievable rate is shown for a received transmit power versus the interference power.

| Interference I (dBW) | Received power Q (in dBW) | | | | |
|---|---|---|---|---|---|
| | BPSK | QPSK | 8-PSK | 16-QAM | 64-QAM |
| 0 | 10 | 13.424 | 18.751 | 20.607 | 26.767 |
| 7.7815 | 14.914 | 18.573 | 23.892 | 25.798 | 32.082 |
| 10.414 | 17.243 | 20.864 | 26.18 | 28.062 | 34.385 |
| 12.041 | 18.633 | 22.355 | 27.597 | 29.614 | 35.894 |
| 13.222 | 19.868 | 23.464 | 28.722 | 30.626 | 36.981 |
| 14.15 | 20.755 | 24.265 | 29.638 | 31.553 | 37.864 |
| 14.914 | 21.461 | 25.011 | 30.273 | 32.304 | 38.558 |
| 15.563 | 22.041 | 25.647 | 30.934 | 32.956 | 39.232 |
| 16.128 | 22.672 | 26.201 | 31.538 | 33.473 | 39.768 |
| 16.628 | 23.139 | 26.693 | 32.055 | 33.953 | 40.255 |
| 17.076 | 23.522 | 27.177 | 32.492 | 34.37 | 40.676 |
| 17.482 | 23.838 | 27.536 | 32.856 | 34.8 | 41.096 |
| 17.853 | 24.314 | 27.903 | 33.181 | 35.152 | 41.449 |
| 18.195 | 24.639 | 28.274 | 33.493 | 35.484 | 41.8 |
| 18.513 | 24.914 | 28.585 | 33.865 | 35.804 | 42.083 |
| 18.808 | 25.289 | 28.82 | 34.108 | 36.037 | 42.4 |
| 19.085 | 25.551 | 29.122 | 34.401 | 36.36 | 42.671 |
| 19.345 | 25.798 | 29.355 | 34.691 | 36.618 | 42.918 |
| 19.59 | 25.999 | 29.6 | 34.914 | 36.866 | 43.133 |
| 19.823 | 26.201 | 29.832 | 35.132 | 37.059 | 43.379 |
| 20.043 | 26.474 | 30.03 | 35.384 | 37.308 | 43.571 |
| 20.253 | 26.665 | 30.261 | 35.581 | 37.517 | 43.806 |
| 20.453 | 26.866 | 30.461 | 35.746 | 37.709 | 43.985 |
| 20.645 | 27.016 | 30.652 | 35.96 | 37.903 | 44.201 |
| 20.828 | 27.243 | 30.888 | 36.133 | 38.069 | 44.379 |
| 21.004 | 27.412 | 31.011 | 36.32 | 38.225 | 44.555 |
| 21.173 | 27.612 | 31.179 | 36.459 | 38.417 | 44.711 |
| 21.335 | 27.686 | 31.326 | 36.632 | 38.555 | 44.862 |

**Figure B.1:** Lookup Table BPSK OFDM user with BPSK DSSS $SF = 3$ interferer in AWGN channel. Received power $Q$ required for each level of Interference $I$. Noise power is equal to unity.

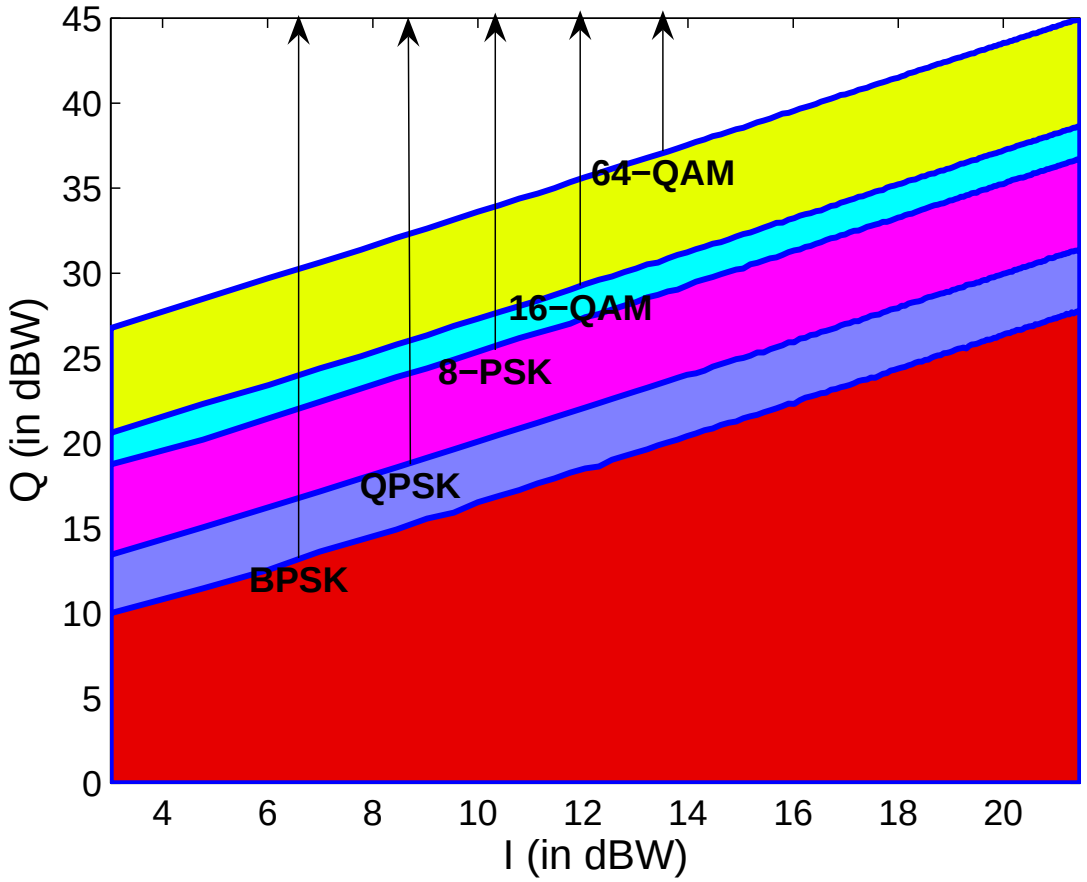


**Figure B.2:** Achievable rate for BPSK OFDM user with BPSK DSSS $SF = 3$ interferer in AWGN channel. Received power $Q$ required for each level of Interference $I$. Noise power is equal to unity.

| | Received power Q (in dBW) | | | |
|---|---|---|---|---|
| Interference I (in dBW) | SF=15 | SF=7 | SF=3 | SF=1 |
| 0 | 0 | 3.0103 | 6.0206 | 10 |
| 7.7815 | 4.7712 | 6.9897 | 10.792 | 15.051 |
| 10.414 | 6.0206 | 9.0309 | 12.788 | 17.324 |
| 12.041 | 7.7815 | 10.414 | 14.314 | 18.921 |
| 13.222 | 8.451 | 11.461 | 15.441 | 19.956 |
| 14.15 | 9.5424 | 12.553 | 16.335 | 20.864 |
| 14.914 | 10 | 13.222 | 17.076 | 21.614 |
| 15.563 | 10.414 | 13.979 | 17.709 | 22.201 |
| 16.128 | 11.139 | 14.472 | 18.195 | 22.788 |
| 16.628 | 11.461 | 14.914 | 18.692 | 23.201 |
| 17.076 | 12.041 | 15.441 | 19.085 | 23.711 |
| 17.482 | 12.553 | 15.682 | 19.542 | 24.031 |
| 17.853 | 12.788 | 16.021 | 19.868 | 24.456 |
| 18.195 | 13.01 | 16.435 | 20.212 | 24.786 |
| 18.513 | 13.424 | 16.721 | 20.569 | 25.079 |
| 18.808 | 13.802 | 16.99 | 20.828 | 25.391 |
| 19.085 | 13.979 | 17.243 | 21.004 | 25.647 |
| 19.345 | 14.314 | 17.559 | 21.367 | 25.922 |
| 19.59 | 14.472 | 17.782 | 21.553 | 26.096 |
| 19.823 | 14.771 | 17.993 | 21.818 | 26.385 |
| 20.043 | 14.914 | 18.129 | 21.987 | 26.561 |
| 20.253 | 15.185 | 18.325 | 22.227 | 26.794 |
| 20.453 | 15.315 | 18.573 | 22.43 | 26.99 |
| 20.645 | 15.563 | 18.751 | 22.625 | 27.177 |
| 20.828 | 15.682 | 18.976 | 22.788 | 27.34 |
| 21.004 | 15.911 | 19.085 | 22.967 | 27.505 |
| 21.173 | 16.128 | 19.294 | 23.139 | 27.657 |
| 21.335 | 16.232 | 19.445 | 23.304 | 27.825 |

**Figure B.3:** Lookup Table BPSK DSSS user with BPSK OFDM interferer in AWGN channel. Received power $Q$ required for each level of Interference $I$. Noise power is equal to unity.

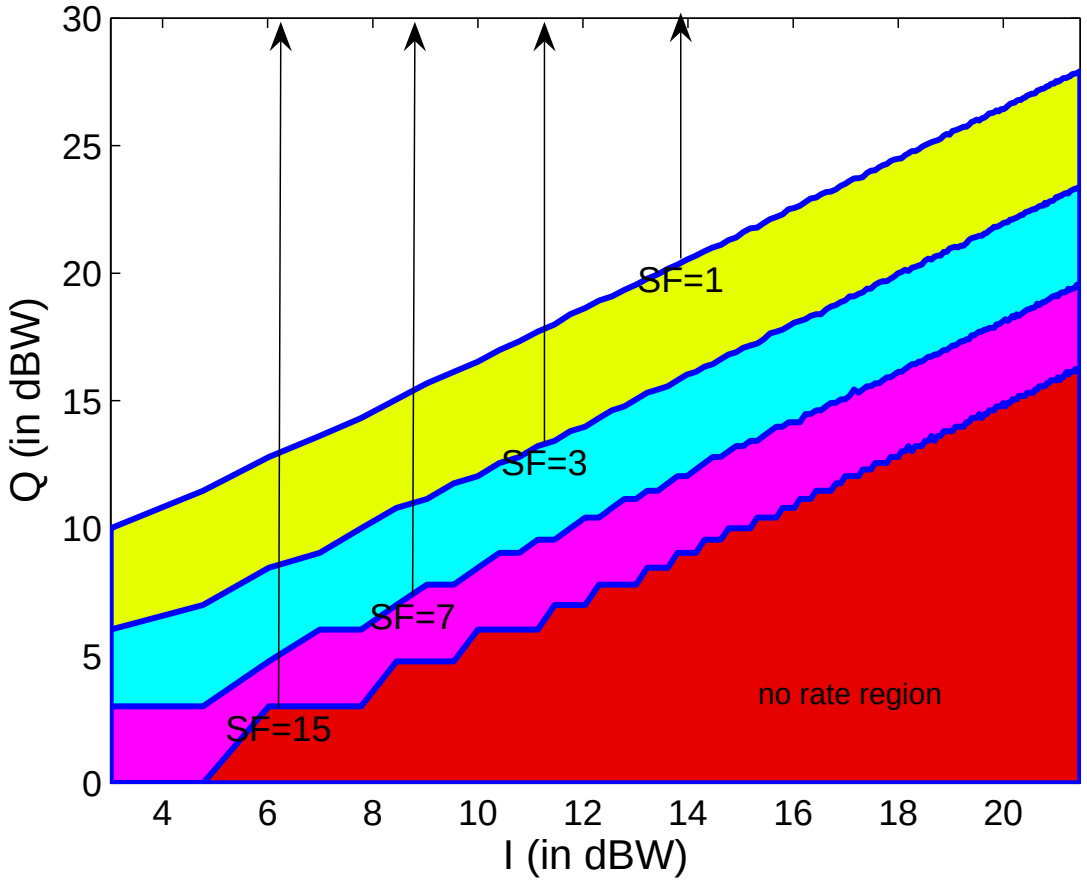


**Figure B.4:** Achievable rate for BPSK DSSS user with BPSK OFDM interferer in AWGN channel. Received power $Q$ required for each level of Interference $I$. Noise power is equal to unity.

| Interference I (dBW) | Received power Q (in dBW) | | | | |
|---|---|---|---|---|---|
| | BPSK | QPSK | 8-PSK | 16-QAM | 64-QAM |
| 0 | 10 | 12.788 | 17.993 | 20 | 26.263 |
| 7.7815 | 13.01 | 16.435 | 21.072 | 23.222 | 29.484 |
| 10.414 | 14.624 | 17.709 | 22.625 | 24.771 | 30.997 |
| 12.041 | 15.682 | 18.692 | 23.579 | 25.74 | 32.009 |
| 13.222 | 16.435 | 19.494 | 24.362 | 26.532 | 32.806 |
| 14.15 | 17.076 | 20.17 | 24.955 | 27.16 | 33.45 |
| 14.914 | 17.634 | 20.755 | 25.539 | 27.745 | 34.002 |
| 15.563 | 18.129 | 21.271 | 25.944 | 28.195 | 34.468 |
| 16.128 | 18.573 | 21.584 | 26.365 | 28.603 | 34.883 |
| 16.628 | 18.921 | 22.014 | 26.749 | 29.004 | 35.261 |
| 17.076 | 19.294 | 22.279 | 27.101 | 29.345 | 35.597 |
| 17.482 | 19.59 | 22.648 | 27.388 | 29.661 | 35.908 |
| 17.853 | 19.868 | 22.878 | 27.694 | 29.934 | 36.199 |
| 18.195 | 20.128 | 23.201 | 27.945 | 30.233 | 36.467 |
| 18.513 | 20.414 | 23.404 | 28.182 | 30.453 | 36.724 |
| 18.808 | 20.645 | 23.692 | 28.439 | 30.719 | 36.957 |
| 19.085 | 20.864 | 23.874 | 28.651 | 30.952 | 37.183 |
| 19.345 | 21.106 | 24.133 | 28.882 | 31.139 | 37.39 |
| 19.59 | 21.303 | 24.298 | 29.074 | 31.351 | 37.591 |
| 19.823 | 21.492 | 24.533 | 29.258 | 31.523 | 37.791 |
| 20.043 | 21.673 | 24.683 | 29.435 | 31.717 | 37.961 |
| 20.253 | 21.818 | 24.9 | 29.605 | 31.889 | 38.141 |
| 20.453 | 21.987 | 25.038 | 29.768 | 32.055 | 38.298 |
| 20.645 | 22.175 | 25.172 | 29.926 | 32.214 | 38.462 |
| 20.828 | 22.33 | 25.366 | 30.077 | 32.368 | 38.617 |
| 21.004 | 22.455 | 25.49 | 30.224 | 32.516 | 38.77 |
| 21.173 | 22.601 | 25.611 | 30.346 | 32.672 | 38.906 |
| 21.335 | 22.742 | 25.786 | 30.484 | 32.799 | 39.038 |

**Figure B.5:** Lookup Table BPSK OFDM user with BPSK OFDM interference in AWGN channel. Received power $Q$ required for each level of Interference $I$. Noise is equal to unity.

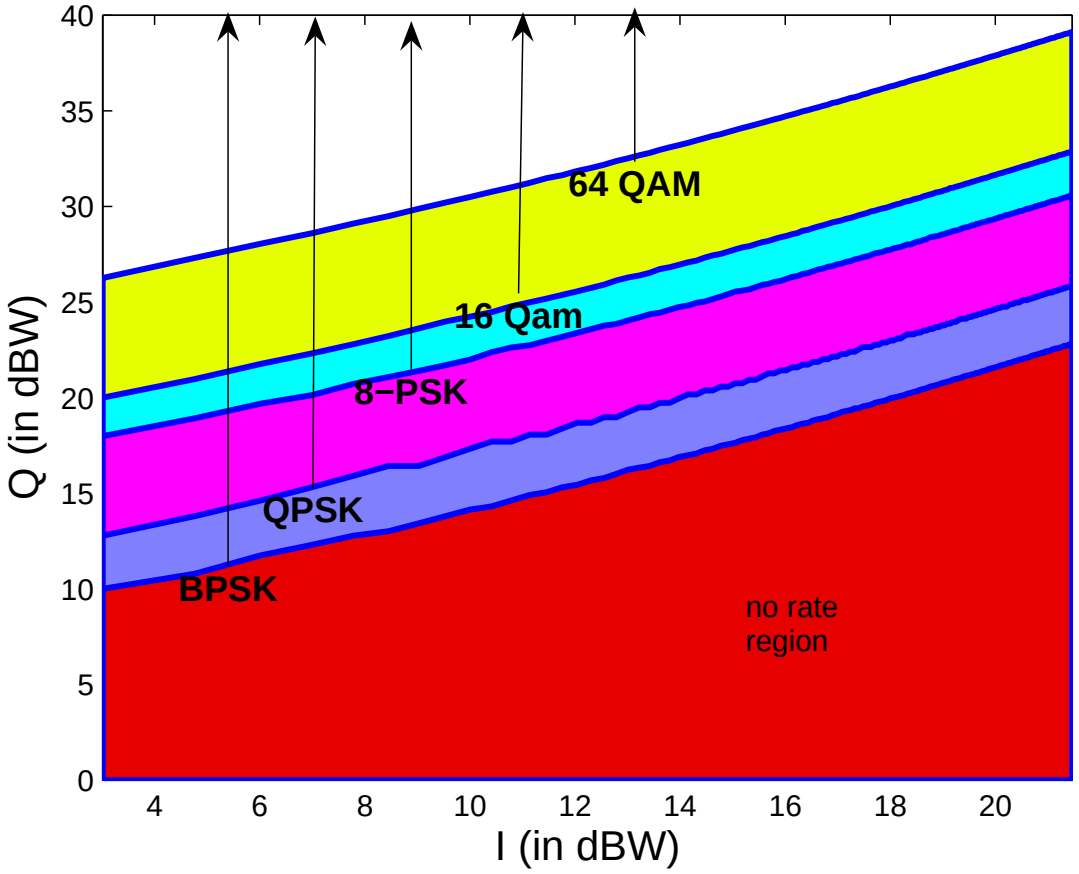


**Figure B.6:** Achievable rate for BPSK OFDM user with BPSK OFDM interference in AWGN channel. Received power $Q$ required for each level of Interference $I$. Noise is equal to unity.

| Interference I (dBW) | Received power Q (in dBW) | | | |
|---|---|---|---|---|
| | **BPSK** | **QPSK** | **8-PSK** | **16-QAM** |
| -10.0 | 15.4 | 21.2 | 27.1 | 29.309 |
| -7.0 | 16.5 | 21.9 | 27.3 | 30.37 |
| -5.2 | 16.5 | 21.9 | 27.5 | 30.618 |
| -4.0 | 17.1 | 22.3 | 27.6 | 31.045 |
| -3.0 | 17.3 | 22.9 | 28.2 | 31.139 |
| -2.2 | 17.8 | 23.0 | 28.7 | 31.139 |
| -1.5 | 18.0 | 23.6 | 28.9 | 31.229 |
| -1.0 | 18.5 | 23.7 | 29.1 | 31.83 |
| -0.5 | 18.8 | 24.3 | 29.6 | 31.945 |
| 0.0 | 19.1 | 24.5 | 29.7 | 32.095 |
| 0.4 | 19.1 | 24.7 | 29.9 | 32.13 |
| 0.8 | 19.2 | 24.8 | 30.0 | 32.253 |
| 1.1 | 19.3 | 25.0 | 30.1 | 32.751 |
| 1.5 | 20.0 | 25.1 | 30.3 | 32.962 |
| 1.8 | 20.2 | 25.1 | 30.3 | 33.081 |
| 2.0 | 20.2 | 25.6 | 30.6 | 33.197 |
| 2.3 | 20.2 | 25.6 | 30.8 | 33.56 |
| 2.6 | 20.2 | 25.7 | 31.1 | 33.585 |
| 2.8 | 20.4 | 26.0 | 31.2 | 33.585 |
| 3.0 | 20.9 | 26.2 | 31.3 | 33.8 |
| 3.2 | 20.9 | 26.3 | 31.5 | 34.089 |
| 3.4 | 21.0 | 26.3 | 31.6 | 34.317 |
| 3.6 | 21.2 | 26.5 | 31.8 | 34.42 |
| 3.8 | 21.2 | 26.8 | 31.8 | 34.555 |
| 4.0 | 21.2 | 26.8 | 32.1 | 34.807 |
| 4.1 | 21.2 | 26.8 | 32.2 | 34.961 |
| 4.3 | 21.4 | 26.9 | 32.3 | 35.027 |
| 4.5 | 21.5 | 27.1 | 32.3 | 35.24 |
| 4.6 | 21.5 | 27.3 | 32.3 | 35.347 |
| 4.8 | 22.0 | 27.3 | 32.3 | 35.382 |
| 4.9136 | 21.959 | 27.372 | 32.509 | 35.403 |
| 5.0515 | 21.987 | 27.551 | 32.914 | 35.577 |
| 5.1851 | 22.014 | 27.612 | 32.978 | 35.656 |
| 5.3148 | 22.148 | 27.612 | 32.989 | 35.817 |
| 5.4407 | 22.148 | 27.731 | 33.043 | 35.853 |
| 5.563 | 22.148 | 27.752 | 33.143 | 35.857 |
| 5.682 | 22.279 | 27.803 | 33.267 | 35.986 |
| 5.7978 | 22.455 | 27.81 | 33.332 | 36.02 |
| 5.9106 | 22.455 | 27.825 | 33.373 | 36.121 |
| 6.0206 | 22.504 | 28.331 | 33.583 | 36.229 |

**Figure B.7:** Lookup Table BPSK OFDM user with BPSK DSSS $SF = 15$ interferer for the frequency selective environment. Received power $Q$ required for each level of Interference $I$. Noise is equal to unity.

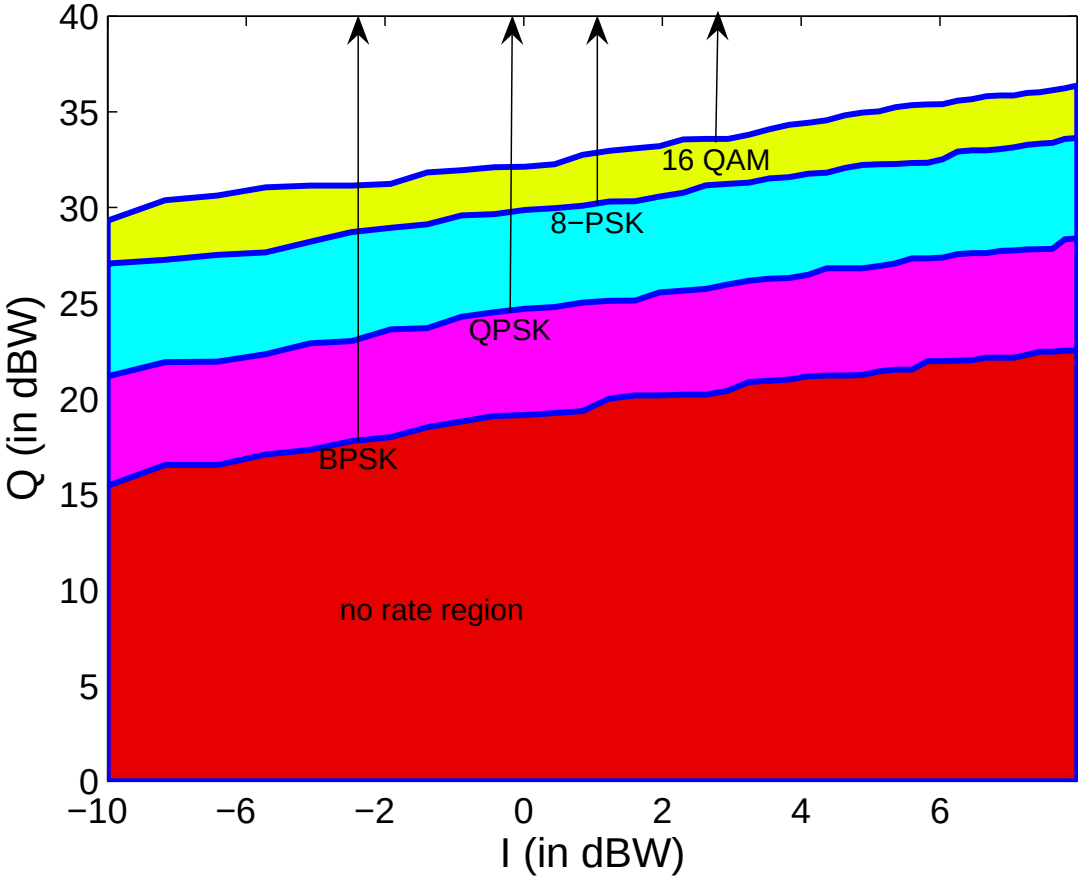


**Figure B.8:** Achievable rate for BPSK OFDM user with BPSK DSSS $SF = 15$ interferer for the frequency selective environment. Received power $Q$ required for each level of Interference $I$. Noise is equal to unity.

| | Received power Q (in dBW) | | | |
|---|---|---|---|---|
| Interference (in dBW) | SF=127 | SF=63 | SF=31 | SF=15 |
| 7.0 | 0.0 | 3.0 | 3.0 | 7.0 |
| 10.0 | 0.0 | 3.0 | 6.0 | 9.0 |
| 11.8 | 3.0 | 4.8 | 7.8 | 10.4 |
| 13.0 | 3.0 | 6.0 | 9.0 | 11.8 |
| 14.0 | 4.8 | 7.0 | 9.5 | 12.8 |
| 14.8 | 4.8 | 7.8 | 10.4 | 14.0 |
| 15.4 | 6.0 | 8.5 | 11.1 | 14.8 |
| 16.0 | 6.0 | 9.0 | 11.8 | 14.8 |
| 16.5 | 7.0 | 9.5 | 12.3 | 15.4 |
| 17.0 | 7.0 | 10.0 | 12.8 | 16.0 |
| 17.4 | 7.0 | 10.0 | 12.8 | 16.5 |
| 17.8 | 7.8 | 10.4 | 14.0 | 17.0 |
| 18.1 | 7.8 | 10.8 | 14.0 | 17.0 |
| 18.5 | 7.8 | 11.1 | 14.0 | 17.0 |
| 18.8 | 8.5 | 11.5 | 14.8 | 17.8 |
| 19.0 | 8.5 | 11.8 | 14.8 | 18.1 |
| 19.3 | 9.0 | 12.0 | 15.4 | 18.1 |
| 19.5 | 9.0 | 11.8 | 15.4 | 18.5 |
| 19.8 | 9.5 | 12.0 | 15.4 | 18.5 |
| 20.0 | 9.5 | 12.3 | 16.0 | 18.8 |
| 20.2 | 9.5 | 12.8 | 16.0 | 19.0 |
| 20.4 | 10.0 | 12.8 | 16.0 | 19.3 |
| 20.6 | 10.4 | 14.0 | 16.5 | 19.3 |

**Figure B.9:** Lookup Table BPSK DSSS $SF = 15$ user with BPSK OFDM interferer for the frequency selective environment. Received power $Q$ required for each level of Interference $I$. Noise is equal to unity.

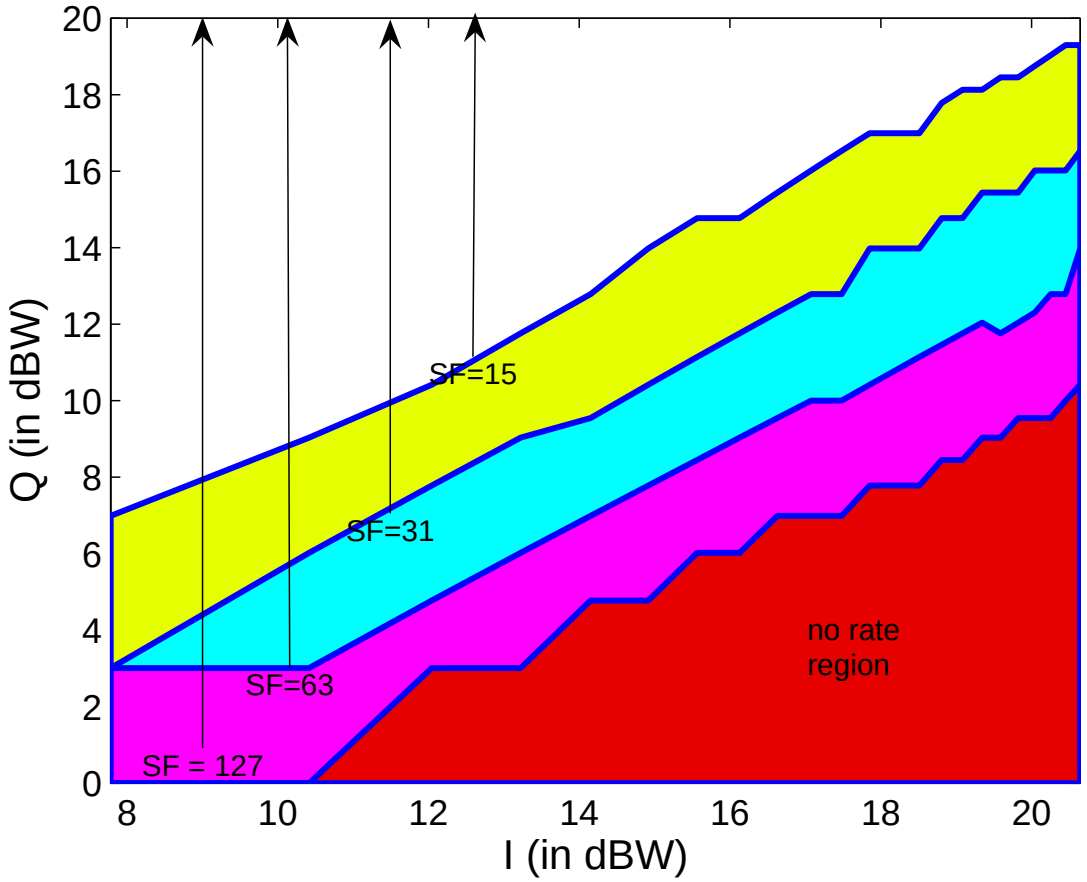


**Figure B.10:** Achievable rate for BPSK DSSS $SF = 15$ user with BPSK OFDM interferer for the frequency selective environment. Received power $Q$ required for each level of Interference $I$. Noise is equal to unity.

| Interference I (dBW) | Received power Q (in dBW) | | | |
|---|---|---|---|---|
| | **BPSK** | **QPSK** | **8-PSK** | **16-QAM** |
| -10.0 | 15.3 | 20.9 | 27.1 | 29.138 |
| -7.0 | 16.6 | 21.2 | 27.3 | 29.175 |
| -5.2 | 17.1 | 21.8 | 27.9 | 29.469 |
| -4.0 | 17.5 | 22.2 | 28.4 | 30.145 |
| -3.0 | 17.6 | 22.4 | 28.5 | 30.191 |
| -2.2 | 17.7 | 22.5 | 29.3 | 30.22 |
| -1.5 | 17.7 | 22.6 | 29.3 | 30.257 |
| -1.0 | 18.3 | 22.9 | 29.3 | 30.257 |
| -0.5 | 18.5 | 23.0 | 29.5 | 30.77 |
| 0.0 | 18.5 | 23.6 | 29.5 | 30.91 |
| 0.4 | 18.6 | 24.1 | 30.0 | 31.099 |
| 0.8 | 18.9 | 24.2 | 30.3 | 31.229 |
| 1.1 | 19.5 | 24.5 | 30.4 | 31.853 |
| 1.5 | 19.7 | 24.7 | 30.6 | 32 |
| 1.8 | 20.1 | 25.0 | 30.8 | 32.079 |
| 2.0 | 20.7 | 25.1 | 30.9 | 32.212 |
| 2.3 | 20.7 | 25.2 | 31.2 | 32.312 |
| 2.6 | 20.8 | 25.3 | 31.3 | 32.41 |
| 2.8 | 20.8 | 25.3 | 31.7 | 32.538 |
| 3.0 | 21.0 | 25.3 | 31.8 | 32.672 |
| 3.2 | 21.0 | 25.4 | 32.0 | 32.735 |
| 3.4 | 21.2 | 25.4 | 32.0 | 32.923 |
| 3.6 | 21.2 | 25.4 | 32.2 | 33.336 |
| 3.8 | 21.4 | 25.5 | 32.4 | 33.564 |
| 4.0 | 21.4 | 25.7 | 32.5 | 33.822 |
| 4.1 | 21.7 | 25.9 | 32.5 | 33.829 |
| 4.3 | 21.7 | 26.4 | 32.7 | 33.993 |
| 4.5 | 21.8 | 26.5 | 32.7 | 34.041 |
| 4.6 | 21.9 | 26.6 | 32.8 | 34.05 |
| 4.8 | 22.0 | 26.9 | 32.9 | 34.219 |
| 4.9136 | 22.175 | 27.093 | 33.049 | 34.354 |
| 5.0515 | 22.227 | 27.193 | 33.265 | 34.395 |
| 5.1851 | 22.279 | 27.308 | 33.326 | 34.464 |
| 5.3148 | 22.504 | 27.308 | 33.416 | 34.701 |
| 5.4407 | 22.648 | 27.364 | 33.444 | 34.767 |
| 5.563 | 22.672 | 27.642 | 33.619 | 34.83 |
| 5.682 | 22.788 | 27.649 | 33.679 | 34.89 |
| 5.7978 | 22.878 | 27.649 | 33.769 | 34.915 |
| 5.9106 | 22.9 | 27.738 | 33.858 | 34.933 |
| 6.0206 | 23.118 | 27.81 | 34.06 | 35.024 |

**Figure B.11:** Lookup Table BPSK OFDM user with BPSK OFDM interferer for the frequency selective environment. Received power $Q$ required for each level of Interference $I$. Noise is equal to unity.

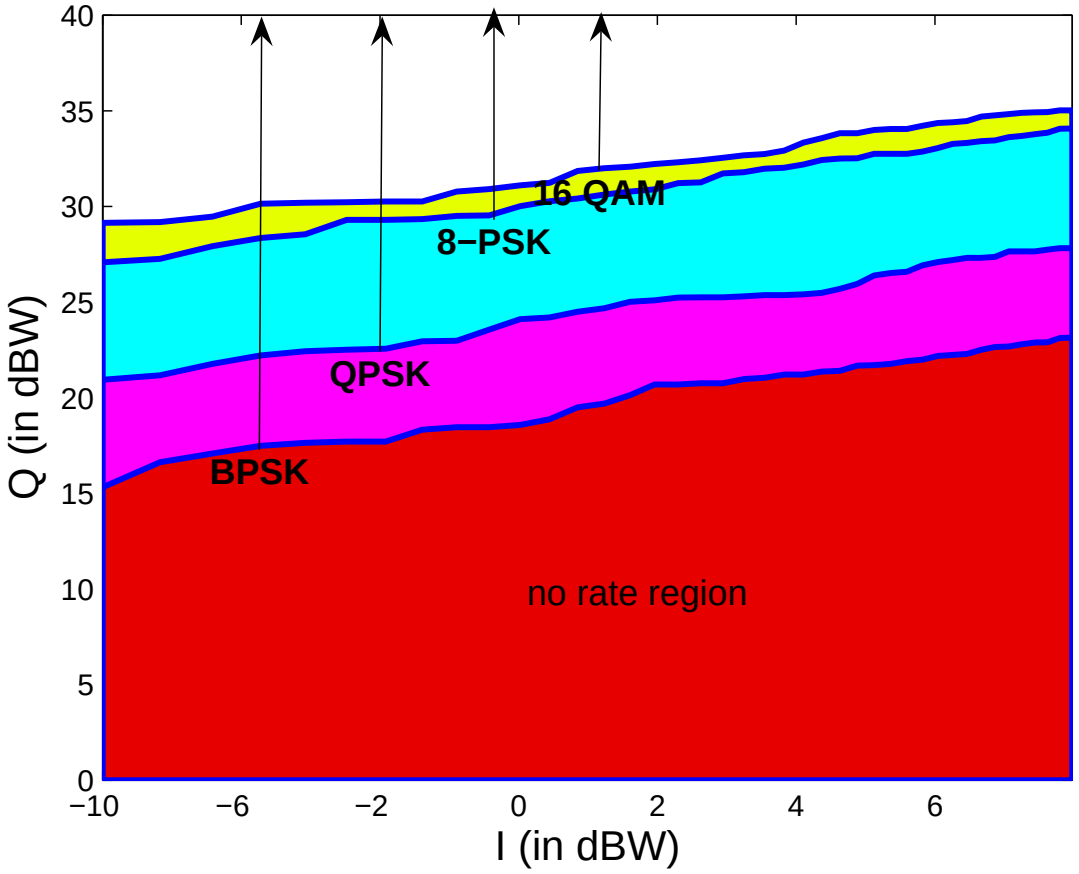


**Figure B.12:** Achievable rate for BPSK OFDM user with BPSK OFDM interferer for the frequency selective environment. Received power $Q$ required for each level of Interference $I$. Noise is equal to unity.

# Bibliography


[1] Federal Communications Commission, "Spectrum policy task force report." `http://transition.fcc.gov/sptf/files/SEWGFinalReport_1.pdf`, 2002.

[2] M. McHenry and D. McCloskey, "Multiband, multilocation spectrum occupancy measurements," in *Proc. Int. Symp. on Advanced Radio Technology*, (Boulder, CO, USA), pp. 167–175, Mar. 2006.

[3] J. Mitola III, *Cognitive radio: an integrated agent architecture for software defined radio*. PhD thesis, KTH Royal Institute of Technology, Sweden, 2000.

[4] S. Haykin, "Cognitive radio: Brain-empowered wireless communications," *IEEE J. Sel. Areas Commun.*, vol. 23, pp. 201–220, Feb. 2005.

[5] I. F. Akyildiz, W.-Y. Lee, M. C. Vuran, and S. Mohanty, "NeXt generation/dynamic spectrum access/cognitive radio wireless networks: a survey," *Computer Networks*, vol. 50, pp. 2127–2159, 2006.

[6] A. Goldsmith, S. A. Jafar, I. Maric, and S. Srinivasa, "Breaking spectrum gridlock with cognitive radios: An information theoretic perspective," *Proc. IEEE*, vol. 97, pp. 894–914, May 2009.

[7] B. A. Fette, *Cognitive Radio Technology*. Elsevier, Academic Press Editions, 2nd ed. ed., 2009.

[8] R. Tandra and A. Sahai, "SNR walls for signal detection," in *IEEE J. Sel. Topics Signal Process.*, vol. 2, pp. 4–17, Feb. 2008.

[9] R. Tandra and A. Sahai, "Fundamental limits on detection in low SNR under noise uncertainty," *Proc. Int. Conf. on Wireless Networks, Commun. and Mobile Comput.*, vol. 5, pp. 464–469, June 2005.

[10] A. Sonnenschein and P. M. Fishman, "Radiometric detection of spread-spectrum signals in noise of uncertain power," *IEEE Trans. Aerosp. Electron. Syst.*, vol. 28, pp. 654–660, July 1992.

[11] G. Ganesan and Y. (G.) Li, "Cooperative spectrum sensing in cognitive radio networks Part I: Two users network," *IEEE Trans. Wireless Commun.*, vol. 6, pp. 2204–2213, June 2007.

[12] T. Yucek and H. Arslan, "A survey of spectrum sensing algorithms for cognitive radio applications," *IEEE Commun. Surveys & Tutorials*, vol. 11, pp. 116–130, Mar. 2009.

[13] D. Cabric, S. M. Mishra, and R. W. Brodersen, "Implementation issues in spectrum sensing for cognitive radios," Nov. 2004.

[14] G. Ganesan and Y. (G.) Li, "Cooperative spectrum sensing in cognitive radio networks Part II: Multiuser networks," *IEEE Trans. Wireless Commun.*, vol. 6, pp. 2214–2222, June 2007.

[15] Y. Xiao and F. Hu, *Cognitive Radio Networks*. Auerbach Publications, 2009.

[16] J. M. Peha, "Sharing spectrum through spectrum policy reform and cognitive radio," *Proc. IEEE*, vol. 97, pp. 708–719, Apr. 2009.

[17] M. Van Der Schaar and F. Fu, "Spectrum access games and strategic learning in cognitive radio networks for delay-critical applications," *Proc. IEEE*, vol. 97, pp. 720–740, Apr. 2009.

[18] W. Yu, G. Ginis, and J. Cioffi, "Distributed multiuser power control for digital subscriber lines," *IEEE J. Sel. Areas Commun.*, vol. 20, pp. 1105–1115, June 2002.

[19] T. J. Willink and P. H. Wittke, "Optimization and performance evaluation of multicarrier transmission," *IEEE Trans. Inf. Theory*, vol. 43, pp. 426–440, Mar. 1997.

[20] Y. Xing, C. N. Mathur, M. A. Haleem, R. Chandramouli, and K. P. Subbalakshmi, "Dynamic spectrum access with QoS and interference temperature constraints," *IEEE Trans. Mobile Comput.*, vol. 6, pp. 423–433, Aug. 2007.

[21] R. Etkin, A. Parekh, and D. Tse, "Spectrum sharing for the unlicensed bands," in *Proc. IEEE DySPAN 2005*, pp. 251–258, Nov. 2005.

[22] N. Nie and C. Comaniciu, "Adaptive channel allocation spectrum etiquette for cognitive radio networks," in *Proc. IEEE DySPAN*, Nov. 2005.

[23] E. Larsson and E. Jorswieck, "Competition versus collaboration on the MISO interference channel," *IEEE J. Sel. Areas Commun.*, vol. 26, pp. 1059–1069, Sept. 2008.

[24] A. Leshem and E. Zehavi, "Cooperative game theory and the gaussian interference channel," *IEEE J. Sel. Areas Commun.*, vol. 26, pp. 1078–1088, Sept. 2008.

[25] R. Gohary and T. J. Willink, "Robust IWFA for open-spectrum communications," *IEEE Trans. Signal Process.*, vol. 57, pp. 4964–4970, Dec. 2009.

[26] G. Scutary, D. P. Palomar, and S. Barbarossa, "Asynchronous iterative water-filling for Gaussian frequency-selective interference channels," *IEEE Trans. Inf. Theory*, vol. 54, pp. 2868–2878, Dec. 2008.

[27] L. Le and E. Hossain, "Resource allocation for spectrum underlay in cognitive radio networks," *IEEE Trans. Wireless Commun.*, vol. 7, pp. 5306–5315, Dec. 2008.

[28] A. B. MacKenzie, L. DaSilva, and W. Tranter, *Game Theory for Wireless Engineers*. Morgan and Caypool, 2006.

[29] Z. Ji and K. J. R. Liu, "Dynamic spectrum sharing: a game theoretical overview," *IEEE Commun. Mag.*, vol. 45, pp. 88–94, May 2007.

[30] F. Wang, M. Krunz, and S. Cui, "Price-based spectrum management in cognitive radio networks," *IEEE J. Sel. Topics Signal Process.*, vol. 2, pp. 74–87, Feb. 2008.

[31] J. E. Suris, L. A. DaSilva, Z. Han, and A. B. MacKenzie, "Cooperative game for distributed spectrum sharing," in *Proc. IEEE Int. Conf. on Commun. (ICC)*, 2007.

[32] I. Budiarjo, H. Nikookar, and L. Ligthart, "Cognitive radio modulation techniques," *IEEE Signal Process. Mag.*, vol. 25, pp. 24–34, Dec. 2008.

[33] Federal Communications Commission, "Establishment of an interference temperature metric to quantify and manage interference and to expand available unlicensed operation in certain fixed, mobile and satellite frequency bands." ET Docket No. 03-237, Nov. 2003.

[34] R. Etkin, D. N. C. Tse, and H. Wang, "Gaussian interference channel capacity within one bit," *IEEE Trans. Inf. Theory*, vol. 54, pp. 5534–5562, Nov. 2008.

[35] T. S. Han and K. Kobayashi, "A new achievable rate region for the interference channel," *IEEE Trans. Inf. Theory*, vol. 27, pp. 49–60, Jan. 1981.

[36] X. He, X. Zhang, and B. Yang, "The effect of imperfect carrier synchronization on the performance of multi-tone DSSS," in *IEEE Int. Conf. on Commun. Technol. (ICCT)*, pp. 637–643, Nov. 2010.

[37] M. G. Khoshkholgh, K. Navaie, and H. Yanikomeroglu, "Achievable capacity in hybrid DS-CDMA/OFDM spectrum-sharing," *IEEE Trans. Mobile Comput.*, vol. 9, pp. 765–777, June 2010.

[38] B. Farhang-Boroujeny and R. R. Kempter, "Multicarrier communication techniques for spectrum sensing and communication in cognitive radios," *IEEE Commun. Mag.*, vol. 46, pp. 80–85, Apr. 2008.

[39] R. Gallager, *Information Theory and Reliable Communication*. New York, USA: John Wiley and Sons, 1968.

[40] D. P. Bertsekas and J. N. Tsitsiklis, *Parallel and Distributed Computation: Numerical Methods*. 2nd ed. ed., 1989.

[41] A. Leshem and E. Zehavi, "Game theory and the frequency selective interference channel," *IEEE Signal Process. Mag.*, vol. 26, pp. 28–40, Sept. 2009.

[42] S. Hayashi and Z.-Q. Luo, "Dynamic spectrum management: When is FDMA sum-rate optimal?," in *Proc. Int. Conf. Acoustics, Speech and Sig. Proc.*, pp. 609–612, Apr. 2007.

[43] R. J. C. Bultitude and G. K. Bedal, "Propagation characteristics on microcellular urban mobile radio channels at 910 MHz," *IEEE J. Sel. Areas Commun.*, vol. 7, pp. 31–39, Jan. 1989.

[44] H. Sari, G. Karam, and I. Jeanclaude, "Transmission techniques for digital terrestrial tv broadcasting," *IEEE Commun. Mag.*, vol. 23, pp. 100–109, Feb. 1995.

[45] J. G. Proakis, *Digital Communications*. McGraw-Hill, 3rd ed. ed., 1995.

[46] A. Tulino, G. Caire, S. Shamai, and S. Verdu, "Capacity of channels with frequency-selective and time-selective fading," *IEEE Trans. Inf. Theory*, vol. 56, pp. 1187–1215, Mar. 2010.

[47] T. Aulin and C. Sundberg, "Continuous phase modulation–Part I: Full response signaling," *IEEE Trans. Commun.*, vol. 29, pp. 196–209, Mar. 1981.

[48] S. Kaiser, "OFDM-CDMA versus DS-CDMA: Performance evaluation for fading channels," in *IEEE Int. Conf. on Commun. (ICC)*, vol. 3, (Seattle, WA, USA), pp. 1722–1726, June 1995.